

DISSERTATION

TRANSPORT VELOCITIES OF BEDLOAD PARTICLES IN ROUGH OPEN  
CHANNEL FLOWS

Submitted by

Bounthanh Bounvilay

Department of Civil Engineering

In partial fulfillment of the requirements

For the Degree of Doctor of Philosophy

Colorado State University

Fort Collins, Colorado

Spring 2003

**COLORADO STATE UNIVERSITY**

November 12, 2002

WE HEREBY RECOMMEND THAT THE DISSERTATION PREPARED UNDER  
OUR SUPERVISION BY **BOUNTHANH BOUNVILAY** ENTITLED **TRANSPORT  
VELOCITIES OF BEDLOAD PARTICLES IN ROUGH OPEN CHANNEL  
FLOWS** BE ACCEPTED AS FULFILLING IN PART REQUIREMENTS FOR THE  
DEGREE OF DOCTOR OF PHILOSOPHY

**Committee on Graduate Work**

---

---

---

---

Advisor

---

Department Head

## ABSTRACT OF DISSERTATION

### TRANSPORT VELOCITIES OF BEDLOAD PARTICLES IN ROUGH OPEN CHANNEL FLOWS

This dissertation aims at defining the bedload particle velocity in smooth and rough open channels as a function of the following variables: bed slope  $S_f$ , flow depth  $y$ , viscosity of the fluid  $\nu$ , particle size  $d_s$ , bed roughness  $k_s$ , particle specific gravity  $G$ , and gravitational acceleration  $g$ .

Sets of aluminum plates were placed on the bottom of an experimental plexiglass-tilting flume, with trapezoidal cross-section, to form a smooth bed. A layer of sand or gravel was glued onto aluminum plates to form bed roughness. Bedload particles used in the experiments were stainless steel ball bearings, glass marbles, and natural quartz particles. The experiments were performed to provide 529 average bedload particle velocities. The analysis of the laboratory measurements showed that: (1) for a smooth bed ( $k_s = 0$ ), the rolling bedload particle velocity  $V_p$  increases with particle sizes  $d_s$ ; (2) for a rough bed ( $k_s > 0$ ), particle velocity decreases with particle density  $G$ , thus lighter particles move faster than heavier ones; and on a very rough boundary  $V_p$  decreases with particle sizes; (3) bedload particles move at values of the Shields parameter  $\tau_{*ds} = u_*^2 / (G-1)gd_s$  below the critical Shields parameter value of  $\tau_{*dsc} = 0.047$ ; (4) few of the observed particles moved at values of Shields roughness parameter  $\tau_{*ks} = u_*^2 / (G-1)gk_s$  less than 0.01; (5) particles are observed to move at values of the Shields roughness parameter 0.01

$< \tau_{*k_s} < 0.15$ ; (6) the ratio of particle velocity  $V_p$  to mean flow velocity  $u_f$  lies in the range of 0.2 to 0.9, while Kalinske (1942) suggested 0.9 to 1.0; and (7) the ratio of particle velocity  $V_p$  to shear velocity  $u_*$  lies in the range of 2.5 to 12.5, compared to the values cited in the literature  $6.0 < V_p/u_* < 14.3$ .

New methods for predicting transport velocity of bedload particles in rough and smooth open channels are examined. Two approaches for transport velocities of bedload particles were considered. The first approach combines dimensional analysis and regression analysis to define bedload particle velocity as a power function of the Shields parameter  $\tau_{*d_s}$ , boundary relative roughness  $k_s/d_s$ , dimensionless particle diameter  $d_*$ , and excess specific gravity  $(G-1)$ . The second approach considers the transport velocity of a single particle on a smooth bed. The reduction in particle velocity due to bed roughness is then examined through a theoretical and empirical analysis. Results show that the bedload particle velocity on smooth beds is approximately equal to the flow at the center of the particle; and the bed roughness gradually decreases the transport velocity of the rolling bedload particles. Comparatively, The first approach gives satisfactory results, except when  $k_s$  equals 0, then  $V_p$  goes to  $\infty$ ; and when  $k_s$  is large,  $V_p$  does not stop (unbounded); for the second approach  $V_p = V_{pmax}$  when  $k_s$  equals 0, and when  $V_p$  equals 0 (no motion), then  $k_s$  follows the criteria a and b described in Chapter 5 (section 5.4).

The analysis shows that the proposed formula, Eq. (5.34) provides much better predictions than the existing formulas. The discrepancy ratio distributions using Eq. (5.34) are normally distributed and have higher density (close to perfect agreement) than all other formulas. In addition, the proposed formula, Eq. (5.34) is also verified with the

devastating flood of the Avila Mountain in Venezuela in December 1999. The results give realistic estimates of particle velocities.

Bounthanh Bounvilay  
Civil Engineering Department  
Colorado State University  
Fort Collins, CO 80523  
Spring 2003

## ACKNOWLEDGMENTS

I would like to express my gratitude to Prof. Pierre Y. Julien, for his inspiration, guidance, encouragement, friendship and financial support during the course of this work. Working with him has been a rewarding and enjoyable experience.

I also wish to express my appreciation to the members of my committee, Prof. Maurice L. Albertson, Dr. Deborah J. Anthony, Dr. Brian P. Bledsoe, and Dr. Daniel Gessler, for their valuable comments and review of this dissertation.

Special appreciation is extended to H.E. Mr. P. Leuangkhamma, Dr. S. Mangnomek (MOE), Duane Smith, Dr. R. Thaemert, Dr. M. Giger, Dr. H. Coowar, Prof. C. Loukides for their help and encouragement. Also, a great deal of thanks is due to Prof. R. Kersten, Dr. M. Chopra, Dr. N. D. Hoan, Dr. F. Nnadi, D. Mowry (UCF), Prof. P. K. Nam, Prof. N. D. Lieu (DHTL), Dr. R. Simmons, Nurse Sharon (Center for Gastroenterology), Dr. R. Risma (HHS), M. Hallett (ISS), L. Howard (CE), Dr. K. Bunte, Dr. J. Guo, M. Casey, R. Rojas, C. Leon (ERC), R. Slosson, P. Schei, D. Marsh, T. Tochtrop, K. Flowers (Smith Geotechnical), T. Pong, K. Phanouvong, S. Akalin, H. Hussain, J. Noh for their encouragement and friendship.

Finally, my deepest gratitude goes to my parents, my brothers and sisters, Khone-Lien, Bi-Ngan, Que-Teo, Noi, Sone, Minh-Nang, Bou, chi Lann, chi Noi, chi Binh (Bouavanh) my aunts and uncles mo Phu, di Duc, cau Be, mo Gai, di Nho, duong Thiene, cau Gai, mo Be, di Hone, duong Duong, bac Bay, bac Tu, bac Nghia, co Ly, co Huong, co Ngoc, co Nga, di Meo, Ama (Pakse), co Phuong, bac Dong, bac Phuong, co The, chu

Ly, bac Quy, anh Ngoc (Hanoi), co Lan, co Quy (BL), my nieces and nephews, Ni, Na, Nu, Piu, Sam, Ky, Kay, Big, Be, Cho, and my friends Hoa (Pakse) and Ha (Hanoi) for their continual support and encouragement throughout this research.

To my Grand parents, Parents, Brothers and Sisters,  
Nieces and Nephews, and aunt Hoang Thi Duc



# TABLE OF CONTENTS

<b>CHAPTER 1</b>	<b>INTRODUCTION</b>	<b>1</b>
1.1.	PROBLEM STATEMENT	1
1.2.	BACKGROUND	1
1.3.	OBJECTIVES	2
1.4.	METHODS	3
1.5.	OUTLINE	3
<b>CHAPTER 2</b>	<b>LITERATURE REVIEW</b>	<b>4</b>
2.1.	EARLIER STUDIES	4
2.2.	DATA COMPILATION	18
2.3.	APPLICATION OF EXISTING METHODS	27
2.4.	SUMMARY	31
<b>CHAPTER 3</b>	<b>DATA COMPILATION</b>	<b>32</b>
3.1.	THE FLUME	32
3.2.	THE PLATES	34
3.3.	THE PARTICLES	38
3.4.	EXPERIMENTAL SET UP	42
3.5.	PRELIMINARY RESULTS	45
3.6.	STATISTICAL ANALYSIS	51
3.7.	PARAMETRIC ANALYSIS OF CSU DATA	52
3.8.	SUMMARY	57
<b>CHAPTER 4</b>	<b>DIMENSIONAL AND REGRESSION ANALYSIS</b>	<b>59</b>
4.1.	EXAMINATION OF SHIELDS APPROACH	60
4.2.	DIMENSIONAL ANALYSIS	66
4.3.	SUMMARY	73
<b>CHAPTER 5</b>	<b>BEDLOAD PARTICLE VELOCITY</b>	<b>74</b>
5.1.	VELOCITY PROFILE NEAR SMOOTH BED	74
5.2.	MAXIMUM VELOCITY OF A PARTICLE ON SMOOTH BED	77
5.3.	SINGLE PARTICLE ROLLING DOWN AN INCLINED ROUGH BED	83
5.4.	ANALYSIS OF THE THRESHOLD CONDITION	92

5.5. SUMMARY	94
<b>CHAPTER 6 LABORATORY AND FIELD APPLICATIONS</b>	<b>95</b>
6.1. PROPOSED METHOD	95
6.2. TESTING EXISTING FORMULAS WITH ENTIRE DATABASE	96
6.3. HALFMOON CREEK, COLORADO	102
6.4. AVILA MOUNTAIN, VENEZUELA	107
<b>CHAPTER 7 SUMMMARY AND CONCLUSIONS</b>	<b>116</b>
<b>CITED REFERENCES</b>	<b>120</b>
<b>APPENDIX I: THE CSU DATABASE</b>	<b>138</b>

## LIST OF FIGURES

Figure 2.1: $V_p/k_s^m$ vs. $u_*d_s^n/k_s$ _____	28
Figure 2.2: Comparison between Calculated and Observed $V_p$ using Eq. (2.9) _____	28
Figure 2.3: $V_p$ vs. $(u_*-0.7u_{*c})$ _____	29
Figure 2.4: Comparison between Calculated and Observed $V_p$ using Eq. (2.15) _____	29
Figure 2.5: $V_p$ vs. $(u_*-u_{*c})$ _____	30
Figure 2.6: Comparison between Calculated and Observed $V_p$ using Eq. (2.22) _____	30
Figure 3.1: Three Point Gages used to Measure Water Depth. _____	34
Figure 3.2: Form Roughened Plates _____	36
Figure 3.3: Plate at Roughness $k_s = 1.2$ mm _____	36
Figure 3.4: Plate at Roughness $k_s = 1.7$ mm _____	37
Figure 3.5: Plate at Roughness $k_s = 2.4$ mm _____	37
Figure 3.6: Plate at Roughness $k_s = 3.4$ _____	38
Figure 3.7: Particles used in the Experiment _____	40
Figure 3.8: The Experiment _____	40
Figure 3.9: $w$ vs. $[(G-1)gd_s]^{1/2}$ _____	43
Figure 3.10: $V_{pobs}$ vs $d_s$ for $k_s = 0$ _____	47
Figure 3.11: $V_{pobs}$ vs $d_s$ for $k_s > 0$ _____	47
Figure 3.12: $V_p/u_*$ vs $d_s$ _____	48
Figure 3.13: $V_p$ vs $u_*$ , a) $V_{p(N,G)} \sim 9.14u_*$ , and b) $V_{p(S)} \sim 3.94u_*$ _____	48
Figure 3.14: $V_p$ vs $\tau_{*ds}$ _____	49
Figure 3.15: $V_p/u_f$ vs $d_s$ _____	49
Figure 3.16: $V_p/u_f$ vs $u_* / [(G-1)gd_s]^{1/2}$ _____	50
Figure 3.17: $\tau_{*ds}$ vs $d_s$ _____	53

Figure 3.18: $\tau_{*ks}$ vs $d_s$	53
Figure 3.19: $\tau_{*ds}/0.047$ vs $d_s/k_s$	54
Figure 3.20: $\tau_{*ds}$ vs $Re^*$	54
Figure 3.21: $V_p/[(G-1)gd_s]^{1/2}$ vs $\tau_{*ds}$	55
Figure 3.22: $V_p/u^*$ vs $\tau_{*ds}/0.047$	55
Figure 3.23: $V_p/u^*$ vs $\tau_{*ks}/0.047$	56
Figure 3.24: $u^*/w$ vs $\tau_{*ks}$	56
Figure 3.25: $u^*/w$ vs $\tau_{*ks}$ , for different database	57
Figure 4.1: $V_p/[(G-1)gk_s]^{1/2}$ vs $\tau_{*ks}$	60
Figure 4.2: $V_p/[(G-1)gd_s]^{1/2} \sim 30.5\tau_{*ds}^{1.0}(d_s/k_s)^{0.583}$	62
Figure 4.3: Comparison between Calculated and Observed $V_p$ using Eq. (4.7)	64
Figure 4.4: Discrepancy Ratio Distribution of $V_p$ using Eq. (4.7)	64
Figure 4.5: Comparison between Calculated and Observed $V_p$ using Eq. (4.8)	65
Figure 4.6: Discrepancy Ratio Distribution of $V_p$ using Eq. (4.8)	65
Figure 4.7: $V_p/[(G-1)gd_s]^{1/2}$ vs $11.5\tau_{*ds}^{0.95}d_s^{0.21}(d_s/k_s)^{0.36}(G-1)^{-0.28}$	68
Figure 4.8: Comparison between Calculated and Observed $V_p$ using Eq. (4.18)	70
Figure 4.9: Discrepancy Ratio Distribution of $V_p$ using Eq. (4.18)	70
Figure 4.10: Comparison between Calculated and Observed $V_p$ using Eq. (4.20)	71
Figure 4.11: Discrepancy Ratio Distribution of $V_p$ using Eq. (4.20)	71
Figure 5.1: Velocity Profile In The Inner Region	75
Figure 5.2: Forces Acting on a Sphere Rolling down an Inclined Smooth Bed	77
Figure 5.3: $V_p/u^*$ vs $Re^*$ using Eq. (5.28)	81
Figure 5.4: Comparison between Calculated and Observed $V_p$ using Eq. (5.28)	81
Figure 5.5: $V_p/u^*$ vs $Re^*$ using Eq. (5.28) for different values of $d^*$	82
Figure 5.6: $V_p/u^*$ vs $Re^*$ using Eq. (5.28) for different values of $\theta$	82

Figure 5.7: Forces Acting on a Sphere Rolling down an Inclined Bed of Roughness	83
Figure 5.8: $V_p/u_*$ vs $Re_*$ for Smooth ( $k_s = 0$ ) and Rough Bed ( $k_s > 0$ )	84
Figure 5.9: $\Delta B_{cal}$ vs $\Delta B_{obs}$ using Eq. (5.33b) for CSU data	86
Figure 5.10: Comparison between Calculated and Observed $V_p$ using Eq. (5.34)	86
Figure 5.11: $\Delta B_{cal}$ vs $\Delta B_{obs}$ using Eq. (5.33b) for total data	87
Figure 5.12: Comparison between Calculated and Observed $V_p$ using Eq. (5.34)	87
Figure 5.13: Discrepancy Ratio Distribution of $V_p$ using Eq. (5.34)	88
Figure 5.14: $\Delta B_{cal}$ vs $\Delta B_{obs}$ using (5.33c) for total data	89
Figure 5.15: Comparison between Calculated and Observed $V_p$ using Eq. (5.35)	89
Figure 5.16: Discrepancy Ratio Distribution of $V_p$ using Eq. (5.35)	90
Figure 5.17: $\tau_{*ds}/0.047$ vs $d_s/k_s$ , for different values of $V_p/u_*$	92
Figure 5.18: $\tau_{*ks}$ vs $d_*$ for different databases	93
Figure 6.1: Comparison between Calculated and Observed $V_p$ using Eq. (2.9)	98
Figure 6.2: Discrepancy Ratio Distribution of $V_p$ using Eq. (2.9)	98
Figure 6.3: Comparison between Calculated and Observed $V_p$ using Eq. (2.15)	99
Figure 6.4: Discrepancy Ratio Distribution of $V_p$ using Eq. (2.15)	99
Figure 6.5: Comparison between Calculated and Observed $V_p$ using Eq. (2.22)	100
Figure 6.6: Discrepancy Ratio Distribution of $V_p$ using Eq. (2.22)	100
Figure 6.7: Track of a single particle at Halfmoon Creek (Dixon and Ryan, 2000); a) the particle move into view and comes to rest.	104
Figure 6.8: Track of a single particle at Halfmoon Creek (Dixon and Ryan, 2000); b) after 17 seconds the particle moves 23 mm and comes to rest again.	104
Figure 6.9: Track of a single particle at Halfmoon Creek (Dixon and Ryan, 2000); c) after being stationary for over 7 minutes, the particle moves out of the view.	105
Figure 6.10: Predicted $V_p$ using Eq. (5.34) for different values of $d_s$ and $k_s$	107
Figure 6.11: Aerial view of Caraballeda looking Southwest (Larsen et al., 2000)	109

Figure 6.12: View of road damaged in Los Corales, Leon and Rojas, 2000 (personal communication) _____	109
Figure 6.13: Aerial view of Caraballeda looking North (Larsen et al., 2000) _____	110
Figure 6.14: View of road damaged in Los Corales, Leon and Rojas, 2000 (personal communication) _____	110
Figure 6.15: View of deposited boulders on the road in Los Corales, Leon and Rojas, 2000 (personal communication) _____	111
Figure 6.16: Big boulder transported by debris flow, Leon and Rojas, 2000 (personal communication) _____	111
Figure 6.17: Boulder transported by debris flow in December 1999 (Larsen et al., 2000) _____	112
Figure 6.18: Aerial view of Los Corales sector of Caraballeda (Larsen et al., 2000) _____	112
Figure 6.19: View of damaged to apartment building in Los Corales, Leon and Rojas, 2000 (personal communication) _____	113
Figure 6.20: Control canal for debris flow at the Saint Julian Ravine, Leon and Rojas, 2000 (personal communication) _____	113
Figure 6.21: Predicted $V_p$ using Eq. (5.34) for different values of $d_s$ and $k_s$ _____	115

## LIST OF TABLES

Table 2.1: Variability of Hydraulic and Bedload Particle Parameters _____	20
Table 2.2: Summary of Literature Review _____	21
Table 2.3: Existing Database _____	24
Table 2.4: Summary of Previous and Recent Studies _____	26
Table 3.1: Gravel Gradations for Roughened Plane Surfaces _____	35
Table 3.2: Particle Size used in the Experiments _____	41
Table 3.3: Classification of Experimental Runs _____	44
Table 3.4. Computed Values of $c$ and $u_{*c}$ for different $k_s$ and Particle type _____	51
Table 4.1: Comparison between Calculated and Observed $V_p$ using Proposed Formulas _____	72
Table 5.1: Summary of Comparison between Calculated and Observed $V_p$ _____	91
Table 6.1: Summary of Comparison between Calculated and Observed $V_p$ _____	102

## LIST OF SYMBOLS

<u>Symbol</u>	<u>Description</u>
$A$	area of the stream cross-section ( $m^2$ ), $A = \frac{1}{2} (T_w + B_w)y$ ;
$b$	constant parameter;
$B_w$	width of the plate, which also defined the bottom width of the channel (mm);
$c$	constant parameter;
$c_c$	$\rho/4\mu$ ( $s/m^2$ );
$C_D$	drag coefficient;
$C_L$	lift coefficient;
$c_a, c_b, c_d, c_e$	constant parameters;
$c_\alpha$	proportionality constant;
$c_\mu$	sliding friction coefficient;
$d_s$	diameter of the rolling particles (mm);
$d_*$	dimensionless particle diameter, $d_* = d_s \left[ \frac{(G-1)g}{v^2} \right]^{1/3}$ ;
$f$	collision coefficient;
$F_D$	drag force;
$F_L$	lift force;
$F_f$	friction force;
$F_N$	support force of the plane;
$Fr$	Froude number;
$g$	gravitational acceleration ( $m/s^2$ );



$G$	specific gravity of the particles;
$H$	energy grade line elevation (m) at the two point gages;  $H_{u.s.} = y_{u.s.} + (S_o \Delta X) + (V_{u.s.})^2 / 2g$ ;  $H_{d.s.} = y_{u.s.} + (V_{u.s.})^2 / 2g$ ;
$k_s$	bed roughness, average diameter of the particles of gravel glued to the plates (see Table 3.1), in mm;
$m$	constant parameter;
$m_\mu$	static friction coefficient;
$n$	number of trials for each particle (between 15 and 21 trials per particle type and size);
$n_a$	$(0.014k_s/u_*)^{0.26}$ ;
$n_\mu$	bulk friction coefficient;
$P$	wetted perimeter of the stream cross-section (mm);  $P = B_w + 2\sqrt{y^2 + \left(\frac{1}{2}(T_w - B_w)\right)^2}$ ;
$Q$	flow rate in liters/s, $Q = 6.45632$ (manometer reading / 12) <sup>0.503</sup> ;
$Re$	Reynolds number;
$Re^*$	Shear Reynolds number;
$R_h$	hydraulic radius of the stream cross-section (m), $R_h = A/P$ ;
$R_i$	discrepancy ratio (%);
$S_f$	friction slope $\Delta H / \Delta X$ ;
$S_o$	bed slope (m/m);
$T_{avg}$	average water temperature in °C (measured at start and end of each run);

$T_w$	top width of the channel (mm); measured at each point gage along the flume;
$u_c$	critical velocity (m/s);
$u_f$	average stream flow velocity (m/s); $u_f = Q/A$ ;
$u_1$	flow velocity at the height of the particle center (m/s);
$u_{1c}$	critical velocity at the threshold motion (m/s);
$u_*$	Shear velocity (m/s), $u_* = \sqrt{gR_h S_f}$ ;
$u_{*c}$	critical shear velocity (m/s);
$V_p$	average velocity over n trials for each particle (mm/s);
$w$	settling velocity of the rolling particles (m/s);
$W_s$	submerged weight of the sphere;
$y$	flow depth in mm (measured at three location with point gages);
$y/k_s$	relative submergence, ratio of average stream depth to bed roughness;
$\Delta X$	distance between two point gages in the test section (1.62 m);
$\Delta H$	energy loss or head loss (m) between the two point gages; $H_{u,s} - H_{d,s}$ ;
$\nu$	kinematic viscosity in $\text{mm}^2/\text{s}$ or $\text{m}^2/\text{s} \times 10^{-6}$ ; $\nu = 0.0003625 (T_{\text{avg}})^2 - 0.038775 (T_{\text{avg}}) + 1.6345$ ;
$\delta$	laminar sub-layer thickness (m), $\delta = 11.6 \frac{\nu}{u_*} \times 10^{-6}$ if $\nu$ in $\text{mm}^2/\text{s}$ ;
$\sigma$	standard deviation of particle velocities (m/s);
$\Delta B$	roughness function;

$\Delta B_c$	calculated rough ness function;
$\tau$	mean bed shear stress (kg/m <sup>2</sup> );
$\tau_c$	shear stress at threshold of motion (kg/m <sup>2</sup> );
$\tau_{oc}$	critical bed shear stress required for the particle to roll (kg/m <sup>2</sup> );
$\tau^*_{ds}$	Shields parameter;
$\tau^*_{ks}$	Shields roughness parameter;
$\rho_s$	particle density (kg-sec <sup>2</sup> /m <sup>4</sup> );
$\rho_f$	fluid density (kg-sec <sup>2</sup> /m <sup>4</sup> );
$\theta$	bed slope angle;
$\mu$	dynamic viscosity of water (kg-sec/m <sup>2</sup> );
$\nu$	kinematic viscosity (m <sup>2</sup> /s);
$\tau_o$	bed shear stress (kg/m <sup>2</sup> );
$\tan \alpha$	dynamic friction coefficient;
$\alpha, \beta, \chi$	particle velocity coefficients;
Pump setting	for major adjustment of the flow (slow, medium, fast);
Valve setting	for fine adjustment of the flow;
Reach length	length of test section (2000 mm);
Slope reading	reading of vertical displacement (mm) for a ruler attached to the flume near the upstream end, the ruler is 7145 mm upstream of the pivot point of at flume support;
Manometer readings	manometer height in inches of water to compute flow rates;
u.s.	upstream -- generally refer to the position of the upstream point gage in the test section;

- d.s. downstream – generally refer to the position of the downstream point gage in the test section;
- $V_{u.s.}$  average flow velocity at the upstream point gage;
- $V_{d.s.}$  average flow velocity at the downstream point gage;

# **CHAPTER 1**

## **INTRODUCTION**

### **1.1. PROBLEM STATEMENT**

The study of rolling bedload particle velocity in rough open channel flows is a basic subject in the field of river mechanics and sediment transport. This study aims at the determination of the velocity of rolling bedload particles in rough open channel flows.

### **1.2. BACKGROUND**

Three major approaches for the study of bedload transport are often found in the literature: (1) deterministic approach; (2) empirical approach; and (3) statistical-mechanical approach. The deterministic approach, which is based on some physical laws, studies the relation between bedload transport rates and the corresponding stream power, flow momentum, or other flow properties. The results are expressed in terms of average

flow conditions. A representative of this type of work is the Bagnold stream power function (Chien and Wan, 1983). The empirical approach relates measured bedload rates with their corresponding flow conditions. The results of many observations provide the basis for engineering applications, but sometimes give conflicting estimates when applied to rivers. The statistical-mechanical approach proposed by Einstein (1950), is a combination of the above two approaches. It considers both flow stochastic and deterministic properties of particle motion. The Einstein bedload function (Einstein 1950) shows that individual particle mechanics is one important aspect in this type of approach. Since bedload particle movement can be divided into rolling, sliding and saltation, this proposed research concentrates on the rolling motion, i.e., the motion of a single particle rolling over a rough open channel bed. The primary interest of this research has been to quantitatively examine the velocity of individual particles moving as rolling bedload on rough beds.

### **1.3. OBJECTIVES**

The specific objectives address in this study are: (1) to compile a large database including observed bedload particle velocity measurements on smooth and rough beds; (2) to analyze the database using existing bedload particle velocity formulas; (3) to develop new functions that computes bedload particle velocity in rough open channel flows using dimensional and regression analysis, and theoretical analysis; (4) to determine threshold conditions; and (5) to test the new functions with laboratory measurements and select the best function for field applications representative of very large floods.

## **1.4. METHODS**

To achieve the objective, an extensive compilation of existing laboratory measurements at CSU and other laboratory data from literature has been done. The theoretical and empirical analyses have been studied, and new theoretical and empirical equations were developed and tested with a database including data from Meland and Norrman (1966), Fernandez Luque and van Beek (1976), Steidtmann (1982), Bridge and Dominic (1984), CSU (1995), and Bigillon (2001).

## **1.5. OUTLINE**

This dissertation includes 7 chapters. Chapter 1 briefly introduces the subject and states the objective. Chapter 2 includes a literature review, presented as a highlight of a few of the major papers written on the particle velocity approximations. Chapter 3 describes the CSU experimental set-up and data analysis. Chapter 4 provides a dimensional and regression analyses and testing of empirical formulas. Chapter 5 describes the theoretical development leading to a particle velocity formula. Chapter 6 describes laboratory and field applications of the proposed formulas. Finally, Chapter 7 summarizes the main results of this research.

# CHAPTER 2

## LITERATURE REVIEW

The purpose of this chapter is to review the pertinent information available from experimental studies on this subject. This material is presented as a highlight of a few of the major papers written on the bedload particle velocity on smooth and rough beds.

### 2.1. EARLIER STUDIES

Krumbein (1942) studied the effect of particle shape on sediment transportation with experiments conducted in flumes. Krumbein related the observed behavior to the settling velocities of particles. His experiments were confined to the bed movement of single particles of different shapes, over a hydraulically smooth bed, for turbulent flow conditions. Through dimensional analysis, Krumbein determined a relationship between sphericity and the ratio of particle velocity to mean flow velocity,  $V_p / u_f$ , as a function



of the Froude number. Krumbein noticed that the curves followed an exponential type of equation, and proposed:

$$\frac{V_p}{u_f} = \left( \frac{V_p}{u_f} \right)_0 (1 - \exp(-bFr)) \quad (2.1)$$

where:  $V_p$  = particle velocity (m/s);  $u_f$  = mean flow velocity (m/s);  $b$  = constant;  $Fr$  = Froude number. In a discussion of Krumbein's paper, Kalinske (1942) noted that all of Krumbein's experiments were made at a constant flow depth of 131 mm, which allowed the Froude number to be written as a function of mean flow velocity:

$$Fr = \frac{u_f}{\sqrt{9.81 \times 0.131}} = 0.88u_f$$

For the case of spheres, Eq. (2.1) can then be written as:

$$\frac{V_p}{u_f} = 0.88[1 - \exp(-1.85u_f)] \quad (2.2)$$

Therefore, Krumbein's equation is not more than a plot of  $V_p/u_f$  vs.  $u_f$ . He did not make any attempts either to correlate against variables other than  $Fr$ , or to find a physical basis for his empirical equation. Moreover, the nominal diameter of all particles tested was kept constant, so that size effects were not taken into account. Finally, even though the flow was turbulent, all of Krumbein's experiments were done over a smooth bed, and therefore have less applicability to real world situations.

Kalinske (1942) reported that the Froude number  $Fr$  has no physical significance in regard to the movement of particles on the bed. Kalinske proposed that the particle

velocity  $V_p$  should be equal, or at least proportional to  $u' - u_c$ . where:  $u'$  = the velocity of the fluid acting on the particle (m/s);  $u_c$  = critical velocity for that particle. As  $u'$  is proportional to  $u_f$ , Kalinske obtained the following expression

$$V_p = c_a (u_f - u_c) \quad (2.3)$$

where:  $c_a$  = constant;  $u_f$  = mean flow velocity (m/s);  $V_p$  = particle velocity (m/s);  $u_c$  = critical velocity (m/s). Kalinske applied his model to Krumbein's data and found the best agreement for  $0.9 < c_a < 1.0$ . No mention is made regarding how to obtain the critical velocity for a given particle.

Ippen and Verma (1955) analyzed the motion of small spheres over beds of different roughness in flume experiments, for turbulent flow conditions. Upon plotting the ratio  $u_f / V_p$  against the Reynolds number, Re, they found that after a transition of variable length (proportional to grain density),  $u_f / V_p$  reached an ultimate value that remained constant over a wide range of Re and that the particle velocity increased directly with size, and attributed this to the fact that larger particles protrude into higher velocities than smaller ones. Assuming that the nearly constant ratio  $u_f / V_p$  is governed by the following variables:  $(G - 1)$ ,  $k_s / d_s$ , and  $1 / S$ , they obtained the following equation as a best fit to the data:

$$\frac{u_f}{V_p} = 1 + \frac{1}{12} (G - 1) \left( \frac{k_s}{d_s} \right) \left( \frac{1}{\sqrt{S}} \right) \quad (2.4)$$

where:  $G$  = the specific gravity of grains;  $d_s$  = particle size (mm);  $k_s$  = roughness size (mm);  $S$  = energy grade line; Eq. (2.4) is explicitly dependent on the particle size, and shows an increase in particle velocity with size. From the definition of shear velocity  $u_*$  and mean bed shear stress  $\tau_o$ :

$$u_* = \sqrt{\frac{\tau_o}{\rho}} \quad (2.5)$$

$$\tau_o = \gamma h S \quad (2.6)$$

one can obtain:

$$S = \frac{u_*^2}{gh} \quad (2.7)$$

and replacing Eq. (2.7) into Eq. (2.4) leads to:

$$\frac{u_f}{V_p} = 1 + c_b \left( \frac{k_s}{d_s} \right) \left( \frac{1}{u_*} \right) \quad (2.8)$$

where:  $c_b = \frac{1}{12}(G-1)\sqrt{gh}$ , a constant for a given flow depth and grain material (m/s);  $u_*$  = shear velocity (m/s);  $V_p$  = particle velocity (m/s);  $u_f$  = mean flow velocity (m/s); Eq. (2.8) clearly shows that particle velocity is directly related to both particle size and shear velocity, while inversely related to roughness size.

Meland and Norrman (1966) represent the most complete up-to-date approach to generate information about single grain transport velocities. Most recent theoretical papers on sediment transport rates rely heavily on Meland and Norrman for data in order

to validate their models. Meland and Norrman investigated the interactive effects of water velocity, bed roughness, and particle size on the transport rate of single particles over rough beds by turbulent flows, keeping particle shape, density and bed packing constant. Meland and Norrman used glass beads only, rolling on top of a bed made from the same beads. Upon analyzing their results, in which particle velocity is plotted against particle size for different values of shear velocity, it can be clearly seen that, for a given bed roughness and shear velocity, larger particles move faster than smaller ones, as concluded by Ippen and Verma (1955). Meland and Norrman give two main reasons for this behavior: First, larger particles ride higher off the bed, being thus exposed to the greater velocities; and second, the rolling resistance decreases when the ratio of particle size to roughness size is increased. They also found that the influence of size upon transport velocity decreases with increasing shear velocity and with decreasing bed roughness size. In other words, at high shear velocities and small bed roughness, the particle velocity tends to be constant with size.

$$\frac{V_p}{k_s^m} = a_m u_* \frac{d_s^{n_a}}{k_s} - b_m \quad (2.9)$$

where:  $u_*$  = shear velocity (m/s);  $V_p$  = particle velocity (m/s);  $k_s$  = roughness size (mm);

$m = 0.75$ ;  $n_a = \left( \frac{0.014 k_s}{u_*} \right)^{0.26}$ ;  $a_m = 7.05$ ; and  $b_m = 5.1$ . This empirical equation applies

only to Meland and Norrman's experiments; the constants appearing in the equation are of no particular importance.  $V_p$  is directly related to  $u_*$  and  $d_s$ , and inversely related to  $k_s$ .

In other words,  $V_p$  is directly related to the ratio  $k_s / d_s$  of particle size, i.e., larger particles roll easier than smaller ones over a given bed, or a given particle rolls more

easily over a smooth than a rough bed. They also observed that transport velocities were lower on beds of loosely packed glass beads than in corresponding fixed, solid beds. This effect was most noticeable at high transport stages, and decreased, or was even reversed for low shear velocities. Eq. (2.9) gives a better results when applied the constants  $a_m = 4$ , and  $b_m = 5.8$  (see Figs. 2.1 and 2.2).

Parson (1972) reported measurements on the rates of travel of several sizes of sand grains and glass beads in laminar sheet flow (i.e., overland flow) at different discharges and slopes, over a smooth bed. Parson found that particles moving in contact with the bed (i.e., rolling and sliding motion) travel at speeds approximately one-half the velocity of water in unobstructed flow, at a distance from the bed equal to the radius of a sphere of equal volume. For some tests with a large number of grains thrown at the same time, Parson overlooked a significant difference in speed. For glass beads, he found good agreement with the following equation:

$$V_p = \frac{\tau_o d_s}{4\mu} \left( 1 - \frac{\tau_{oc}}{\tau_o} \right) \quad (2.10)$$

where:  $V_p$  = particle velocity (m/s);  $\mu$  = fluid dynamic viscosity (kg-s/m<sup>2</sup>);  $d_s$  = grain diameter (mm);  $\tau_o$  = bed shear stress (kg/m<sup>2</sup>);  $\tau_{oc}$  = critical bed shear stress required for the glass beads to roll (kg/m<sup>2</sup>). Using Eq. (2.5), one can express  $\tau_o$  and  $\tau_{oc}$  as:

$$\tau_o = \rho u_*^2 \quad (2.11)$$

$$\tau_{oc} = \rho u_{*c}^2 \quad (2.12)$$

replacing (2.11) and (2.12) into Eq. (2.10), and defining  $c_c = \frac{\rho}{4\mu}$  (s/m<sup>2</sup>), results in:

$$V_p = c_c d_s (u_*^2 - u_{*c}^2) \quad (2.13)$$

where:  $u_*$  = shear velocity (m/s);  $u_{*c}$  = critical velocity (m/s). Eq. (2.13) not only shows that  $V_p$  depends directly on  $d_s$ , but also that  $V_p$  is proportional to the difference between a velocity and a critical velocity. In this case, it is shear velocity squared.

Ikeda (1971) made a theoretical analysis of the mechanics of the motion of a single spherical grain rolling on the bed, by considering the four main forces acting on the particle: drag, lift, gravity and friction with the bed. The resulting equation is as follows:

$$\frac{V_p}{u_*} = \frac{u_f}{u_*} - \left[ \frac{4}{3} c_\mu \frac{(G-1) g d_s}{(c_\mu C_L + C_D) u_*^2} \right]^{1/2} \quad (2.14)$$

where:  $V_p$  = particle velocity (m/s);  $u_*$  = shear velocity (m/s);  $u_f$  = fluid velocity at the center of the spherical grain (m/s);  $c_\mu$  = sliding friction coefficient;  $G$  = particle specific gravity;  $g$  = gravitational acceleration (m/s<sup>2</sup>);  $C_D$  and  $C_L$  = the drag and lift coefficients respectively; However, Ikeda did not give a method to specify the values of  $c_\mu$ ,  $C_D$  and  $C_L$ , which makes this formula inapplicable in practice. Besides, Ikeda assumed that the particle velocity is always behind the fluid velocity. This is not true for the case of steep slopes at very low fluid velocities.

Francis (1973) studied the motion of solitary grains along the bed of a flume. Francis' investigation was limited to particles moving over a fixed-plane bed made out of particles of the same type as those being transported, and he did not consider the effects

of grain size relative to roughness size. Francis found a satisfactory correlation between  $V_p$  (m/s) and the particle settling velocity,  $w$  (m/s). He also found a considerable difference in  $V_p$  for grains of different shapes. Specifically, he concluded that rounded particles always roll faster than angular ones.

The effect of grain size on  $V_p$  was always accounted for by using the regression with  $w$ , but shape effects could not be reduced. Francis performed the experiments with spherical particles traveling over a bed consisting of cylinders of the same diameter as the grains laid perpendicular to the flow. In this case, spherical particles traveled faster than any natural grains. Finally, he observed marked grains moving in the company of many other grains, in order to test the applicability of results derived from single grain experiments. In this case, speed was reduced 5% on average below that corresponding to solitary grains. This effect was most noticeable for low transport stages, and disappeared altogether for very high shear velocities.

Fernandez Luque and van Beek (1976) used a different approach than the one in previous studies, by using a loose bed for all of their experiments. They measured particle velocities as a function of bed shear stress in a closed-flow rectangular flume. The measured grains were scoured from the bed and then rolled on top of it. The average transport velocity of particles, which were saltating, or even in suspension, for most of the time was found to be equal to the average fluid velocity for turbulent flow without bed load at about three particle diameters above the bed surface minus a constant proportional to  $u_{*c}$ , as shown below:

$$V_p = c(u_* - 0.7u_{*c}) \quad (2.15)$$

where:  $u_{*c}$  = critical shear velocity at Shields condition for entrainment (m/s);  $V_p$  = particle velocity (m/s);  $u_*$  = shear velocity (m/s) and  $c$  = constant (11.5). Eq. (2.15) is valid over a wide range of slopes. The form of this equation is quite misleading, since it seems that  $V_p$  will decrease with size (because  $u_{*c}$  is higher for larger particles), but this is not the case because the points through which the equation was plotted correspond to all different experiments. Thus, in Eq. (2.15),  $u_*$  is also a function of size; because in experiments with larger particles, larger shear velocities were required not only to entrain grains, but also to keep them moving. As in Francis (1973), the particles were rolling on top of a bed made from the same material, so that the effect of size cannot be described.

Romanovskiy (1977) not only shows his own experimental results, but he also discusses previous approaches to the problem of modeling grain transport velocity. In particular, he presents Goncharov's (1938) empirical equation:

$$V_p = u_1 - u_{1c} \quad (2.16)$$

where:  $V_p$  = particle velocity (m/s);  $u_1$  = flow velocity at the height of the particle center (m/s);  $u_{1c}$  = critical value at the threshold of motion (m/s). Assuming a logarithmic velocity profile, it is possible to relate  $u_1$  to the mean flow velocity,  $u_f$ , through a constant, so that one obtains:

$$V_p = c_a (u_f - u_c) \quad (2.17)$$

where:  $c_a$  = constant;  $u_f$  = mean flow velocity (m/s);  $u_c$  = critical velocity (m/s). This is identical to Kalinske' Eq. (2.3). One considers the shear velocity as:



$$u_* = \sqrt{\frac{f}{8}} u_f \quad (2.18)$$

where:  $f$  = Darcy-Weisbach coefficient;  $u_*$  = shear velocity (m/s); we can write Eqs. (2.3) and (2.17) in terms of shear velocities:

$$V_p = c(u_* - u_{*c}) \quad (2.19)$$

where:  $c = (f/8)^{1/2}$ , which is assumed constant;  $u_{*c}$  = critical shear velocity (m/s). The later equation is quite similar to the form of Fernandez Luque and van Beek's (1976) Eq. (2.15). Romanovskiy (1977) made a simplified analysis of the forces acting on a rolling grain and proposed:

$$V_p = c_e \left( u_f - u_c \sqrt{\frac{\tan \alpha}{m_\mu}} \right) \quad (2.20)$$

where:  $\tan \alpha$  = dynamic friction coefficient;  $m_\mu$  = static friction coefficient;  $u_f$  = mean flow velocity (m/s);  $c_e$  = constant;  $u_c$  = critical velocity (m/s). For a particle at repose,  $\tan \alpha = m_\mu$ ; and if  $u_f$  is allowed to increase slowly from zero, at a certain velocity  $u_f = u_c$ , the particle will be entrained. From his experimental work he concluded that the form of Eq. (2.20) adequately represents the data.

Abbott and Francis (1977) continued the investigations reported by Francis (1973). More experiments were carried out and the following equation was found to represent all data sets with very low scatter:

$$V_p = c(u_* - u_{*c}) \quad (2.21)$$

where:  $u_*$  = shear velocity (m/s);  $u_{*c}$  = critical shear velocity (m/s); and  $c$  = constant parameter ( $13.5 < c < 14.5$ ); A particle riding on top of the bed has a far lower threshold of motion than one nested into it. Abbott and Francis obtained  $u_{*c}$ , based on actual measurements of overriding grains. Thus, instead of using Shields' criterion, the critical shear velocity was derived assuming a Shields parameter value of  $\theta_o = 0.02$ .

Bridge and Dominic (1984) made an extensive analysis of bed load grain transport velocity data in order to calibrate their proposed physically based model to estimate sediment transport rates. On theoretical grounds they showed that:

$$V_p = c(u_* - u_{*c}) \quad (2.22)$$

where:  $cu_{*c} = w\sqrt{\tan \alpha}$ ;  $w$  = the settling velocity of particles (m/s);  $\tan \alpha$  = dynamic friction coefficient;  $6 < c < 14.3$ ;  $u_*$  = shear velocity (m/s);  $u_{*c}$  = critical shear velocity (m/s); Application of this model to the existing data sets on single grain transport velocities yielded good results.

Wiberg and Smith (1987) developed an expression for the critical shear stress in non-cohesive sediment derived from the balance of forces on individual particles at the surface of a bed. The resulting equation, for a given grain size and density, depends on near bed drag force, the lift force to drag force ratio, and the particle angle of repose. Calculated values of the critical shear stress for uniformly sized sediment correspond closely to those determined from Shields' diagram. The initial motion problem for mixed grain sizes additionally depends on the relative protrusion of the grains into the flow and the particle angle of repose. The latter decreases when the diameter of a moving grain,  $d_s$ ,

is larger than the length scale of the bed roughness,  $k_s$  ( $d_s / k_s > 1$ ), and increases when  $d_s / k_s < 1$ , producing a corresponding decrease or increase in critical shear stress. Using the Miller and Byrne (1966) experimental relationship between  $d_s / k_s$ , and particle angle of repose, which is consistent with Shields' definition of initial motion, Wiberg and Smith obtain results that are in good agreement with the available experimental critical shear stress data for heterogeneous beds. Wiberg and Smith used a physically based model of bedload sediment transport and data sets from Francis (1973), Fernandez Luque and van Beek (1976) and Abbott and Francis (1977) to derive the semi-empirical equation:

$$\frac{V_p}{u_*} = 4.2 \frac{\left[ \frac{(\tau - \tau_c)}{\tau_c} \right]^{1/2}}{\left( \frac{\tau}{\tau_c} \right)} + 2.4 \quad (2.23)$$

where:  $\tau$  = mean bed shear stress ( $\text{kg/m}^2$ );  $\tau_c$  = shear stress at threshold of motion ( $\text{kg/m}^2$ );  $V_p$  = particle velocity (m/s); and  $u_*$  = shear velocity (m/s).

Jan (1992) addressed the relative contribution of the stresses developed in granular fluid flows (viscosity, collision and friction stresses). Jan determined how much each of the examined stresses contributed to the total stress acting on a rolling sphere. Experiments were conducted for the steady movement of a sphere rolling down smooth and rough inclines in air, water and salad oil. An equation was derived expressing the velocity of a sphere rolling down a roughened incline without acceleration or deceleration based on the principle of conservation of momentum. Jan's average terminal velocity  $V_p$  was derived as the following:

$$V_p = \sqrt{\frac{(\rho_s - \rho_f)gd_s(\sin\theta - n_\mu \cos\theta)}{f_c\rho_s + \frac{3}{4}C_D\rho_f}} \quad (2.24)$$

where:  $\rho_s, \rho_f$  = particle and fluid densities ( $\text{kg}\cdot\text{s}^2/\text{m}^4$ );  $C_D$  = drag coefficient;  $\theta$  = bed slope angle;  $d_s$  = particle diameter (mm);  $g$  = gravitational acceleration ( $\text{m}/\text{s}^2$ );  $f_c$  = collision coefficient (0.667); and  $n_\mu$  = bulk friction coefficient (0.13). Both  $f$  and  $n_\mu$  were determined via regression analysis using experiment data. Jan' experiments were performed for situations where the tested particle was identical to those comprising the roughness over which it rolled. Roughness particles were tightly spaced in a single layer on a smooth wooden bed of a tilting flume. Several conclusions were made as a result of the experiments and analysis. First, velocity is independent of rolling particle density. Second, collision stresses increase with increased bed inclination. Third, side wall friction from particles interacting with the side boundaries of the flume is negligible.

Meier (1995) completed the literature review on the existing formulas of transport velocity, in which he analyzed seventeen equations. Most of the equations can be written in the following form:

$$V_p = c_\alpha(u_* - u_{*c}) \quad (2.25)$$

where:  $V_p$  = particle velocity (m/s);  $u_*$  = shear velocity (m/s);  $u_{*c}$  = critical shear velocity (m/s); and  $c_\alpha$  = proportionality constant. The differences between various investigators is how they correlate  $c_\alpha$  and  $u_{*c}$  with the flow parameters. A shortcoming of this type of equation is that it does not apply for a steep bed slope.

Steidtmann (1982) conducted an experiment to assess the effects of size and density, with sand-size spheres of two densities being transported and deposited under controlled flume conditions. Observations on the motion of discrete particles show that grains smaller than bed roughness grains move continuously and have the same transport velocities regardless of density. For grains near and slightly larger than the roughness, movement is intermittent; and, for a given size, heavy particles move more slowly than light particles. For grains much larger than bed roughness grains, movement is continuous over the rough surface, and light and heavy grains have nearly the same transport velocities. Steidtmann's analysis of bulk sediment deposited from plane-bed transport, show that the size and proportion of heavy grains decrease and that of light grains increase with distance transported. For ripple bed transport, the size relations between associated light and heavy grains remains essentially unchanged with transport distance and the proportion of light and heavy grains is extremely variable. The results suggest that size-density sorting in plane-bed transport is a function of the transportability identified in the discrete grain studies but that sorting in ripple-bed transport is related to deposition on, and recycling through, the bed forms.

Bigillon (2001) conducted an experiment in a tilted, narrow, glass-sided channel, 2m in length and 20 cm in height. The channel inclination ranged from 0° to 12°. Two types of spherical particles were used in the experiments: glass beads and steel beads, the particle density was 2500 and 7750 kg/m<sup>3</sup> respectively. The water supply at the channel entrance was controlled by an electromagnetic flow meter provided by Krohne (France). The flow depth was a few particle diameters. Most of the time, channel slope was in excess of 1°, the water flow regime was supercritical, that is the Froude number exceeded

unity. The channel bed was made up of regularly juxtaposed half-cylinders of equal size. Bigillon selected three sizes of cylinder: their radius are 1.5 mm, 3 mm, and 4 mm. The motion of mobile beads was recorded using the Pulnix camera. A single particle was dropped from above into the water stream 1 m upstream from the measuring window. Bigillon filmed the motion of the particle with the Pulnix camera. For each flow condition  $(u_f, \theta)$ , the variability of the results was evaluated by repeating the run between three and five times, and only the average value was reported. The standard deviation was low relative to the mean (less than 5%) when the particle rolled. Bigillon noted that, these mean velocities cannot be rigorously assimilated to asymptotic velocities  $V_p$ , they provide a reasonable approximation of  $V_p$ . Fifty experimental data points were collected and the variability for hydraulic and particle parameters include: the range of shear velocity  $u_* = 0.018-0.038$  m/s,  $T_{\text{water}} = 20^\circ\text{C}$ ,  $\nu_{\text{water}} = 1.004 \times 10^{-6}$  m<sup>2</sup>/s, particle diameter  $d_s = 1.5$  mm and 3 mm,  $G = 2.5$  (glass bead) and 7.75 (steel bead),  $k_s = 1.5$  mm and 3 mm, bed slope  $S_f = 0.02$  and 0.05, mean flow velocity  $u_f = 0.223-0.492$  m/s, flow depth  $y = 2.13-28.65$  mm, and observed bedload particle velocity  $V_{\text{pobs}} = 0.076-0.496$  m/s.

## 2.2. DATA COMPILATION

A complete set of the experimental and data measurements is provided in Chapter 3. It includes the laboratory data of Meland and Norrman (1966), Fernandez Luque and van Beek (1976), Steidtmann (1982), Bridge and Dominic (1984), CSU (1995), and Bigillon (2001). A summary of this database is given in Table 2.1. It is comprised of 6 data sets containing a total of 1038 data points. These data are limited to the particle sizes

with median diameters in the range of 0.21 to 29.3 mm, bed roughness in the range of 0.19 to 7.76 mm, average flow velocity in the range of 0.22 to 1.00 m/s, shear velocity in the range of 0.0097 to 0.1108 m/s, flow depth in the range of 2.13 to 180 mm, and slope in the range of 0.00073 to 0.05. Details on the variability of hydraulic and bedload particle parameters are given in the appendices. Table 2.2 to 2.4 provides the summary of literature review, including existing equations, data sources and previous and recent studies.

Table 2.1: Variability of Hydraulic and Bedload Particle Parameters

Variables	Existing Experiments Data				Recent Experiments Data	
	Meland and Norrman (1966)	Fernandez Luque and van Beek (1976)	Steidtmann (1982)	Bridge and Dominic (1984)	CSU (1995)	Bigillon (2001)
(1)	(2)	(3)	(4)	(5)	(6)	(7)
Number	120	85	330	77	356	50
$S_f$	-	-	-	-	0.00073-0.011	0.02-0.05
T (°C)	20	22	18-22	20	17.25-21.5	20
$\nu \times 10^{-6}$ (m <sup>2</sup> /s)	1.004	1.26	0.98-1.095	1.004	0.968-1.08	1.004
y (mm)	-	-	180	-	50.3-71.15	2.13-28.65
$u_*$ (m/s)	0.0172-0.1108	0.0122-0.0641	0.0172-0.0277	0.0122-0.0641	0.0097-0.0641	0.018-0.038
$u_f$ (m/s)	0.25-1.0	-	0.29-0.44	-	0.25-0.89	0.22-0.49
$k_s$ (mm)	2.09-7.76	0.9-3.3	0.35	0.19-3.5	1.2-3.4	1.5-3
$d_s$ (mm)	2.09-7.76	0.9-3.3	0.21-1.25	0.19-3.5	2.4-29.3	1.5-3
$d_s/k_s$	1.0	1.0	0.6-3.57	1.0	2.02-24.4	1.0
Shape of Particles	Spherical	Angular	Spherical	Spherical Angular	Spherical Angular	spherical



Table 2.2: Summary of Literature Review

Sources	Equations	Notes
Krumbein (1942)	$\frac{V_p}{u_f} = 0.88(1 - \exp(-1.85u_f))$	where: $V_p$ = particle velocity; $u_f$ = mean flow velocity; $b$ = constant; $Fr$ = Froude number
Kalinske (1942)	$V_p = c_a(u_f - u_c)$	where: $c_a$ = constant; $u_f$ = mean flow velocity; $V_p$ = particle velocity; $u_c$ = critical velocity; Kalinske applied his model to Krumbein's data and found the best agreement for $0.9 < c_a < 1.0$
Ippen and Verma (1955)	$\frac{u_f}{V_p} = 1 + c_b \left( \frac{k_s}{d_s} \right) \left( \frac{1}{u_*} \right)$	Where: $c_b = \frac{1}{12}(G-1)\sqrt{gh}$ , $k_s$ = roughness size, $d_s$ = grain size, $u_*$ = shear velocity, $V_p$ = particle velocity and $u_f$ = mean flow velocity
Meland and Norrman (1966)	$\frac{V_p}{k_s^m} = 7.05u_* \frac{d_s^n}{k_s} - 5.1$	Where: $u_*$ = shear velocity, $V_p$ = particle velocity, $k_s$ = roughness size, $m = 0.75$ and $n = \left( \frac{0.014k_s}{u_*} \right)^{0.26}$
Ikeda (1971)	$\frac{V_p}{u_*} = \frac{u_f}{u_*} - \left[ \frac{4}{3} c_\mu \frac{(G-1)}{(c_\mu C_L + C_D)} \frac{gd_s}{u_*^2} \right]^{1/2}$	where, $V_p$ = particle velocity, $u_*$ = shear velocity, $u_f$ = fluid velocity

		at the center of the spherical grain, $c_\mu$ = sliding friction coefficient, $G$ = the particle specific gravity, $g$ = gravitational acceleration, and $C_D$ and $C_L$ = drag and lift coefficients
Parson (1972)	$V_p = c_c d_s (u_*^2 - u_c^2)$	where, $u_*$ = shear velocity, $u_c$ = critical velocity, $d_s$ = grain size and $c_c = \rho/4\mu$ .
Fernandez Luque and van Beek (1976)	$V_p = c(u_* - 0.7u_{*c})$	Where: $u_{*c}$ = critical shear velocity at Shield's condition for entrainment, $V_p$ = particle velocity and $u_*$ = shear velocity, and $c = 11.5$ ;
Romanovskiy (1977)	$V_p = c_e \left( u_f - u_c \sqrt{\frac{\tan \alpha}{m_\mu}} \right)$	Where: $\tan \alpha$ = dynamic friction coefficient, $m_\mu$ = static friction coefficient, $u_f$ = mean flow velocity, $c_e$ = constant and $u_c$ = critical velocity
Abbott and Francis (1977)	$V_p = c(u_* - u_{*c})$	Where: $u_*$ = shear velocity, $u_{*c}$ = critical shear velocity and $13.5 < c < 14.3$ , $c$ = constant parameter.
Bridge and Dominic (1984)	$V_p = c(u_* - u_{*c})$	$c_h u_{*c} = w \sqrt{\tan \alpha}$ , $w$ = the settling velocity of particles, $\tan \alpha$ = the dynamic coefficient

		friction, $6 < c < 14.3$ , $u_* =$ shear velocity and $u_{*c} =$ critical shear velocity
Wiberg (1987)	$\frac{V_p}{u_*} = 4.2 \frac{\left[ \frac{(\tau - \tau_c)}{\tau_c} \right]^{1/2}}{\left( \frac{\tau}{\tau_c} \right)} + 2.4$	Where: $\tau =$ mean bed shear stress, $\tau_c =$ shear stress at threshold of motion, $V_p =$ particle velocity and $u_* =$ shear velocity
Jan (1992)	$V_p = \sqrt{\frac{(\rho_s - \rho_f)gd_s(\sin\theta - n_\mu \cos\theta)}{f\rho_s + \frac{3}{4}C_D\rho_f}}$	Where: $\rho_s, \rho_f =$ particle and fluid density, $C_D =$ drag coefficient, $\theta =$ bed slope angle, $d_s =$ particle diameter, $g =$ gravitational acceleration, $f =$ collision coefficient, and $n_\mu =$ bulk friction coefficient
Meier (1995)	$V_p = c_\alpha (u_* - u_{*c})$	Where: $V_p =$ particle velocity, $u_* =$ shear velocity, $u_{*c} =$ critical shear velocity, and $c_\alpha =$ proportionality constant

Table 2.3: Existing Database

Sources	Number of Data Points	Bed-load Particle Size	Notes
Meland and Norrman (1966)	120	$d_s=2.09, 3.15, 3.93, 5.1, 5.95, 7.0$ and $7.76\text{mm}$ ; $k_s=2.09$ and $7.76\text{mm}$	Glass spheres $G=2.65$
Fernandez Luque and van Beek (1976)	85	$d_{\text{walnut}}=1.5\text{mm}$ $0.9\text{mm}<d_{\text{sand}}<1.8\text{mm}$ $d_{\text{gravel}}=3.3\text{mm}$ $d_{\text{magnetite}}=1.8\text{mm}$	Walnut, sand (I), sand (II), gravel and magnetite; $G=2.64$ and $4.58$ Shape, density,...
Steidtmann (1982)	330	$0.21\text{mm}<d_{\text{sand}}<1.25\text{mm}$ $k_s=0.35\text{mm}$ (Glass sphere)	Sand-size spheres ( $d_s$ ) Glass spheres ( $k_s$ ) 154 with $G_s=4.5$ 176 with $G_s=2.5$
Bridge and Dominic (1984)	77		Glass spheres $G=2.56$
Wiberg (1987)	115	$d_s = 0.35, 0.5, 0.8, 1.5, 2.0, 2.5, 5, 10, 28.6\text{mm}$	Shape, density,...
Rakoczi (1991)	100	$d_{s1}=5-10\text{mm}, d_{s2}=10-15\text{mm}, d_{s3}=15-20\text{mm};$ $d_{s4}=20-25\text{mm}$ and $d_{s5}=25-36\text{mm}$	Gravel $G=2.65$
Jan (1992)	158	$13.5\text{mm}<d_{\text{glass}}<24.1\text{mm}$ $d_{\text{steel}} = 13.5\text{mm}$ $d_{\text{golf}} = 42.5\text{mm}$ $13.5\text{mm}<k_s<42.5\text{mm}$	Golf, steel balls; water, air and salad oil
CSU (1995)	356	$1.57\text{mm}<d_{\text{steel}}<19.04\text{mm}$ $d_{\text{tin}}=4.375\text{mm}$	Glass, natural and steel spherical and angular

		$14.48\text{mm} < d_{\text{glass}} < 29.3\text{mm}$ $1.2\text{mm} < d_{\text{natural}} < 13.6\text{mm}$ $k_s = 1.2, 1.7, 2.4 \text{ and } 3.4\text{mm}$	shapes
Bigillon (2001)	50	$1.5\text{mm} < d_{\text{steel}} < 3\text{mm}$ $1.5\text{mm} < d_{\text{glass}} < 3\text{mm}$ $k_s = 1.5 \text{ and } 3\text{mm}$	Glass and steel spherical shape

Table 2.4: Summary of Previous and Recent Studies

Author	Equation	Data	Particle Size	Particle Shape	Particle Density	Smooth Bed	Rough Bed	Still Fluid	Flowing Fluid
Meland and Norrman (1966)	Yes	Yes	Yes	Spherical			Yes		Yes
Fernandez Luque and van Beek (1976)	Yes	Yes	Yes	Angular	Yes		Yes		Yes
Steidtman (1982)		Yes	Yes	Spherical	Yes	Yes	Yes		Yes
Bridge and Dominic (1984)	Yes	Yes	Yes	Spherical, Angular			Yes		Yes
Wiberg (1987)	Yes	Yes	Yes	Spherical, Angular	Yes		Yes		Yes
Jan (1992)	Yes	Yes	Yes	Spherical	Yes	Yes	Yes	Yes	
CSU (1995)	Yes	Yes	Yes	Spherical, Angular	Yes	Yes	Yes	Yes	Yes
Bigillon (2001)	Yes	Yes	Yes	Spherical	Yes		Yes		Yes

### **2.3. APPLICATION OF EXISTING METHODS**

Figs. 2.1 to 2.6 show the application of the equations of Meland and Norrman (1966), Fernandez Luque and van Beek (1976), and Bridge and Dominic (1984) to their own database. The results show that the equations of Meland and Norrman, Fernandez Luque and van Beek, and Bridge and Dominic predict very well with their own data.

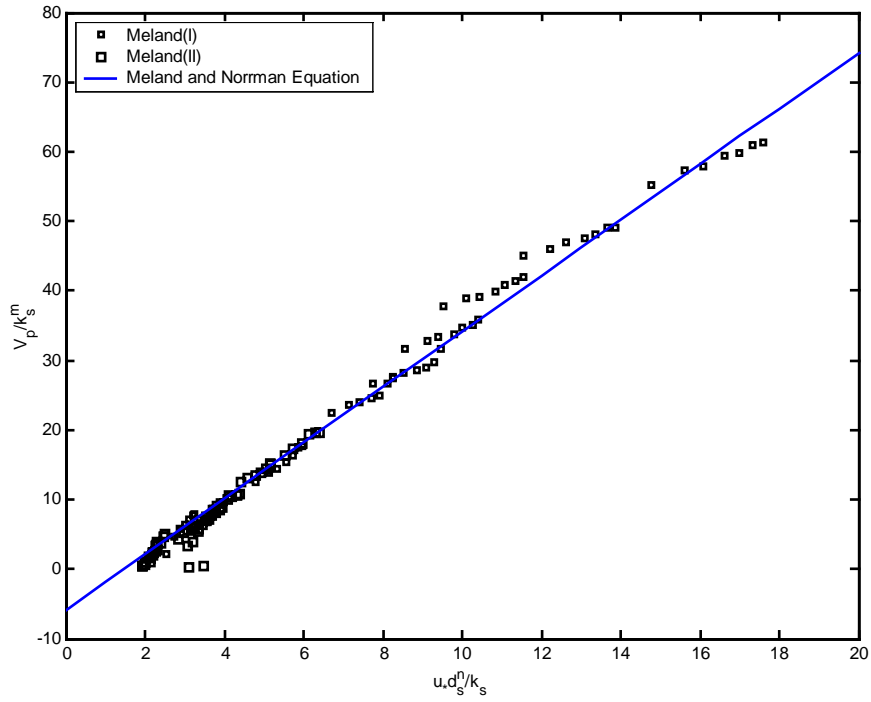


Figure 2.1:  $V_p/k_s^m$  vs.  $u \cdot d_s^n/k_s$

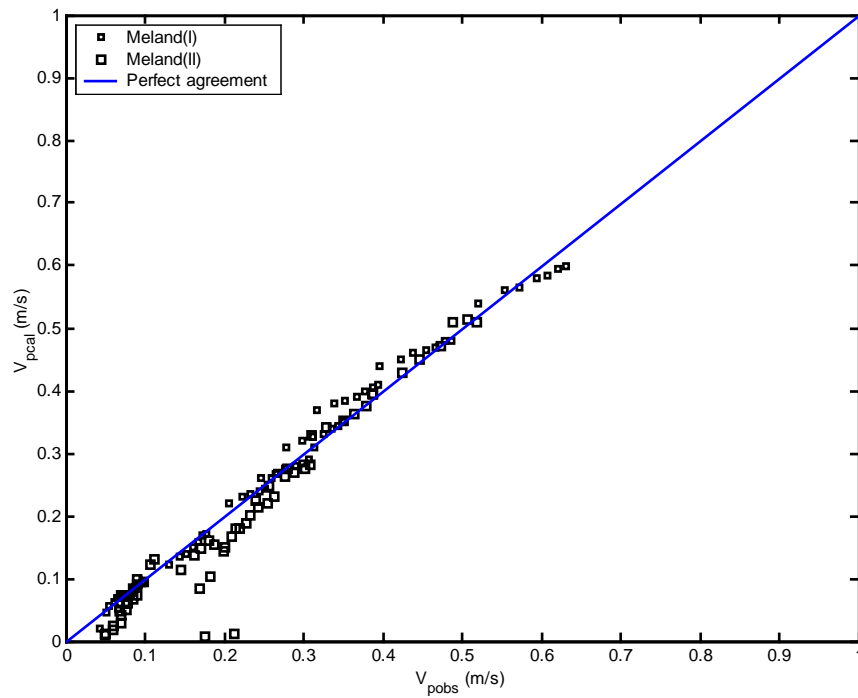


Figure 2.2: Comparison between Calculated and Observed  $V_p$  using Eq. (2.9)



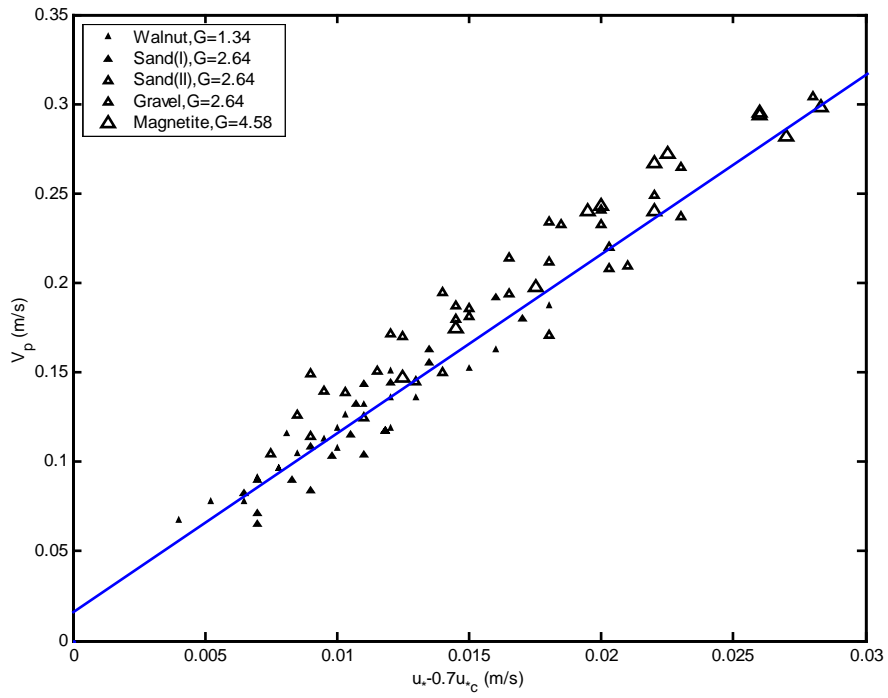


Figure 2.3:  $V_p$  vs.  $(u_* - 0.7u_{*c})$

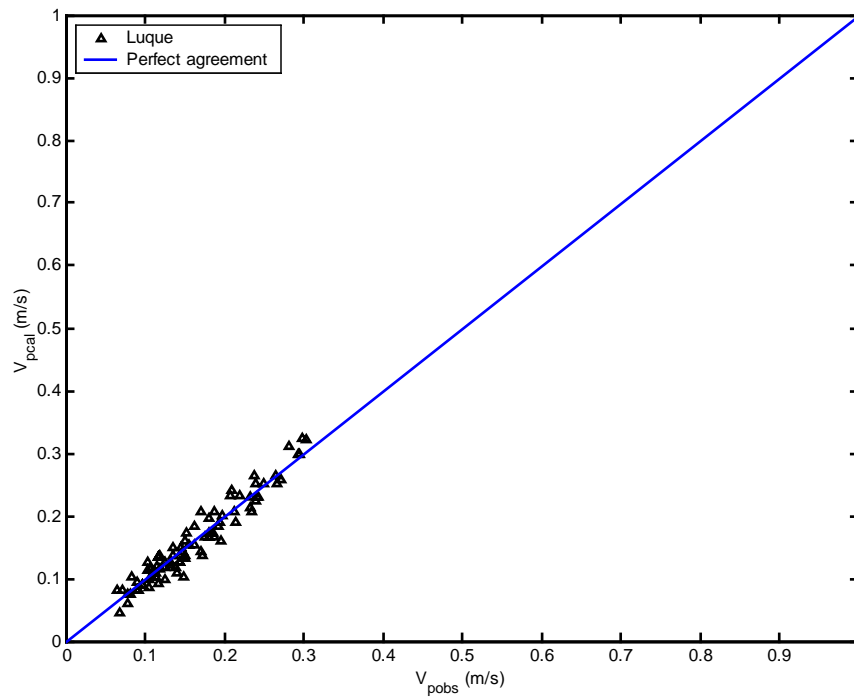
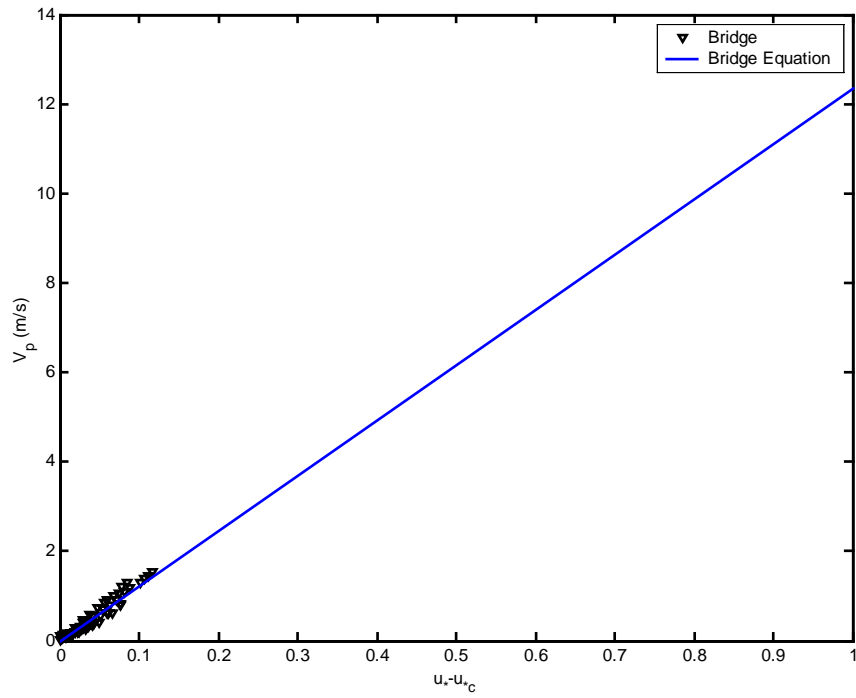
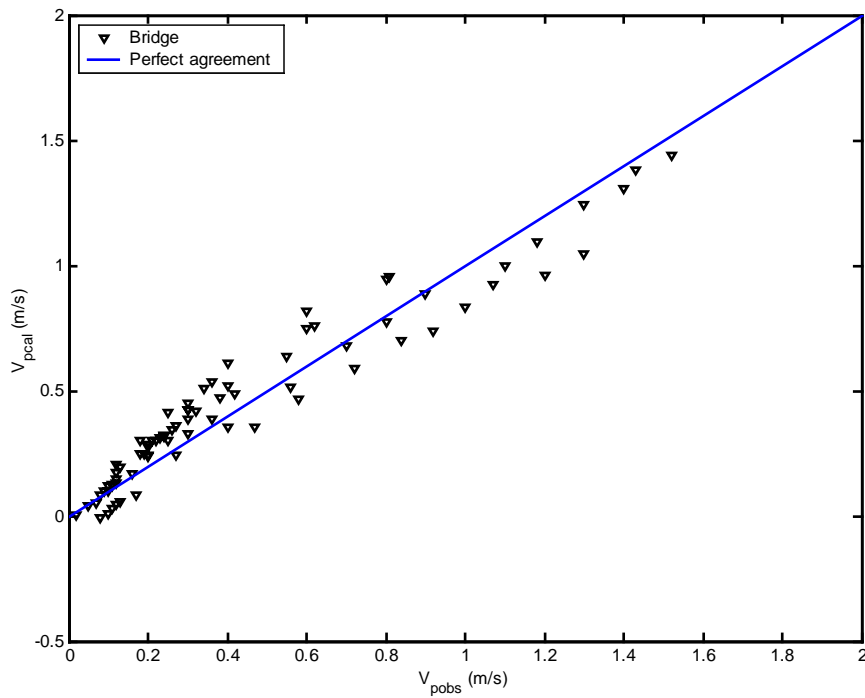


Figure 2.4: Comparison between Calculated and Observed  $V_p$  using Eq. (2.15)



**Figure 2.5:  $V_p$  vs.  $(u_* - u_{*c})$**



**Figure 2.6: Comparison between Calculated and Observed  $V_p$  using Eq. (2.22)**

## **2.4. SUMMARY**

The existing methods, i.e., Meland and Norrman, Fernandez Luque and van Beek, and Bridge and Dominic compare well with their own data. There is a shortage of laboratory data on particle specific gravity  $G$  (density), particle shape, bed roughness  $k_s$ , particle size  $d_s$ , etc., therefore more extensive physical experiments are needed to cover a greater range of variability for hydraulic and particle parameters.

# **CHAPTER 3**

## **DATA COMPILATION**

Julien, Meier, and Blackard (1995) conducted experiments at the Engineering Research Center (ERC) of Colorado State University on transport velocities of bedload particles in smooth and rough open channel flows. This chapter represents the descriptions of the flume, plates, particles, set up, experiments, and methodology used in the experiments.

### **3.1. THE FLUME**

A 9.77m long plexiglass tilting flume shown in Fig. 3.1, with trapezoidal cross-section was used for the experiment. The bed slope has a range of approximately 0% to 4%, although 1% was the largest slope used (run 18, 20, 28 and 37). The side walls of the flume are adjustable, allowing for the channel cross-section to be varied. In these experiments the side walls were kept fixed at a 3 H to 1 V ratio, in order to minimize

their influence on the flow. A 2 m long test reach near the downstream end of the flume was used to measure particle velocities.

The location of the test reach was chosen by visual inspection as that portion of the flume with most uniform flow conditions. An adjustable weir located at the downstream end of the flume was used in some of the runs to control the test reach water levels. Many runs with higher flow rates were performed with the weir removed as long as the flow was steady and uniform in the test section. The system re-circulated water collected at the downstream end of the flume in a stilling tank with a pump driven by an electric motor.

The motor has three speed settings (slow, medium, and fast) and the return pipe has a valve for fine adjustment of the flow rate. Three point gages were used to measure flow depths. Two gages were located at the beginning and end of the test section, the third was used to record flow depth over the weir. Flow rates were measured using an orifice plate located in the water return pipe. Pressure taps on each side of the construction were connected to two manometers in parallel, with water and mercury as manometric fluids. The mercury manometer was needed for the higher flow rates.



**Figure 3.1: Three Point Gages used to Measure Water Depth.**

### **3.2. THE PLATES**

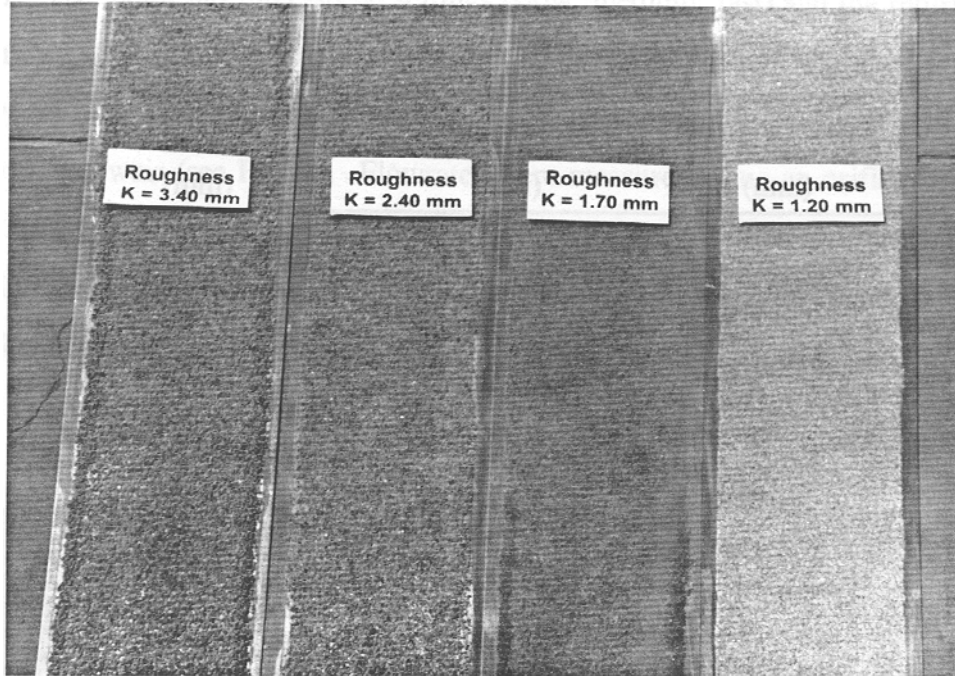
Sand or gravel was glued to aluminum plates to achieve various bed roughnesses. Four sets of plates with rounded sand and gravel were used, one set with angular gravel and one smooth aluminum plate (bed roughness  $k_s=0$ ). Grain sizes used as bed roughness are shown in Table 3.1. Two 12-ft long plates were used for each bed roughness condition. The upstream plate used the same roughness as the downstream plate in order to establish the velocity profile of the stream. The test reach was located over the downstream plate.

Table 3.1: Gravel Gradations for Roughened Plane Surfaces

Sieve Retained (mm)	Sieve Passed (mm)	Bed Roughness (mm)
No gravel	No gravel	0
1.0	1.4	1.2
1.4	2.0	1.7
2.0	2.8	2.4
2.0	2.8	2.4(angular)
2.8	4.0	3.4

Various adhesives were used to bond the sand and gravel to the plates. The first set of plates was produced using a spray lacquer made by Krylon to glue 2.4 mm (angular) gravel particles. This attempt failed as the gravel did not stick to the plates well. A vanish substitute called “EnviroTex Lite pour-on” made by Environmental Technology, Inc. was then used; the particles of gravel adhered much better. A contact cement from DAP was also used. It performed as well as the EnviroTex and the contact cement avoided the difficulty in producing a uniform layer of gravel without having “clumps” on the plates. For the 1.2 mm sand, a waterproof paint was used (Tile Clad II from Sherwin Williams). This held the sand in place very well, although clumping was difficult to prevent with this paint as well.

In the early runs, particles had a tendency to roll off the sides of the plates. To solve this problem extra sand/gravel was glued to the sides, creating small ridges that acted as “guard rails” to keep the particles on the plate. The roughened plates are shown in Fig. 3.2, 3.3, 3.4, 3.5 and 3.6



**Figure 3.2: Form Roughened Plates**

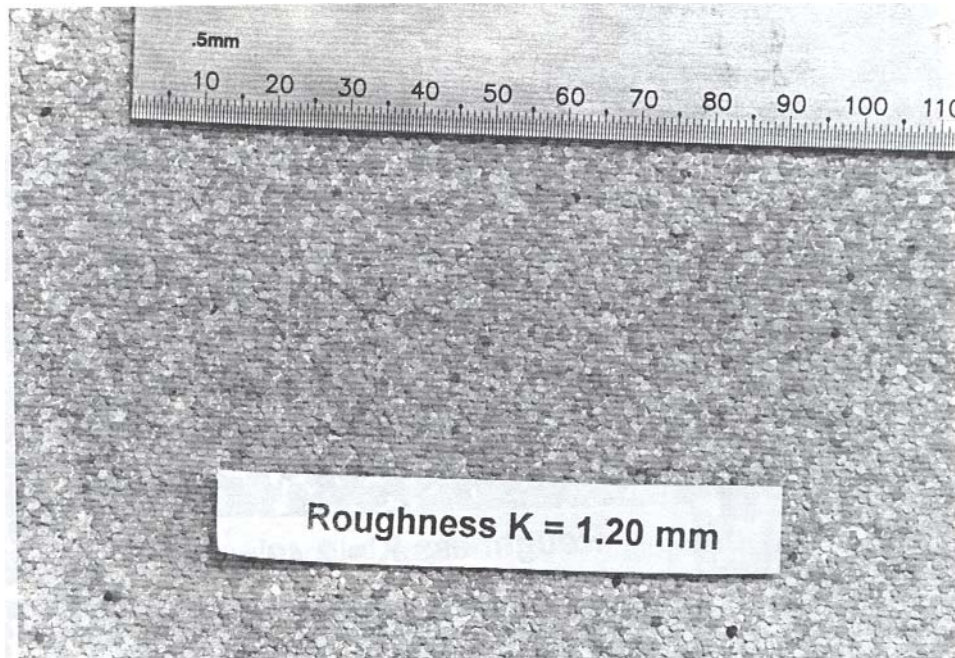


**Figure 3.3: Plate at Roughness  $k_s = 1.2$  mm**



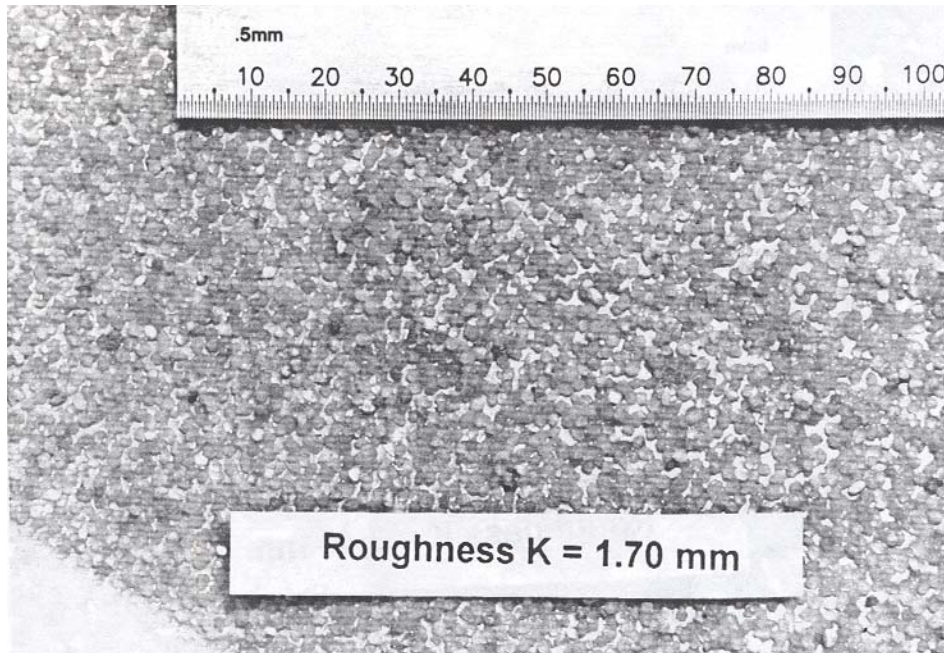


**Figure 3.4: Plate at Roughness  $k_s = 1.7$  mm**

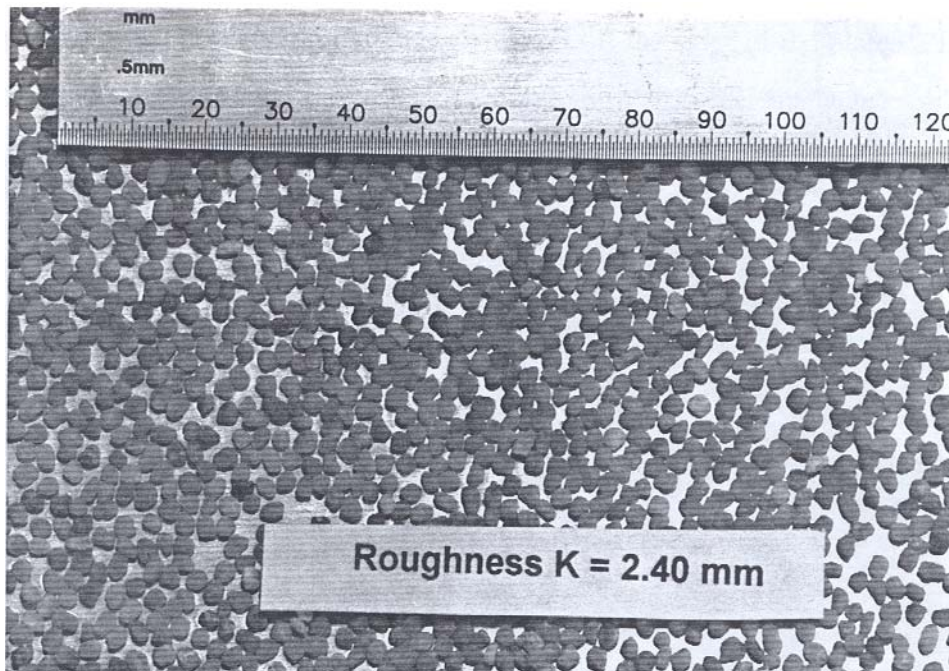


**Figure 3.5: Plate at Roughness  $k_s = 2.4$  mm**

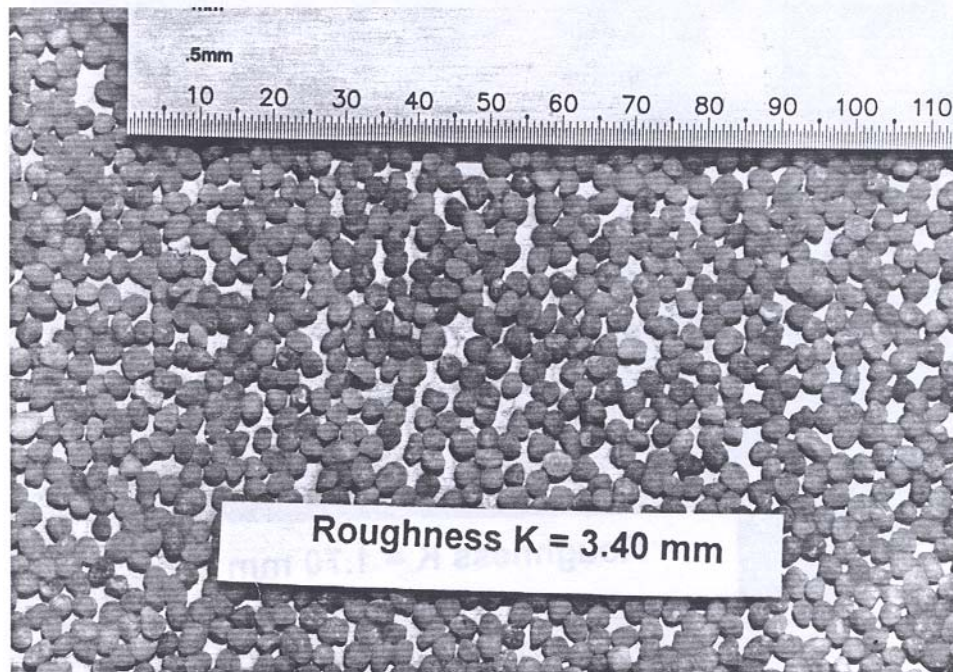


**Figure 3.6: Plate at Roughness  $k_s = 3.4$**

### **3.3. THE PARTICLES**

Three types of particles were run in the experiment: stainless steel ball bearings, glass marbles and natural quartz particles. The steel ball bearing and glass marbles were used because of their precise spherical shape. Using steel and glass also gave results for particles of two different densities. The quartz particles were used to emulate conditions closer to natural conditions for slope and density, and also to examine the effects of particle angularity.

As can be seen from Fig. 3.7 and Table 3.2, a large number of particle types and diameters were tested. Not all of them moved in every run. For the lower transport rates, most steel particles didn't move at all, or did so only for short distances before halting, because of their high density. The natural particles also rolled very little at low transport

stages, tending to sit on their flatter sides. For the higher transport stages the smaller steel and natural particles simply disappeared when dropped in the water, presumably whisked away in suspension. The glass marbles were the most consistent across all transport stages. Almost every run used all five marbles. Many different particles were used for each size. The particles were sieved and categorized accordingly. For example, the 3.4 mm diameter “particle” was in fact a set of particles, all passing through the 4.00 mm sieve and retained in the 2.8 mm sieve.



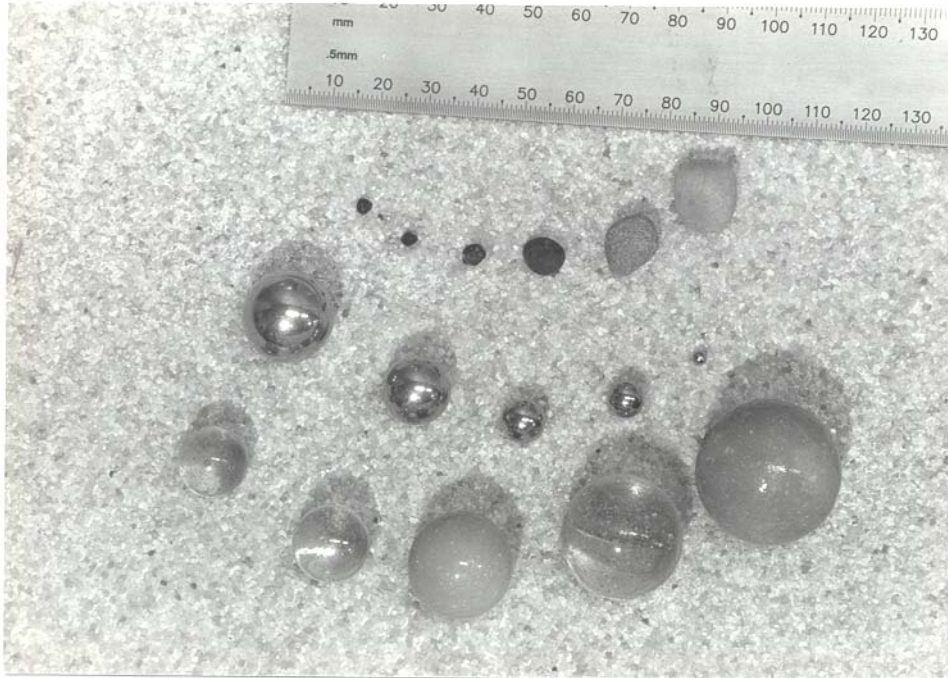


**Figure 3.7: Particles used in the Experiment**

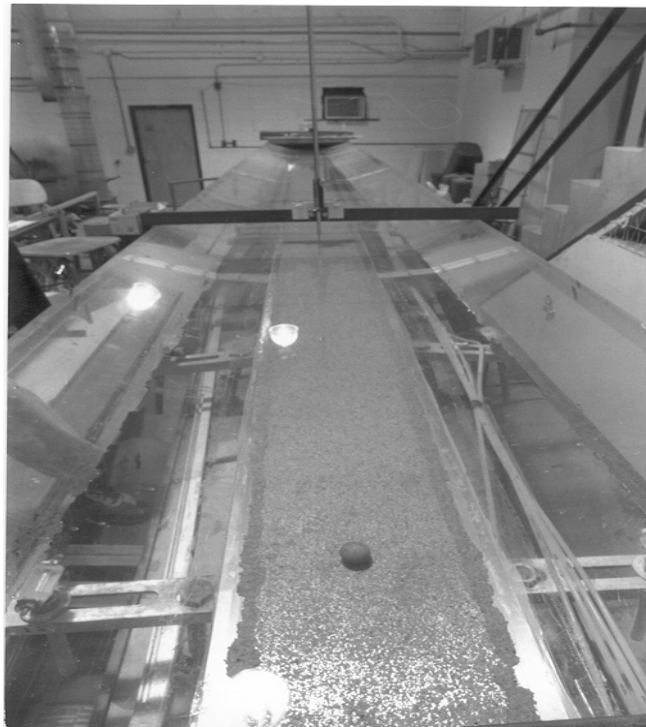


**Figure 3.8: The Experiment**

Table 3.2: Particle Size used in the Experiments

Type	G	Diameter (mm)	Sieve Retained (mm)	Sieve Passed (mm)
Steel	8.02	19.04		
		15.88		
		14.28		
		9.50		
		7.90		
		6.34		
		4.75		
		3.14		
Glass	2.60	29.30		
		25.17		
		21.70		
		15.97		
		14.48		
Natural	2.65	13.60	11.2	16.0
		9.60	8.0	11.2
		6.80	5.6	8.0
		4.80	4.0	5.6
		3.40	2.8	4.0
		2.40	2.0	2.8
		1.70	1.4	2.0
		1.20	1.0	1.4

### 3.4. EXPERIMENTAL SET UP

Establishing the desired hydraulic conditions for each run involved setting the bed slope, pump, valve and (optionally) adjusting the weir in order to reach a predetermined value of shear velocity  $u_*$ . In general, a bed slope and pump setting were selected, then the valve and weir adjusted until the two point gages in the test section indicated approximately the same flow depth. If the flow depth was too shallow ( $<50$  mm), or if the value of  $u_*$  undesirable, bed slope and/or pump setting were changed and the process started over. Adjustments were made until the difference in flow depths between point gages was smaller than 15% of the drop in bed elevation between the point gages (due to the bed slope).

After the hydraulic conditions were set (and recorded) for a given run, the particles were released upstream and their times measured over the 2 m test section. Notes were taken on any non-uniform particle motion, such as surging of particles, suspension or halting. If a particle ran off the plate, that measurement was discarded and repeated. Each particle was run at least 15 times. Hydraulic conditions were measured and recorded at the middle and end of each run, allowing an average over three readings for flow depths, top flow widths, and manometer readings. A total of 49 runs have been completed on plates with six different roughness. For each roughness, a range of values of shear velocity  $u_* = (\tau_o/\rho)^{1/2}$  were used in the range where the particles are expected to be in motion and in contact with the bed. A summary of the runs is presented in Tables 3.3 and Table 3.4. One set of plates had no roughness and the experiments for the 2.4 mm gravel were repeated using rounded versus angular material to identify possible differences owing to the angularity of the surface material. Fig. 3.9 Shows a linear relationship

between settling velocity  $w$ , and  $[(G-1)gd_s]^{1/2}$ , the plot indicated that  $w \cong 0.9423 [(G-1)gd_s]^{1/2}$  with  $R^2 = 1.0$ .

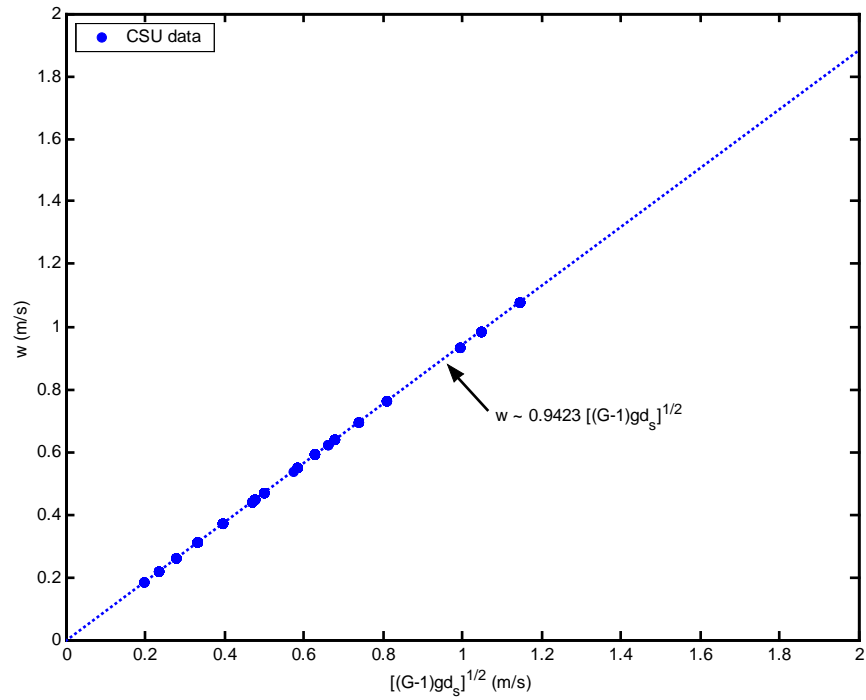


**Figure 3.9:**  $w$  vs.  $[(G-1)gd_s]^{1/2}$

Table 3.3: Classification of Experimental Runs

Run Number	$u_*$ (m/s)	Roughness (mm)	Run Number	$u_*$ (m/s)	Roughness (mm)
1	0.0111	0	26	0.0501	3.4 (rounded)
2	0.0176	0	27	0.055	3.4 (rounded)
3	0.016	0	28	0.0625	1.7 (rounded)
4	0.0119	0	29	0.0593	1.7 (rounded)
5	0.0141	0	30	0.0516	1.7 (rounded)
6	0.0152	0	31	0.048	1.7 (rounded)
7	0.0194	0	32	0.0419	1.7 (rounded)
8	0.0249	0	33	0.0359	1.7 (rounded)
9	0.0299	0	34	0.0242	1.7 (rounded)
10	0.0176	0	35	0.0285	1.7 (rounded)
11	0.0356	0	36	0.0186	1.7 (rounded)
12	0.0097	0	37	0.0616	2.4 (rounded)
13	0.0301	2.4 (angular)	38	0.0558	2.4 (rounded)
14	0.0386	2.4 (angular)	39	0.0514	2.4 (rounded)
15	0.025	2.4 (angular)	40	0.0467	2.4 (rounded)
16	0.0339	2.4 (angular)	41	0.0378	2.4 (rounded)
17	0.0506	2.4 (angular)	42	0.0317	2.4 (rounded)
18	0.0641	2.4	43	0.019	2.4 (rounded)
19	0.0424	0	44	0.0248	2.4 (rounded)
20	0.0623	3.4 (rounded)	45	0.019	1.2 (rounded)
21	0.024	3.4 (rounded)	46	0.027	1.2 (rounded)
22	0.0231	3.4 (rounded)	47	0.036	1.2 (rounded)
23	0.0298	3.4 (rounded)	48	0.044	1.2 (rounded)
24	0.0362	3.4 (rounded)	49	0.051	1.2 (rounded)
25	0.0438	3.4 (rounded)			



The voluminous data set in Appendix A provides a substantial compilation of particle velocity information for each size fraction for plane surfaces of different roughnesses and particles of different size, density and angularity.

### **3.5. PRELIMINARY RESULTS**

The data set shows the following overall characteristics: (1) under given hydraulic and surface roughness conditions, coarse particles generally roll faster than fine particles; (2) exceptions to (1) were observed, either when smaller particles were partly in saltation, or when the standard deviation of repeated particle velocity measurements were large compared to the mean velocity; (3) the most convincing results are found on runs 3 and 5 for a smooth plate, and runs 34, 36, and 44 for rough plates; (4) at a given roughness size, particles roll slightly faster on a plane boundary of rounded particles as opposed to angular particles; and (5) as shear velocity  $u_*$  increases, the smaller particles enter saltation and tend to move faster than coarse particles.

A plot of particle velocity against particle diameter for a smooth bed ( $k_s = 0$ ) is shown in Fig. 3.10. where larger particles move faster than smaller ones for all values of shear velocity. Larger particles protrude higher into the flow, in regions with higher flow velocities. There are no clear differences in transport velocities for particles of different densities; Fig. 3.11 shows that lighter particles move faster than heavier particles, and particle velocity tends to decrease with the increase of the particle size; for natural particles, the variability of particle velocity with respect to particle size is high, this may

be the effect of particle shape; and for glass particles, larger particles move faster than smaller ones.

Fig 3.12 shows the ratio of particle velocity  $V_p$  to shear velocity  $u_*$  lies in the range of 2.5 to 12.5; Fig. 3.13 shows, for glass and natural particles (lighter),  $V_p \cong 9.14u_*$ , and for steel particles (heavier),  $V_p \cong 3.94u_*$ ; Fig. 3.14 shows the variation of particle velocity,  $V_p$  against Shields parameter,  $\tau_{*ds}$ . Fig. 3.15 shows the ratio of particle velocity  $V_p$  to mean flow velocity  $u_f$  lies in the range of 0.2 to 0.9; Fig. 3.16 shows that spherical particles move faster than angular particles at the same  $u_* / [(G-1)gd_s]^{1/2}$ .

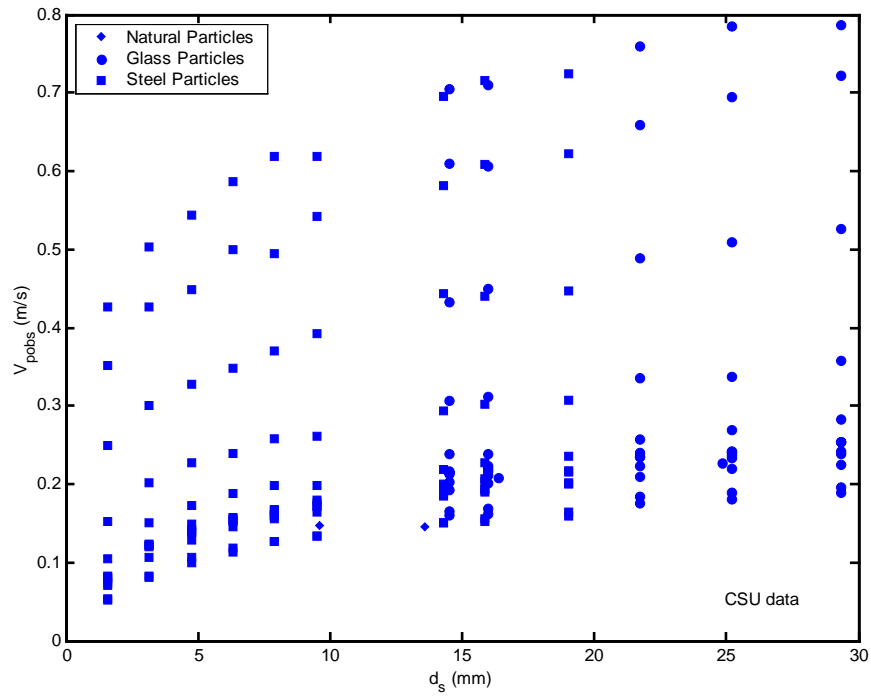


**Figure 3.10:  $V_{\text{pobs}}$  vs  $d_s$  for  $k_s = 0$**

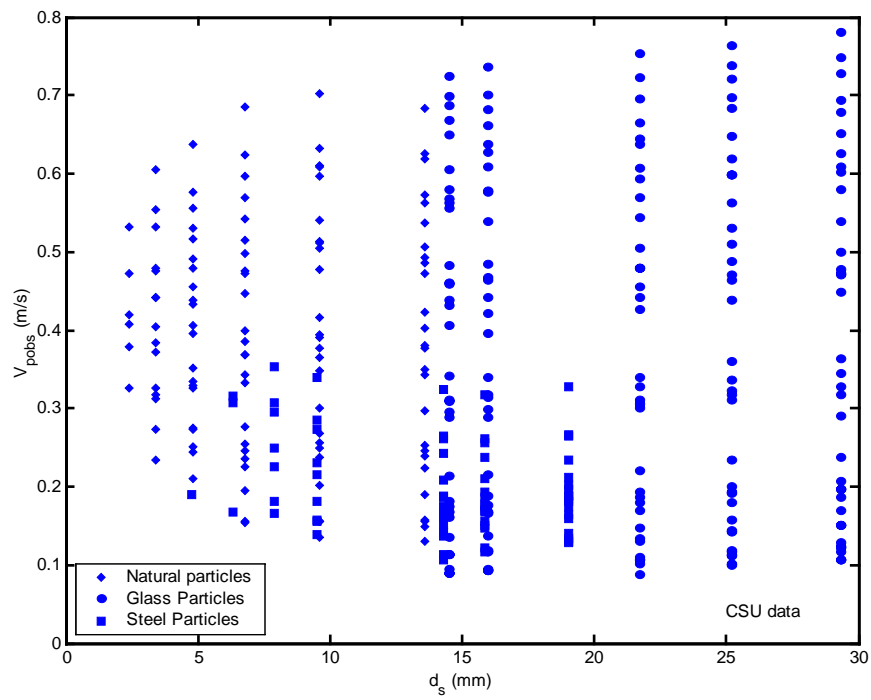


**Figure 3.11:  $V_{\text{pobs}}$  vs  $d_s$  for  $k_s > 0$**

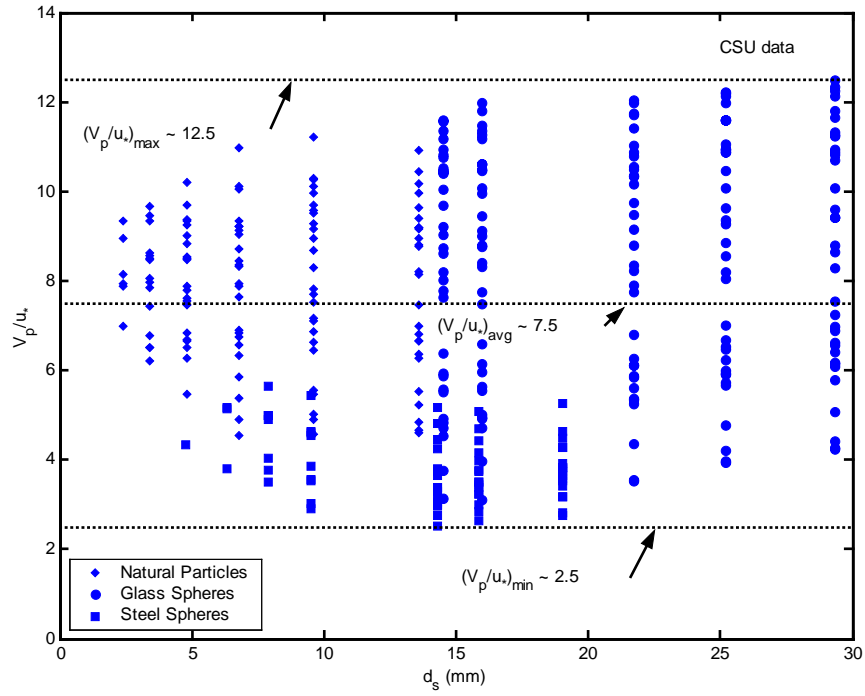


Figure 3.12:  $V_p/u_{*}$  vs  $d_s$

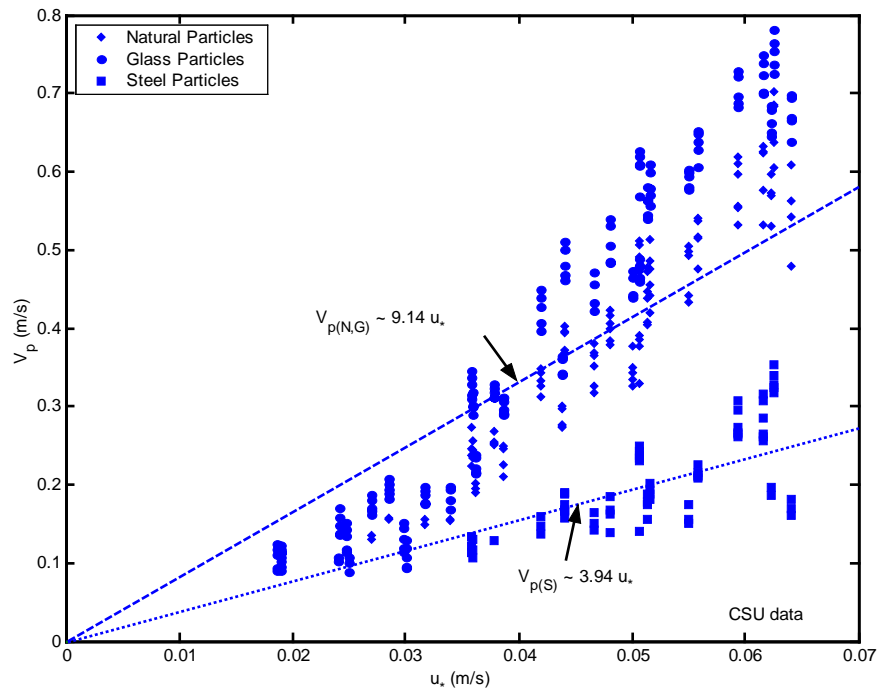


Figure 3.13:  $V_p$  vs  $u_{*}$ , a)  $V_{p(N,G)} \sim 9.14u_{*}$ , and b)  $V_{p(S)} \sim 3.94u_{*}$

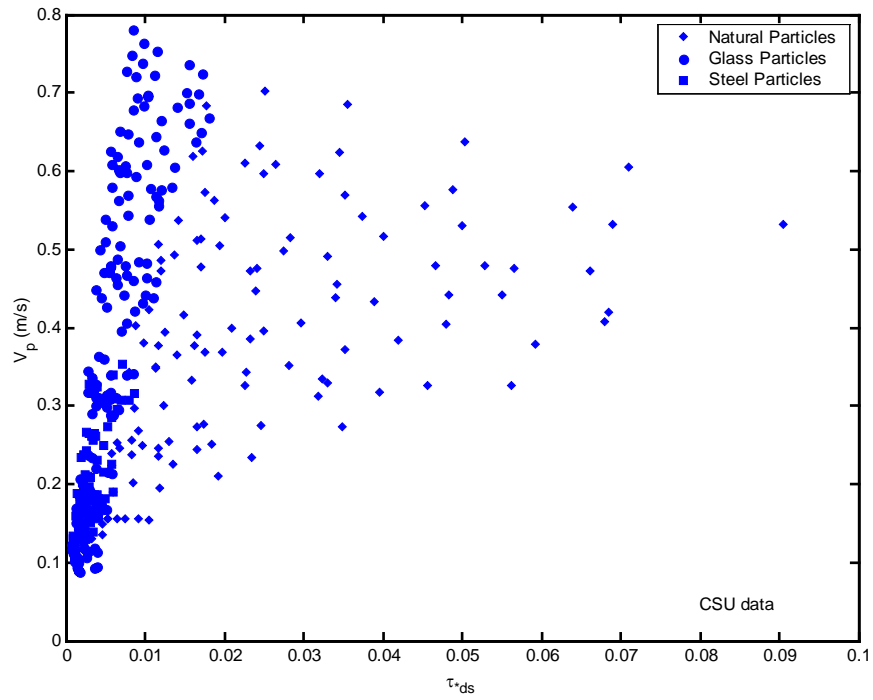


Figure 3.14:  $V_p$  vs  $\tau^*d_s$

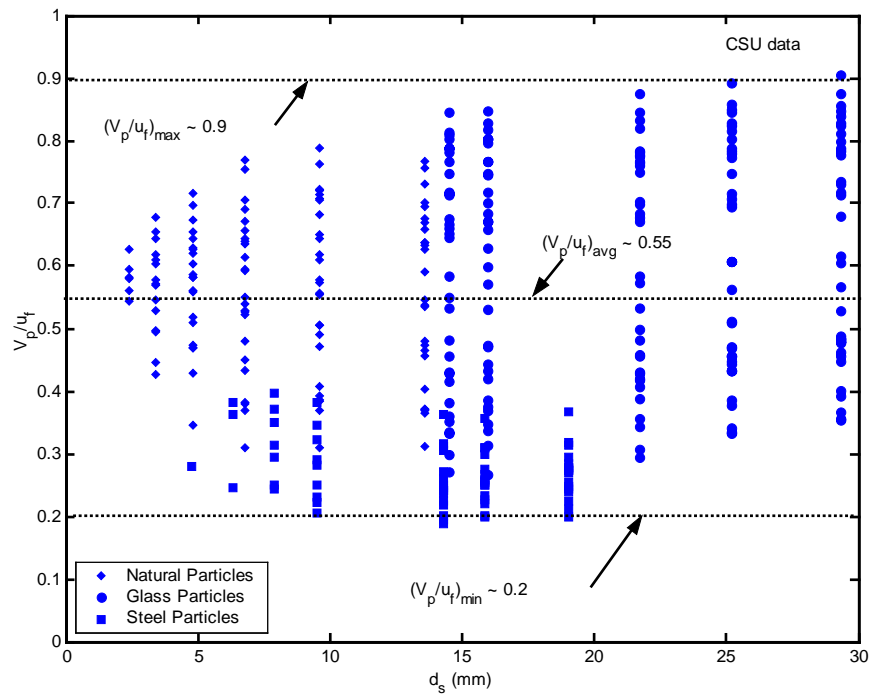
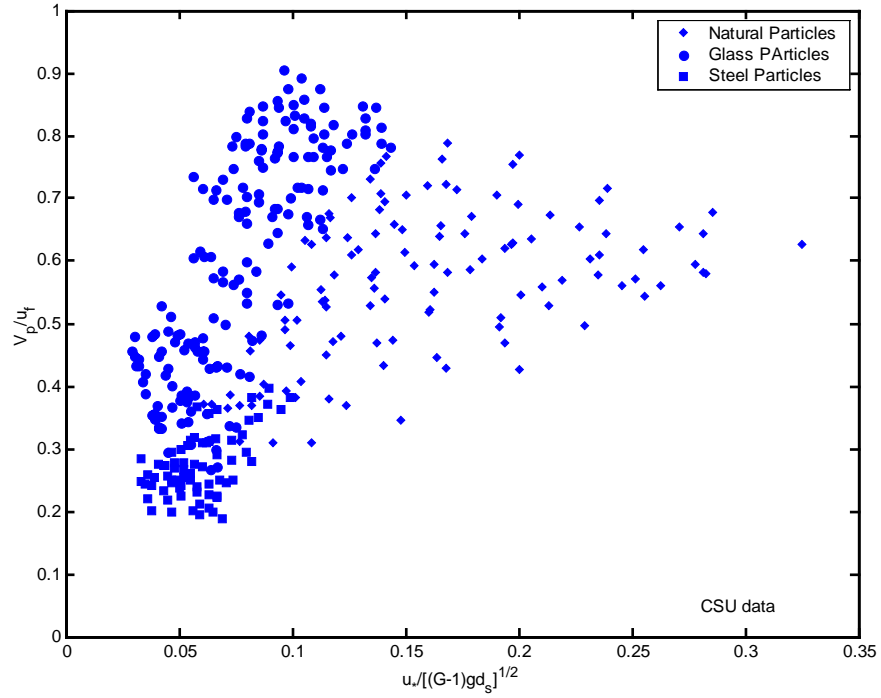


Figure 3.15:  $V_p/u_f$  vs  $d_s$



**Figure 3.16:  $V_p/u_f$  vs  $u^*/[(G-1)gd_s]^{1/2}$**

From Fig. 3.13, we generated linear equations of the following form, for each bed roughness and particle type:

$$V_p = C_1 + C_2 u_* \quad (3.1)$$

where:  $C_1$  and  $C_2$  are constants, these equations were then reduced to the form of Eq. (2.19) by introducing the absolute value of  $C_1/C_2$  as a new positive constant:

$$V_p = C_2 (u_* - |C_1 / C_2|) \quad (3.2)$$

where:  $c = C_2$  and  $|C_1/C_2| = u_{*c}$ . The computed values of  $c$  and  $u_{*c}$  for different bed roughness and particle types is shown in Table 3.4.

Table 3.4. Computed Values of  $c$  and  $u_{*c}$  for different  $k_s$  and Particle type

Particle Type	$k_s$ (mm)	$c$	$u_{*c}$ (m/s)	$R^2$
Natural ( $G = 2.6$ )	0	NA	NA	NA
	1.2	15.51	0.0192	0.98
	1.7	14.83	0.0197	0.97
	2.4	14.03	0.0212	0.93
	3.4	14.83	0.0244	0.95
Glass ( $G = 2.65$ )	0	18.61	0.0033	0.94
	1.2	16.29	0.0145	0.98
	1.7	15.39	0.0143	0.99
	2.4	15.87	0.0187	0.95
	3.4	16.33	0.0214	0.98
Steel ( $G = 8.02$ )	0	15.08	0.0044	0.85
	1.2	7.93	0.0213	0.93
	1.7	8.21	0.0251	0.89
	2.4	5.08	0.0152	0.42
	3.4	4	0.0147	0.77

### 3.6. STATISTICAL ANALYSIS

In the statistical analysis, the discrepancy method is adopted to indicate the goodness of fit between the calculated and observed results. The discrepancy ratio,  $R_i$

$$R_i = \frac{V_{pcal(i)}}{V_{pobs(i)}} \quad (3.1)$$

in which  $V_{p\text{cal}(i)}$ ,  $V_{p\text{obs}(i)}$  = calculated and observed bedload particle velocity corresponding to data point number in a data set. For a perfect fit,  $R_i = 1.0$ .

### 3.7. PARAMETRIC ANALYSIS OF CSU DATA

Fig. 3.17, 3.19, and 3.20 show that  $\tau_{*d_s}/0.047 \approx 0.01$  ( $\tau_{*d_s} \approx 0.00047$ ), when  $k_s < d_s$ , bedload particles move at values of shear stress below the threshold value given by the Shields diagram, and  $\tau_{*d_s} = 0.047$  when  $d_s = k_s$ . Fig. 3.18 shows the values of  $\tau_{*k_s}$  is in the range of 0.01 to 0.15; Fig. 3.20 shows values of  $Re_* > 100$ ; Fig. 3.21 shows  $V_p/[(G-1)gd_s]^{1/2} < 2$ , then combined with Fig. 3.9, resulted in  $V_p/w < 2$ , and therefore  $V_p < 2w$ ; and Figs. 3.22 and 3.23 show the values of  $V_p/u_*$  is in the range of 2.5 to 12.5, and the threshold value for  $\tau_{*k_s}$  is 0.01; Figs. 3.24 and 3.25 show the values of  $u_*/w < 0.5$ , which is in agreement with the criterion for bedload sediment transport in Julien (1995, p.187, Figure 10.4).



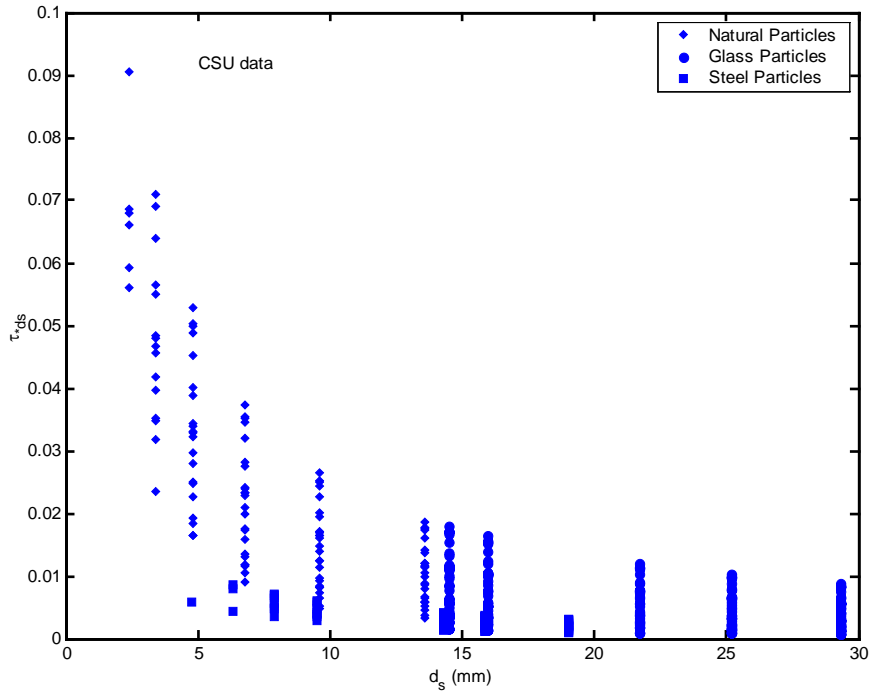


Figure 3.17:  $\tau_{*ds}$  vs  $d_s$

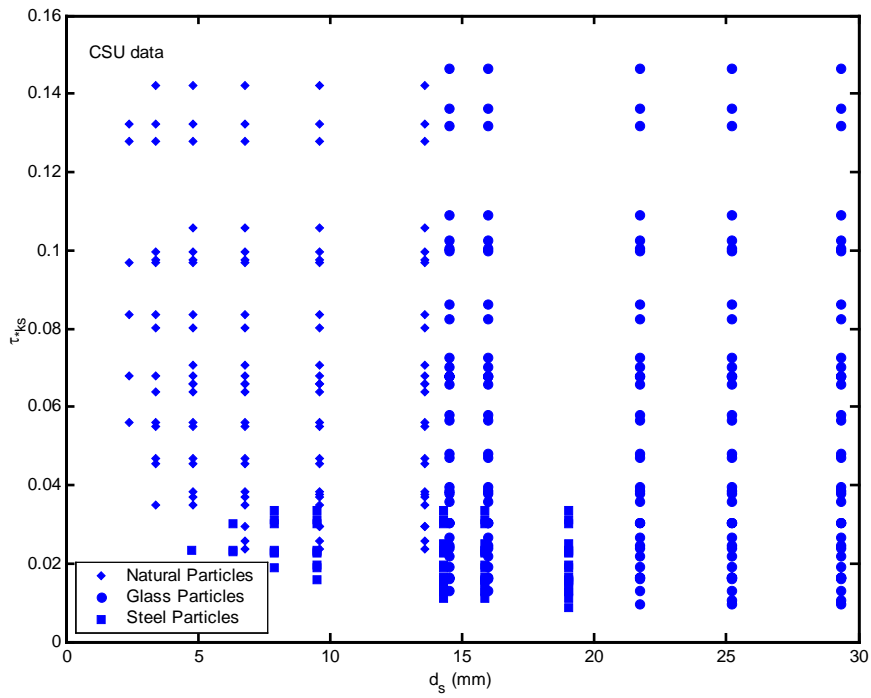
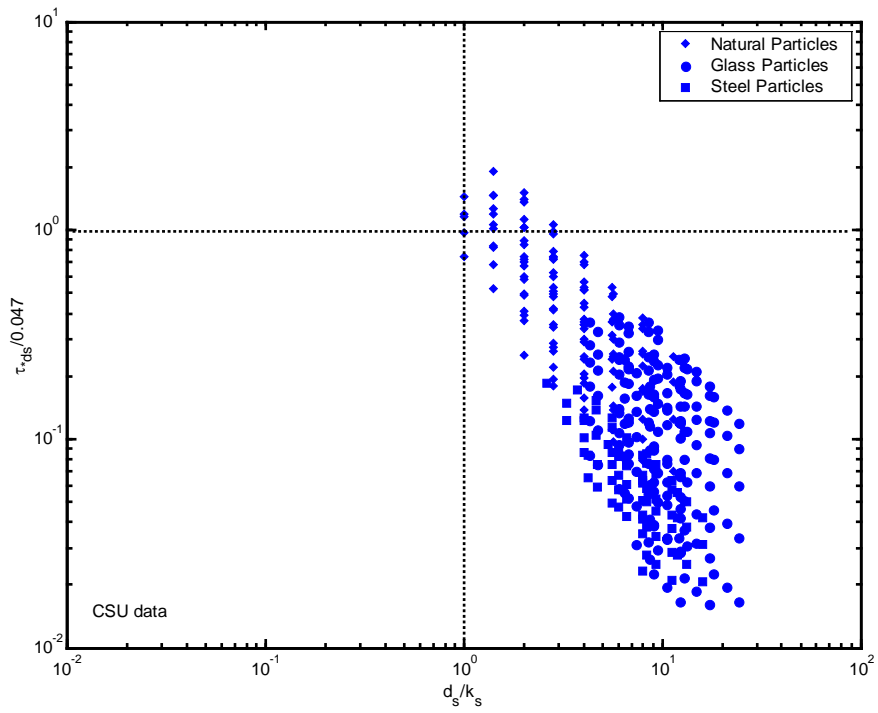
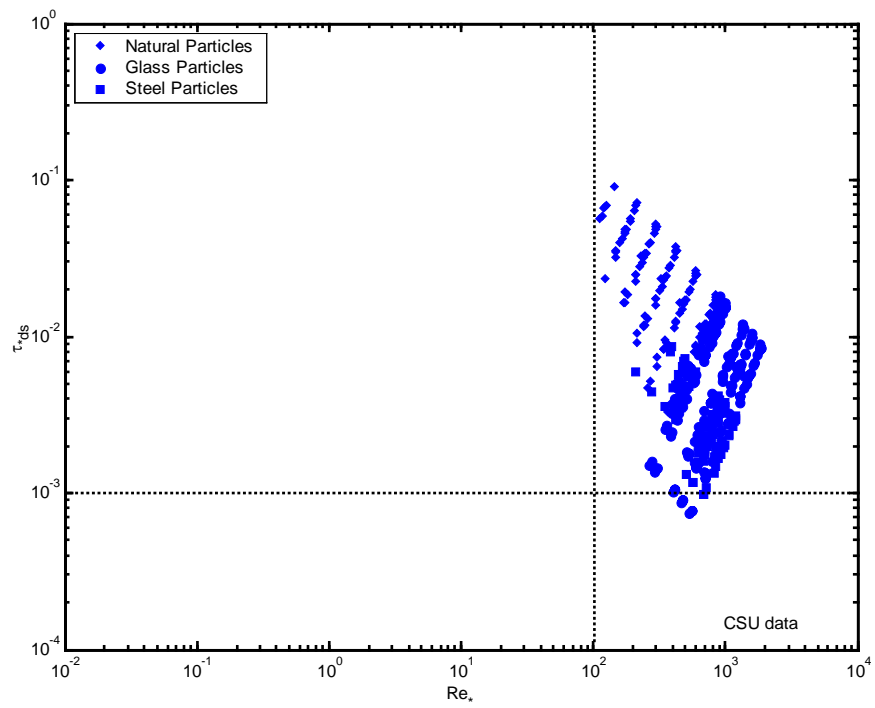


Figure 3.18:  $\tau_{*ks}$  vs  $d_s$



**Figure 3.19:**  $\tau_{*ds}/0.047$  vs  $d_s/k_s$



**Figure 3.20:**  $\tau_{*ds}$  vs  $Re_*$

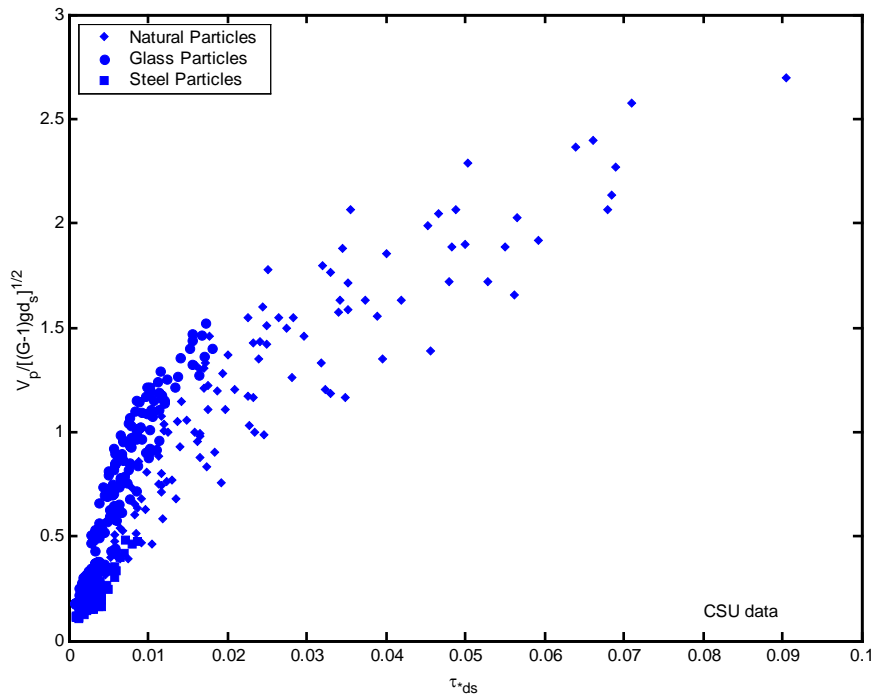


**Figure 3.21:  $V_p/[(G-1)gd_s]^{1/2}$  vs  $\tau_{*ds}$**

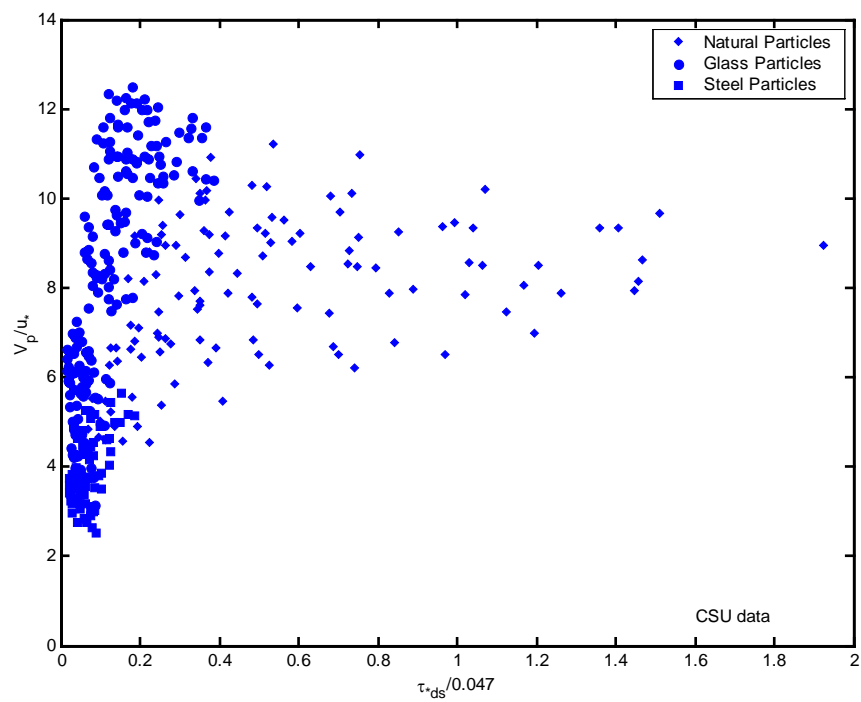


**Figure 3.22:  $V_p/u_*$  vs  $\tau_{*ds}/0.047$**

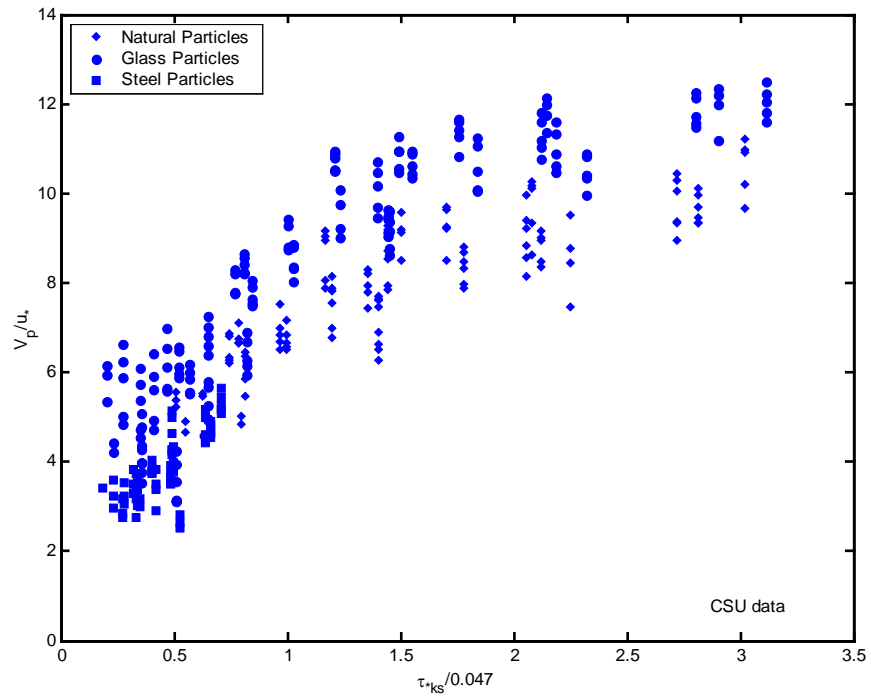


Figure 3.23:  $V_p/u_*$  vs  $\tau_{*ks}/0.047$

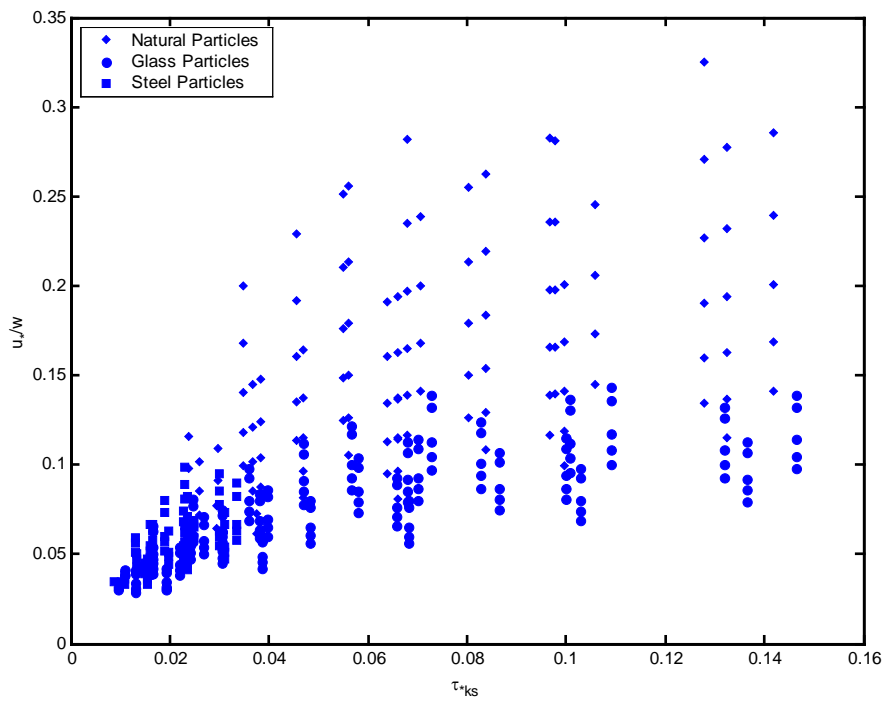
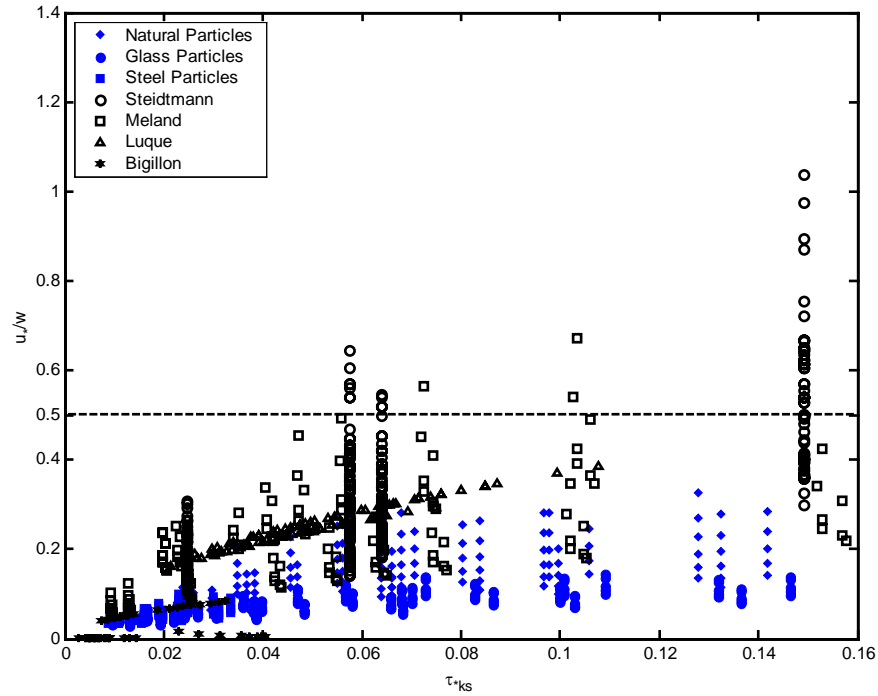


Figure 3.24:  $u_r/w$  vs  $\tau_{*ks}$



**Figure 3.25:  $u^*/w$  vs  $\tau^*_{ks}$ , for different database**

### 3.8. SUMMARY

Analysis of the data showed that: (i) for a smooth bed ( $k_s = 0$ ) larger particles move faster than smaller ones. In other words, rolling bedload particle velocity increases with particle sizes; (ii) for a rough bed ( $k_s > 0$ ) lighter particles move faster than heavier ones; (iii) bedload particles move at values of the Shields parameter  $\tau^*_{ds} < 0.047$  when  $d_s > k_s$ ; (iv) the ratio of particle velocity  $V_p$  to mean flow velocity  $u_f$  lies in the range of 0.2 to 0.9, while Kalinske (1942) suggested 0.9 to 1.0; (v) the ratio of particle velocity  $V_p$  to shear velocity  $u^*$  lies in the range of 2.5 to 12.5, while Kalinske (1947) suggested 11.0, Bagnold (1956, 1973) suggested 8.5, Francis (1973) suggested 8.3 to 11.8, Fernandez Luque and van Beek (1976) suggested 11.5, Engelund and Fredsoe (1976, 1982)

suggested 6.0 to 10.0, Fleming and Hunt (1976) suggested 9.0, Abbott and Francis (1977) suggested 13.5 to 14.3, Mantz (1980) suggested 9.2, and Naden (1981) suggested 11.8; (vi)  $0.01 < \tau_{*ks} < 0.15$ ; (vii)  $Re_* > 100$ ; (viii)  $V_p < 2w$ ; (ix) the threshold value for  $\tau_{*ks}$  appears to be 0.01; (x)  $u_*/w < 0.5$ .

# **CHAPTER 4**

## **DIMENSIONAL AND REGRESSION**

### **ANALYSIS**

The subject of transport velocity of a single particle over rough open channel flow is complicated since it involves several unknown parameters, such as the drag coefficient and the friction coefficient. To date, theoretical solutions of particle velocities are uncertain at best. The approach of this Chapter is to combine the methods of dimensional and regression analysis. Roughness and rolling particle interactions have been proven to be highly dependent on geometrical constraints such as: particle sizes (both roughness and rolling), relative roughness, and bed slope.

The challenge becomes one of deriving an equation that encompasses the correct variables without being too awkward to use. Ideally, the derived equation should predict the desired output relatively well, without the inclusion of empirical coefficients. This Chapter first examines the CSU data and particularly the Shields parameter in term of

rolling particle diameter  $d_s$  and boundary roughness  $k_s$ . The dimensional and regression analyses are then presented. An empirical equation is finally tested with data from CSU, other laboratories and field measurements.

#### 4.1. EXAMINATION OF SHIELDS APPROACH

The simplest empirical form of estimated bedload particle velocity based on analysis of CSU data is shown in Fig. 4.1, and is a variation of  $V_p/[(G-1)gd_s]^{1/2} \sim u_*^2/(G-1)gk_s$ .

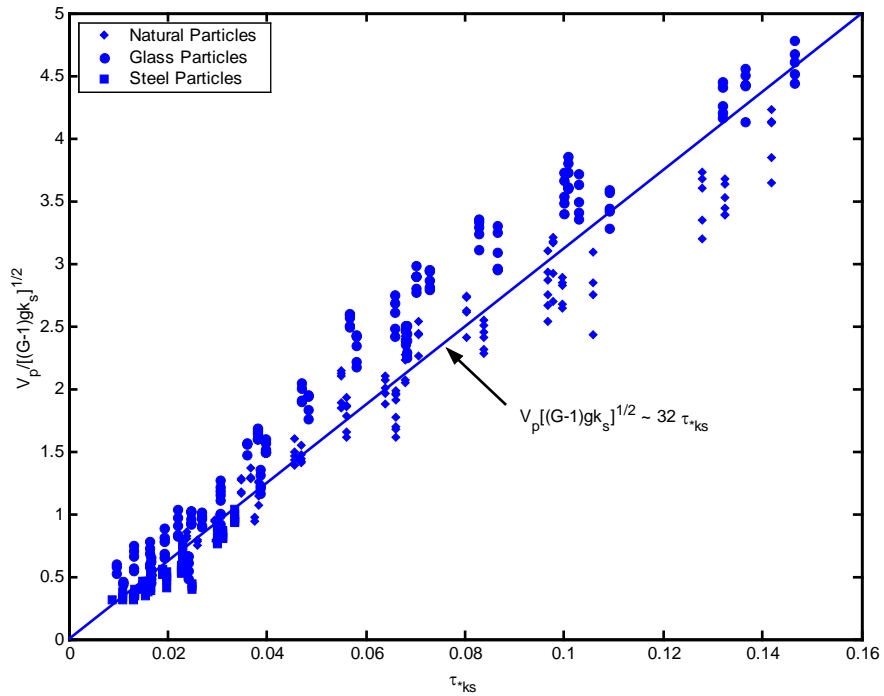


Figure 4.1:  $V_p/[(G-1)gk_s]^{1/2}$  vs  $\tau_{*k_s}$

From Fig. 4.1, we have



$$\frac{V_p}{\sqrt{(G-1)gd_s}} \sim 32 \frac{u_*^2}{(G-1)gk_s} \quad (4.1)$$

or

$$\frac{V_p}{u_*} \sim 32 \frac{u_*}{\sqrt{(G-1)gk_s}} \quad (4.2)$$

or

$$\frac{V_p}{u_*} \sim 32 \tau_{*k_s}^{1/2} \quad (4.3)$$

The bedload particle velocity can be estimated by

$$V_p \cong 32 u_* \tau_{*k_s}^{1/2} \quad (4.4)$$

Since the Shields parameter is usually written in term of  $d_s$ , a three-parameter empirical model is introduced. The variation of  $V_p/[(G-1)gd_s]^{1/2}$  with Shields parameter  $\tau_{*d_s} = u_*^2/[(G-1)gd_s]$ , and  $(k_s/d_s)$ , then transforms (4.4) into power form equation as shown below

$$\frac{V_p}{\sqrt{(G-1)gd_s}} = a \left[ \frac{u_*^2}{(G-1)gd_s} \right]^b \left( \frac{d_s}{k_s} \right)^c \quad (4.5)$$

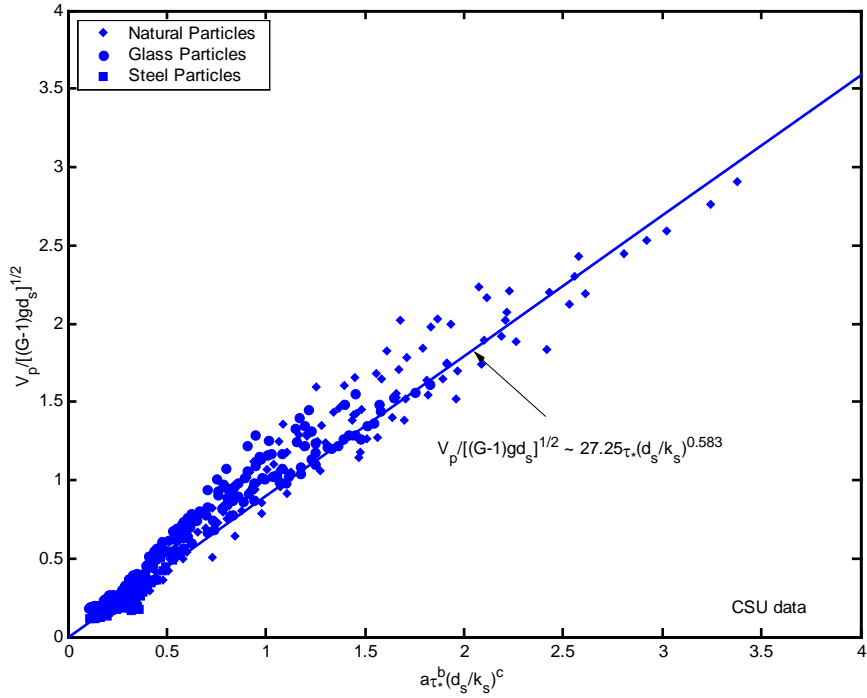


**Figure 4.2:**  $V_p / [(G-1)gd_s]^{1/2} \sim 30.5\tau_{*ds}^{1.0} (d_s/k_s)^{0.583}$

Using EXCEL multiple regression analysis toolbox, the coefficients  $a$ ,  $b$ , and  $c$  can be determined using:

$$\log \frac{V_p}{\sqrt{(G-1)gd_s}} = \log a + b \log \tau_{*ds} + c \log \left( \frac{d_s}{k_s} \right) \quad (4.6)$$

Applied to CSU's (1995) database, one obtains

$$V_p = 30.5 \left[ \frac{u_*^2}{(G-1)gd_s} \right]^1 \left( \frac{d_s}{k_s} \right)^{0.583} \sqrt{(G-1)gd_s} \quad (4.7)$$

Similarly, when applied to the entire database, one obtains

$$V_p = 6.59 \left[ \frac{u_*^2}{(G-1)gd_s} \right]^{0.94} \left( \frac{d_s}{k_s} \right)^{1.1} \sqrt{(G-1)gd_s} \quad (4.8)$$

The rolling bedload particle velocity can be estimated by Eqs. (4.7) and (4.8), where: shear velocity  $u_* = [gR_h S_f]^{1/2}$  (m/s),  $d_s$  = particle size (mm),  $k_s$  = bed roughness (mm),  $G$  = particle specific gravity, and  $g$  = gravitational acceleration ( $m/s^2$ ). The comparison between calculated and observed rolling bedload particle velocity  $V_p$  is shown in Figs. 4.3 and 4.5; Figs 4.4 and 4.6 show a discrepancy ratio distribution using Eqs. (4.7), and (4.8). Since the empirical regression coefficients  $b$  and  $c$  are quite close to unity, the basic form of Eq. (4.1) is found to be representative of laboratory conditions. It is concluded that the Shields roughness parameter  $\tau_{*k_s} = u_*^2 / [(G-1)gk_s]$  can be useful to determine bedload particle velocity.

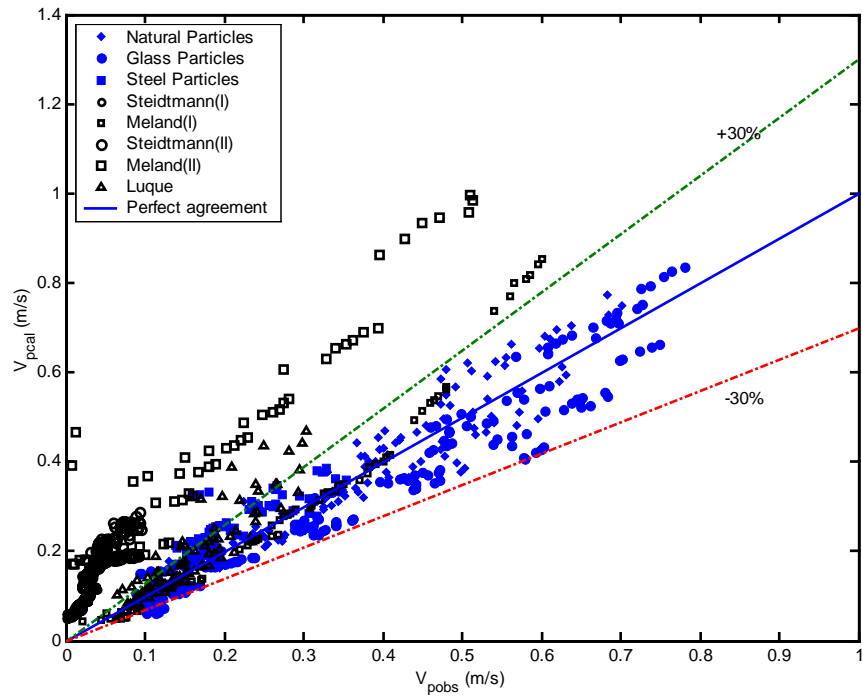


Figure 4.3: Comparison between Calculated and Observed  $V_p$  using Eq. (4.7)

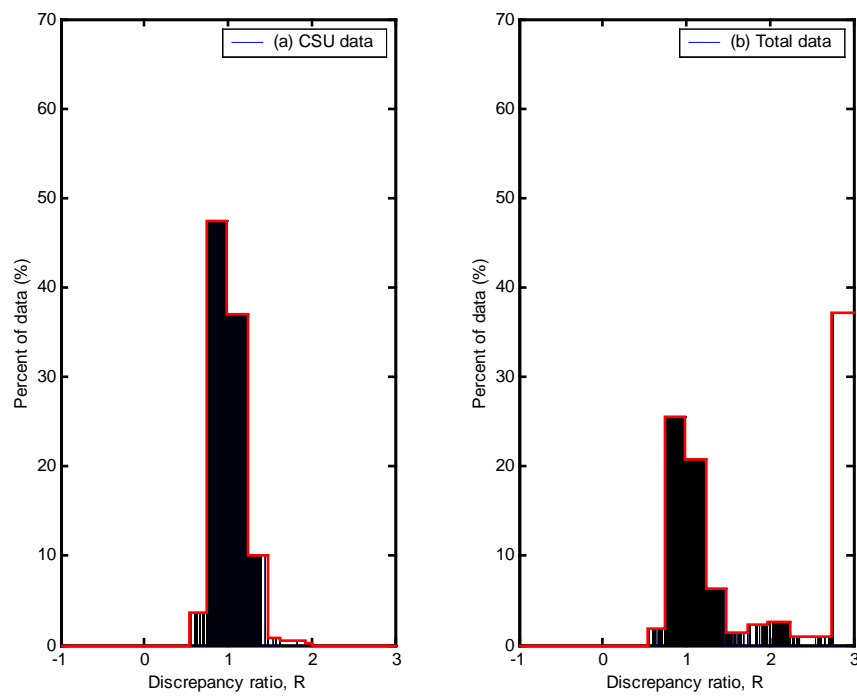


Figure 4.4: Discrepancy Ratio Distribution of  $V_p$  using Eq. (4.7)

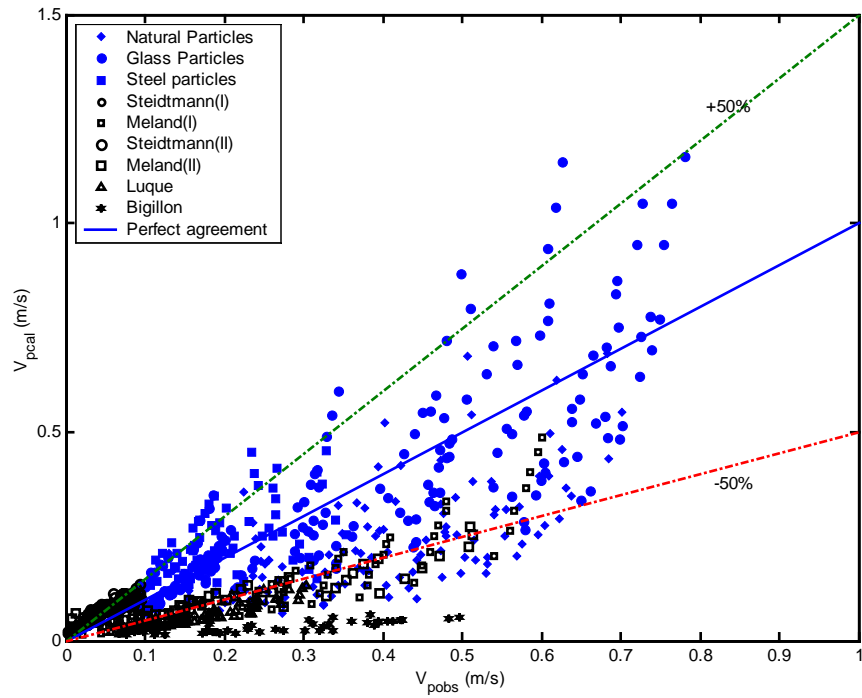


Figure 4.5: Comparison between Calculated and Observed  $V_p$  using Eq. (4.8)

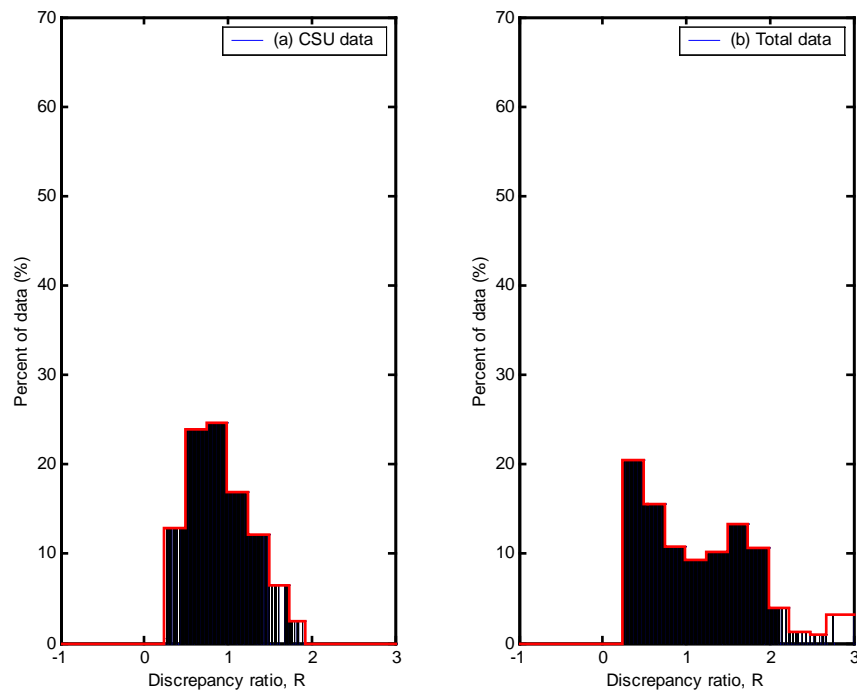


Figure 4.6: Discrepancy Ratio Distribution of  $V_p$  using Eq. (4.8)

## 4.2. DIMENSIONAL ANALYSIS

Dimensional analysis is adopted to find a functional relationship between the parameters affecting bedload particle velocity. The dependent variable is a function of six independent variables, with a total  $n = 7$  variables:

$$V_p = f(u_*, (G-1), \nu, d_s, k_s, g) = 0 \quad (4.9)$$

in which  $f$  represents an unspecified function of the shear velocity  $u_*$ , particle specific gravity  $(G-1)$ , kinematic viscosity of the fluid  $\nu$ , bedload particle diameter  $d_s$ , bed roughness  $k_s$ , and gravitational acceleration  $g$ . After  $d_s$  and  $g$  are selected as repeating variables, the two fundamental dimensions ( $j = 2$ ) are rewritten in terms of repeating variables:

$$\left. \begin{array}{l} d_s = L \\ g = \frac{L}{T^2} \end{array} \right\} \text{thus} \left\{ \begin{array}{l} L = d_s \\ T = \sqrt{\frac{d_s}{g(G-1)}} \end{array} \right.$$

After the relationships for  $L$ ,  $T$  are substituted into the non-repeating variables, five  $\pi$  terms ( $n-j = 7-2 = 5$ ) are obtained, respectively, from  $V_p$ ,  $u_*$ ,  $\nu$ ,  $(G-1)$ , and  $k_s$

$\pi_1$ :

$$\frac{V_p T}{L} = \frac{V_p}{d_s} \sqrt{\frac{d_s}{g(G-1)}} = \frac{V_p}{\sqrt{(G-1)gd_s}} \quad (4.10)$$

$\pi_2$ :

$$\frac{u_* T}{L} = \frac{u_*}{d_s} \sqrt{\frac{d_s}{g(G-1)}} = \frac{u_*}{\sqrt{(G-1)gd_s}} \quad (4.11)$$

$\pi_3$ :

$$\frac{vT}{L^2} = \frac{v}{d_s^2} \sqrt{\frac{d_s}{g(G-1)}} = \frac{v}{d_s^{3/2} [g(G-1)]^{1/2}} \quad (4.12)$$

$$\pi_3^2 = \frac{v^2}{d_s^3 (G-1)g} = \frac{1}{d_*^3} \quad (4.13)$$

$\pi_4$ :

$$\frac{k_s}{L} = \frac{k_s}{d_s} \quad (4.14)$$

$$\pi_5 = (G-1)$$

From  $\pi_1$  to  $\pi_5$ , the five dimensionless parameters can thus be written

$$\frac{V_p}{\sqrt{(G-1)gd_s}} = F \left\{ \frac{u_*}{\sqrt{(G-1)gd_s}}, \frac{1}{d_*^3}, \frac{k_s}{d_s}, (G-1) \right\} \quad (4.15)$$

The results from this dimensional analysis indicate that the dimensionless bedload particle velocity parameter is a function of the Shields parameter  $\tau_{*ds}$ , boundary relative roughness  $k_s/d_s$ , dimensionless particle diameter  $d_*$ , and excess particle specific gravity  $(G-1)$ . Further progress can be achieved only through physical understanding or an analysis of laboratory or field experiments. The bedload particle velocity is assumed to be proportional to the product of the powers of the dimensionless parameters

$$\frac{V_p}{\sqrt{(G-1)gd_s}} = a \left[ \frac{u_*}{\sqrt{(G-1)gd_s}} \right]^b d_*^c \left( \frac{d_s}{k_s} \right)^d (G-1)^e \quad (4.16)$$

in which  $a$ ,  $b$ ,  $c$ ,  $d$ , and  $e$  are coefficients to be determined from the multiple regression analysis.

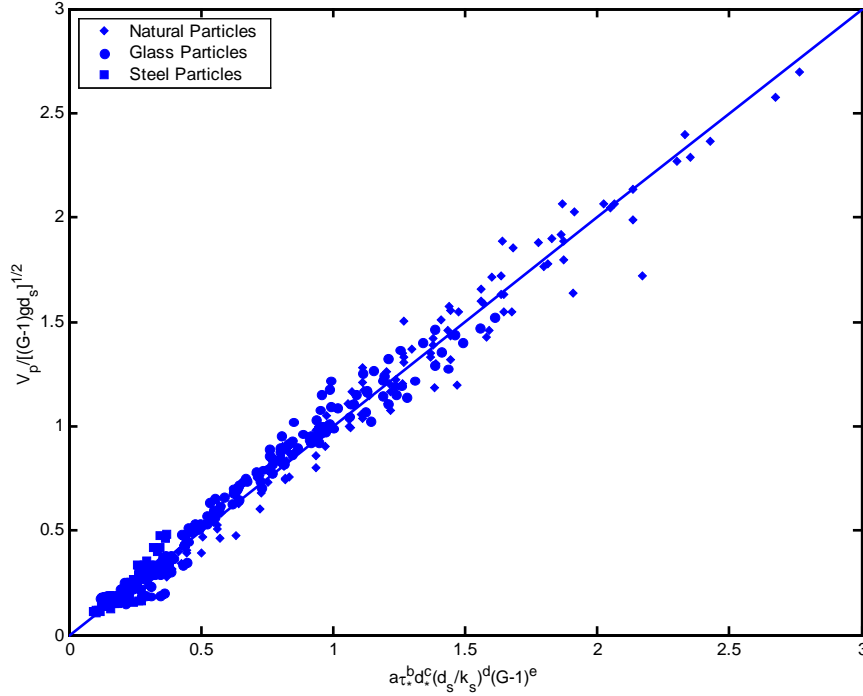


**Figure 4.7:**  $V_p / [(G-1)gd_s]^{1/2}$  vs  $11.5\tau_*^{0.95}d_*^{0.21}(d_s/k_s)^{0.36}(G-1)^{-0.28}$

Using EXCEL multiple regression analysis toolbox, the coefficients  $a$ ,  $b$ ,  $c$ ,  $d$ , and  $e$  can be determined as follow

$$\log \frac{V_p}{\sqrt{(G-1)gd_s}} = \log a + b \log \left[ \frac{u_*}{\sqrt{(G-1)gd_s}} \right] + c \log d_* + d \log \left( \frac{d_s}{k_s} \right) + e \log(G-1) \quad (4.17)$$

Applied to CSU's (1995) database we have

$$V_p = 11.5 \left[ \frac{u_*}{\sqrt{(G-1)gd_s}} \right]^{1.9} d_*^{0.21} \left( \frac{d_s}{k_s} \right)^{0.36} (G-1)^{-0.28} [(G-1)gd_s]^{0.5} \quad (4.18)$$

Similarly, applied to the total database, one obtains



$$V_p = 2.2 \left[ \frac{u_*}{\sqrt{(G-1)gd_s}} \right]^2 d_*^{0.5} \left( \frac{d_s}{k_s} \right)^{0.57} (G-1)^{-0.4} [(G-1)gd_s]^{0.5} \quad (4.19)$$

or

$$V_p = 2.2\tau_{*ds} d_*^{0.5} \left( \frac{d_s}{k_s} \right)^{0.57} (G-1)^{-0.4} [(G-1)gd_s]^{0.5} \quad (4.20)$$

The comparison between calculated and observed bedload particle velocity using Eqs. (4.18) and (4.20) is shown in Figs. 4.8 and 4.10; Figs. 4.9 and 4.11 show a discrepancy ratio distribution using Eqs. (4.18) and (4.20).

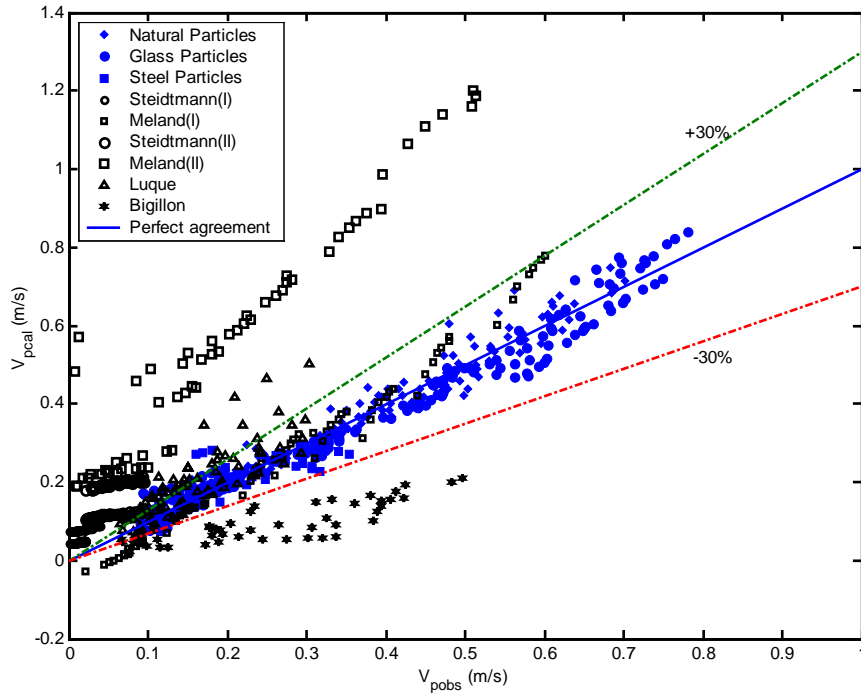


Figure 4.8: Comparison between Calculated and Observed  $V_p$  using Eq. (4.18)

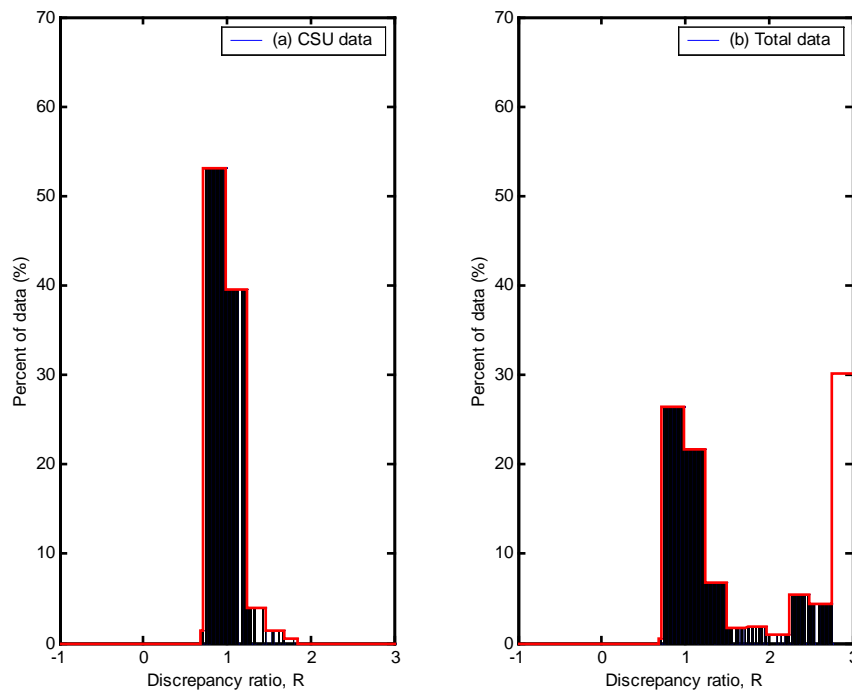


Figure 4.9: Discrepancy Ratio Distribution of  $V_p$  using Eq. (4.18)

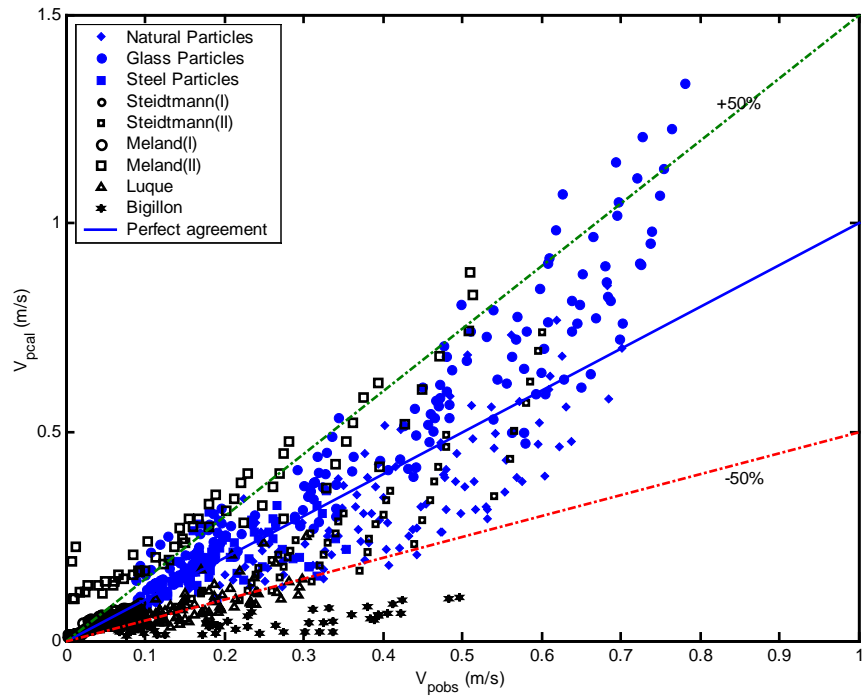


Figure 4.10: Comparison between Calculated and Observed  $V_p$  using Eq. (4.20)

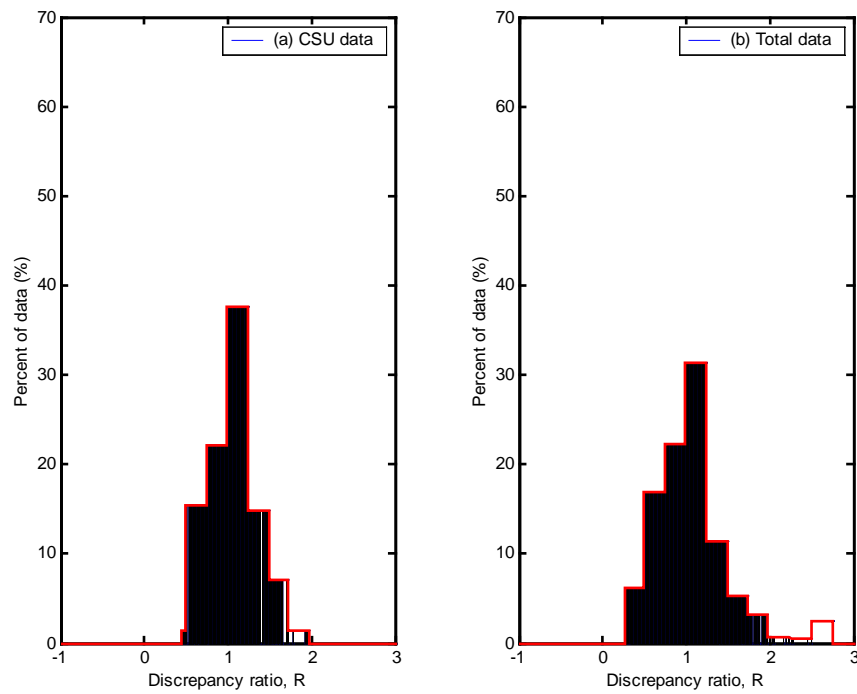


Figure 4.11: Discrepancy Ratio Distribution of  $V_p$  using Eq. (4.20)

The comparison between calculated and observed particle velocity using the proposed formula and the values is summarized in Table 4.1. A discrepancy ratio method is used to indicate the goodness of fit between calculated and observed results. It can be seen that for Eqs. (4.7) and (4.8) the percentages of data falling within the range of discrepancy ratios between 0.75 to 1.25 were in the range of 42.5 to 84.5% using the CSU database and 22.5 to 47.5% using the Total database; and for Eqs. (4.18) and (4.20) the percentages of data falling within the range of discrepancy ratios between 0.75 to 1.25 were in the range of 60 to 93% using the CSU database and 49 to 56% using the Total database.

Table 4.1: Comparison between Calculated and Observed  $V_p$  using Proposed Formulas

Equation	Data Sources	Data in Range of				No. of Data Points	$R^2$
		Discrepancy Ratio, $R_i$ (%)					
		0.75-1.25	0.5-1.5	0.25-1.75	0-2.0		
(1)	(2)	(3)	(4)	(5)	(6)	(7)	(8)
Eq. (4.7)	CSU	84.5	98.5	100	100	356	0.9
	Total	47.5	58	63.5	100	1018	0.7
Eq. (4.8)	CSU	42.5	79	98	100	356	0.54
	Total	22.5	49.5	84.5	100	1018	0.69
Eq. (4.18)	CSU	93	96.75	100	100	356	0.96
	Total	49	56.5	59	100	1018	0.7
Eq. (4.20)	CSU	60	92	98.5	100	356	0.77
	Total	56	85	97.5	100	1018	0.84

Eqs. (4.7), (4.8), (4.18), and (4.20) can be reduced to a simple form shown in Eq. (4.21); From Eq. (4.8), the exponents  $b$  and  $c$  are close to unity, one can approximate with

$$\frac{V_p}{\sqrt{(G-1)gd_s}} = a \left( \frac{u_*^2}{(G-1)gk_s} \right)$$

or

$$\frac{V_p}{u_*} = f \left[ \left( \frac{u_*^2}{(G-1)gd_s} \right)^x \left( \frac{d_s}{k_s} \right)^y \right] \quad (4.21)$$

Notice that  $V_p \rightarrow \infty$  when  $k_s \rightarrow 0$ ; and there is no threshold for  $V_p \rightarrow 0$  other than  $k_s \rightarrow \infty$ . Also, when  $k_s = d_s$  at  $\tau_{*ds} = 0.047$ , Eq (4.21) does not reduce to  $V_p = 0$ .

### 4.3. SUMMARY

This proposed bedload particle velocity function, Eq. (4.20) is derived through the combination of dimensional analysis and regression analysis with a proposed formula in power form. Eq. (4.20) accounts for various flow and particle parameters, such as bed slope  $S$ , flow depth  $y$  (mm), viscosity of the fluid  $\nu$  ( $m^2/s$ ), particle size  $d_s$  (mm), bed roughness  $k_s$  (mm), specific gravity of the particles  $G$ , and gravitational acceleration  $g$  ( $m/s^2$ ). Results showed that calculated and observed rolling bedload particle velocity fit very well when applied to both CSU and the total database.

The proposed rolling bedload particle velocity Eq. (4.20) predicts very well when  $k_s \neq 0$ , but when  $k_s \rightarrow 0$  (smooth bed), then bedload particle velocity  $V_p \rightarrow \infty$  (unbounded); when  $d_s = k_s$ , there is no value of  $\tau_{*ds}$  (no threshold) as  $V_p \rightarrow 0$ . The following Chapter provides further analysis to define the maximum bedload particle velocity on smooth bed, and also the threshold condition for beginning of motion when  $k_s \neq d_s$ .

# CHAPTER 5

## BEDLOAD PARTICLE VELOCITY

The results of the dimensional and regression analysis in Chapter 4 indicate that: (i) when  $k_s \rightarrow 0$  (smooth bed), then the bedload particle velocity  $V_p \rightarrow \infty$ ; and (ii) there is no threshold value ( $V_p \rightarrow 0$ ) when  $k_s = d_s$ . This Chapter examines the maximum bedload particle velocity over smooth beds. A theoretical analysis of particle velocity on smooth and rough surfaces are presented. The theoretical equation is then tested with laboratory and field databases. Sections 5.1 and 5.2 were modified from Guo (1997).

### 5.1. VELOCITY PROFILE NEAR SMOOTH BED

Since the particle moves near the smooth bed, the determination of the particle velocity profile is important. A turbulent flow over a smooth bed is composed of two regions: an inner and an outer region. The inner region is influenced by viscous shear, while the outer region is influenced by turbulent shear. The inner region is further divided

into three layers: the viscous sub-layer, the buffer layer and the log layer. Since the bedload movement always occurs near the bed, it relates to the velocity profile in the inner region. In the viscous sub-layer, the velocity distribution is

$$u^+ = y^+ \quad (5.1)$$

in which  $u^+ = u_f / u_*$ ,  $y^+ = u_* y / \nu$ ,  $u_f$  is the velocity at distance  $y$  from the bed,  $u_*$  is the shear velocity, and  $\nu$  is the water kinematic viscosity. In the log layer, the velocity distribution is

$$u^+ = \frac{1}{\kappa} \ln y^+ + 5.5 \quad (5.2)$$

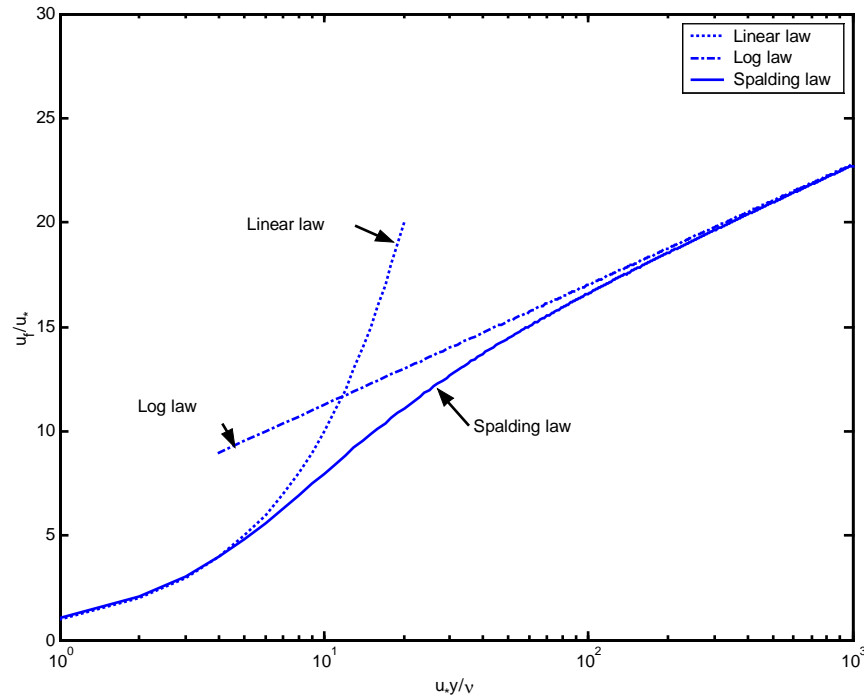


**Figure 5.1: Velocity Profile In The Inner Region**

In the buffer layer, Spalding's equation can be used (White, 1991, p.415), which is

$$y^+ = u^+ + \exp(-\kappa B) \left[ \exp(\kappa u^+) - 1 - \kappa u^+ - \frac{(\kappa u^+)^2}{2} - \frac{(\kappa u^+)^3}{6} \right] \quad (5.3)$$

in which  $\kappa = 0.4$  and  $B = 5.5$ . From equations (5.1) and (5.2), one has

$$\frac{du^+}{dy^+} = 1, \text{ for } y^+ \rightarrow 0 \quad (5.4a)$$

$$\frac{du^+}{dy^+} = \frac{1}{\kappa y^+}, \text{ for } y^+ \rightarrow \infty \quad (5.4b)$$

From the above expression, a general velocity gradient may be approximated by

$$\frac{du^+}{dy^+} = \frac{\kappa a^2 + y^+}{\kappa a^2 + \kappa y^{+2}} \quad (5.5)$$

The above equation satisfies the two asymptotic expressions. The integration of the Eq.

(5.5) with the boundary condition  $u^+ = 0$  at  $y^+ = 0$  gives

$$u^+ = a \tan^{-1} \left( \frac{y^+}{a} \right) + \frac{1}{2\kappa} \ln \left[ 1 + \left( \frac{y^+}{a} \right)^2 \right] \quad (5.6)$$

When  $y^+ \rightarrow \infty$ , the above equation reduces to

$$u^+ = \frac{1}{\kappa} \ln y^+ + \frac{\pi}{2} a - \frac{1}{\kappa} \ln a \quad (5.7a)$$

Comparing (5.7) with (5.2) gives

$$\frac{\pi}{2} a - \frac{1}{\kappa} \ln a = 5.5 \quad (5.7b)$$

Solving for  $a$  gives



$$a = 6.47 \quad (5.7c)$$

A plot of Eqs. (5.1) and (5.5) with  $a = 6.47$  is shown in Figure 5.1.

## 5.2. MAXIMUM VELOCITY OF A PARTICLE ON SMOOTH BED

Consider that, for a sphere of diameter  $d_s$ , the slope angle of the plane is  $\theta$ . The forces acting on the sphere include drag force,  $F_D$ , lift force,  $F_L$ , submerged weight of the sphere  $W_s$ , and resistance to the movement of the sphere  $F_f$ .

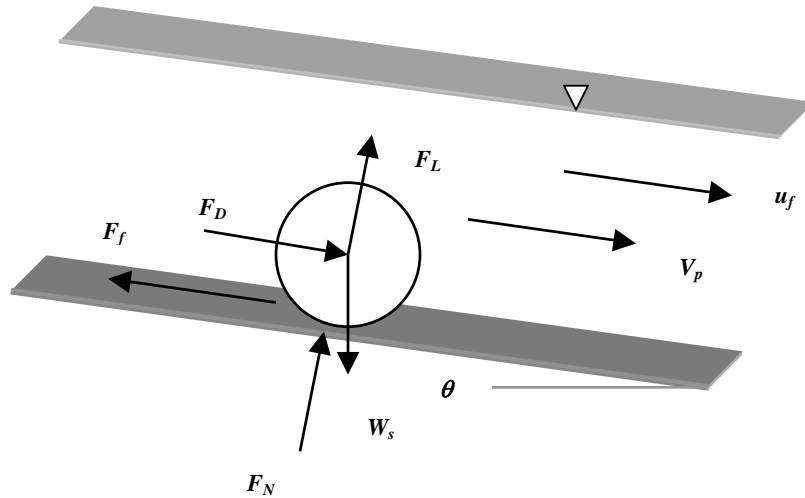


**Figure 5.2: Forces Acting on a Sphere Rolling down an Inclined Smooth Bed**

Considering the steady state, one can write the following equilibrium equations

$$W_s \sin \theta = F_D - F_f \quad (5.8)$$

$$W_s \cos \theta = F_N + F_L \quad (5.9)$$

The submerged weight is

$$W_s = \frac{1}{6} \pi \rho (G-1) g d_s^3 \quad (5.10)$$

Assumed that the fluid moves faster than the particle, the drag force in the flowing fluid can be used

$$F_D \approx \frac{1}{2} C_D \rho (u_f - V_p)^2 \frac{\pi d_s^2}{4} \quad (5.11)$$

in which  $\alpha$  is an experimental coefficient. The lift force points upward and can be calculated

$$F_L = \frac{2}{3} \pi \rho d_s^2 (u_f - V_p) V_p \quad (5.12)$$

The frictional force is

$$F_f \leq \mu F_N \quad (5.13)$$

considering the equilibrium in the  $z$ -direction, one has

$$F_N = W_s \cos \theta - F_L = \frac{1}{6} \pi \rho (G-1) g d_s^3 \cos \theta - \frac{2}{3} \pi \rho d_s^2 (u_f - V_p) V_p \quad (5.14)$$

similarly, considering the equilibrium in the  $x$ -direction, one obtains

$$\frac{1}{6} \pi \rho (G-1) g d_s^3 \sin \theta + \frac{1}{2} C_D \rho (u_f - V_p)^2 \frac{\pi d_s^2}{4} \leq \mu \left[ \frac{1}{6} \pi \rho (G-1) g d_s^3 \cos \theta - \frac{2}{3} \pi \rho d_s^2 (u_f - V_p) V_p \right] \quad (5.15)$$

which shows that the particle accelerates all the time and a steady state is achieved when the equal sign is used in (5.15). The above equation can be rearranged in terms of  $(u_f - V_p)$ , i.e.

$$\left(1 - \frac{16}{3} \frac{\mu}{C_D}\right)(u_f - V_p)^2 + \frac{16}{3} \frac{\mu}{C_D} u_f (u_f - V_p) + \frac{4}{3C_D} (G-1)gd_s (\sin \theta - \mu \cos \theta) = 0 \quad (5.16)$$

solving for  $(u_f - V_p)$  gives

$$u_f - V_p = \frac{-b \pm \sqrt{b^2 - 4ac}}{2a} \quad (5.17)$$

in which

$$a = 1 - \frac{16}{3} \frac{\mu}{C_D} \quad (5.18)$$

$$b = \frac{16}{3} \frac{\mu u_f}{C_D} \quad (5.19)$$

$$c = \frac{4}{3C_D} (G-1)gd_s (\sin \theta - \mu \cos \theta) \quad (5.20)$$

since the fluid goes faster than the particle, the positive value of  $(u_f - V_p)$  is the required solution, since  $b > 0$ , the particle velocity is

$$V_p = u_f - \frac{\sqrt{b^2 - 4ac} - b}{2a} \quad (5.21)$$

For an experimental study, assume  $\mu$  constant,  $C_D$  function of a Reynolds number  $Re_* = u_* d_s / \nu$ , then the second term on the right hand side of (5.21) has the following function form

$$\frac{\sqrt{b^2 - 4ac} - b}{2a} = u_* f \left( Re_*, \frac{u_f}{u_*}, (G-1) \frac{gd_s}{u_*^2}, \theta, \mu \right) \quad (5.22)$$

Considering  $u_f / u_*$  at  $y = d_s$  is also a function of  $Re_*$  from the velocity profile equation in a smooth bed, and  $\theta$  has been merged into the shear velocity  $u_*$ , the above relation should become primarily dependent on  $Re_*$  and to a lesser degree depend on  $\theta$ ,  $\mu$ , and  $d_*$

$$\frac{V_p}{u_*} = f(Re_*, d_*, \mu, \theta) \quad (5.23)$$

As approximation, one can plot  $V_p/u_*$  vs  $Re_*$  as shown in Fig. 5.3. Applying Eq. (5.6) with a correction factor  $\beta$ , one obtains

$$\frac{V_p}{u_*} = a \tan^{-1}\left(\frac{Re_*}{\beta a}\right) + \frac{1}{2\kappa} \ln\left[1 + \left(\frac{Re_*}{\beta a}\right)^2\right] \quad (5.27)$$

in which  $\kappa = 0.4$  and  $a = 6.47$ , as for Eq. (5.6), Guo (1997) used the Matlab Nonlinear Optimization Toolbox to determine that  $\beta = 4$ . The rolling bedload particle velocity for smooth bed can be estimated by

$$V_p = \left\{ 6.47 \tan^{-1}\left(\frac{Re_*}{25.88}\right) + \frac{1}{2\kappa} \ln\left[1 + \left(\frac{Re_*}{25.88}\right)^2\right] \right\} \times u_* \quad (5.28)$$

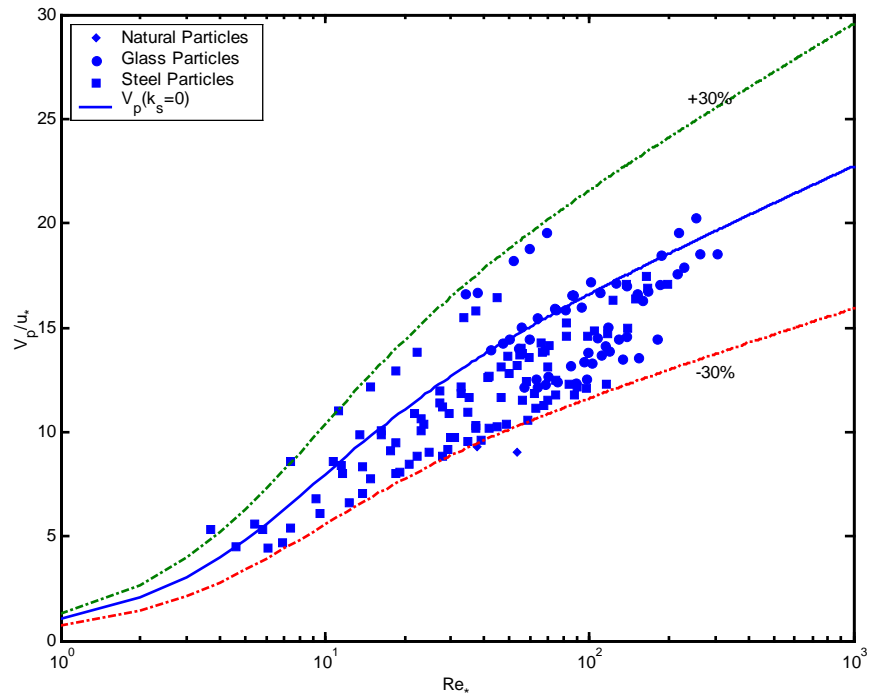


Figure 5.3:  $V_p/u_*$  vs  $Re_*$  using Eq. (5.28)

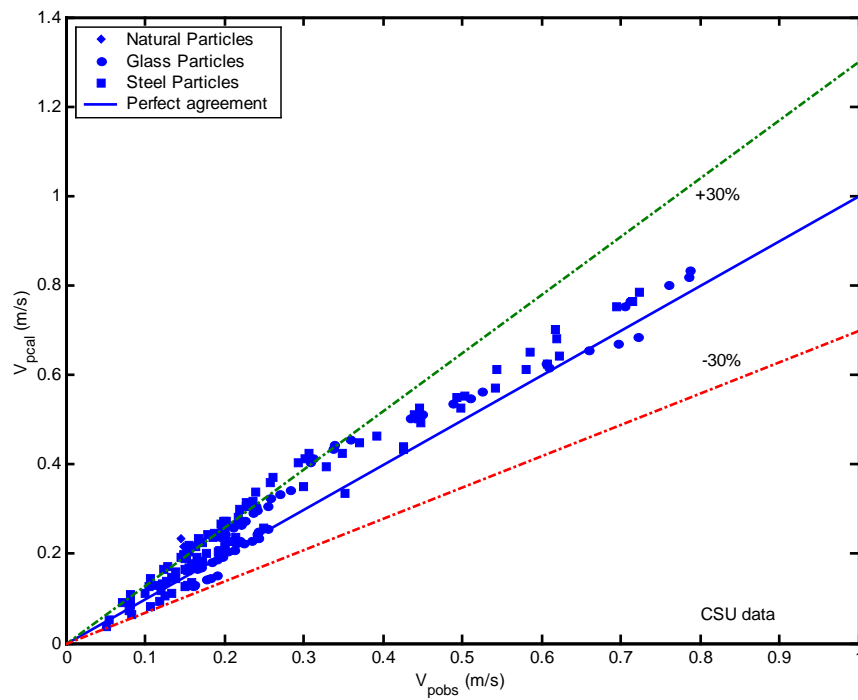


Figure 5.4: Comparison between Calculated and Observed  $V_p$  using Eq. (5.28)

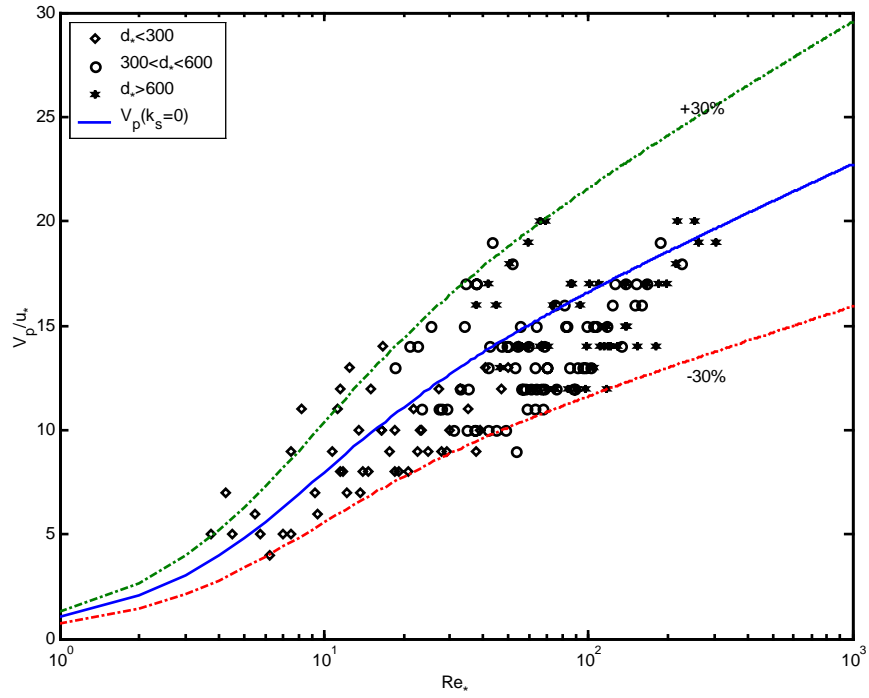


Figure 5.5:  $V_p/u_*$  vs  $Re_*$  using Eq. (5.28) for different values of  $d$ \*

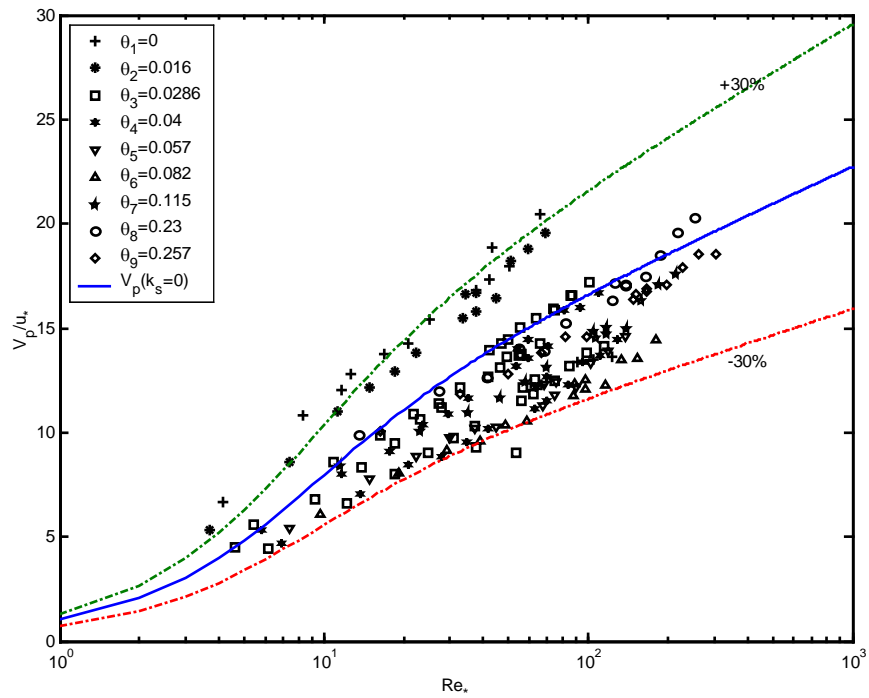
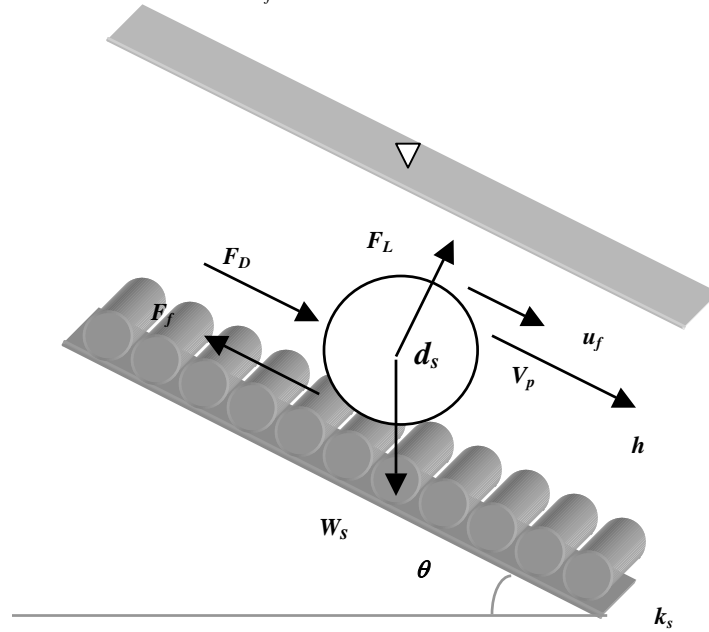


Figure 5.6:  $V_p/u_*$  vs  $Re_*$  using Eq. (5.28) for different values of  $\theta$

### 5.3. SINGLE PARTICLE ROLLING DOWN AN INCLINED ROUGH BED

Consider a sphere of diameter  $d_s$  rolling in a flowing fluid over an inclined bed of roughness. The slope angle of the plane is  $\theta$ . The forces acting on the sphere include drag force,  $F_D$ , lift force,  $F_L$ , submerged weight of the sphere  $W_s$ , and resistance to the movement of the sphere from boundary  $F_f$ .



**Figure 5.7: Forces Acting on a Sphere Rolling down an Inclined Bed of Roughness**

$$\frac{V_p}{u_*} = \frac{V_{psmooth}}{u_*} - \Delta B \quad (5.29)$$

where the boundary roughness function  $\Delta B = f(k_s, \tau_{*ds}, d_*)$ . A plot of  $V_p/u_*$  as a function of  $Re_*$  and  $\Delta B$  for both smooth and rough beds is shown in Fig. 5.9. After substituting Eq. (5.29) to particle velocity on smooth bed, Eq. (5.29) reduces to

$$\frac{V_p}{u_*} = 6.47 \tan^{-1}\left(\frac{Re_*}{25.88}\right) + \frac{1}{2\kappa} \ln \left[ 1 + \left(\frac{Re_*}{25.88}\right)^2 \right] - \Delta B \quad (5.30)$$

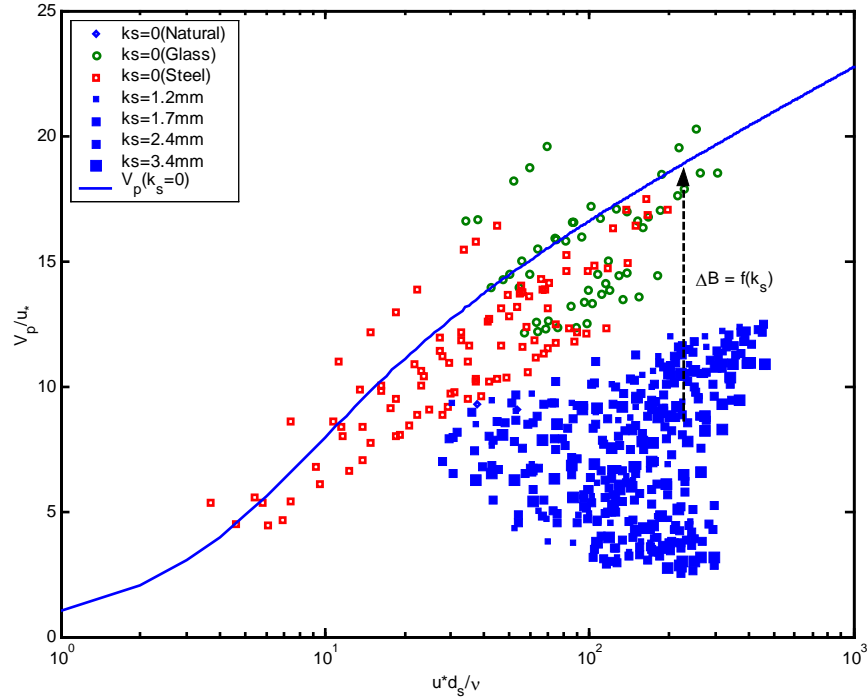


**Figure 5.8:  $V_p/u_*$  vs  $Re_*$  for Smooth ( $k_s = 0$ ) and Rough Bed ( $k_s > 0$ )**

or

$$\Delta B = 6.47 \tan^{-1}\left(\frac{Re_*}{25.88}\right) + \frac{1}{2\kappa} \ln\left[1 + \left(\frac{Re_*}{25.88}\right)^2\right] - \frac{V_p}{u_*} \quad (5.31)$$

Due to the effect of bed roughness  $k_s$ , particle size  $d_s$ , shear velocity  $u_*$ , and fluid kinematic viscosity  $\nu$ , on bedload particle velocity  $V_p$ , we can assume that the calculated value  $\Delta B_c$  can be obtained as a function of Shields parameter  $\tau_{*ds}$ , dimensionless particle diameter  $d_*$ , and relative roughness ( $k_s/d_s$ ) as

$$\Delta B_c = a \tau_{*ds}^b d_*^c \left(\frac{k_s}{d_s}\right)^d \quad (5.32)$$

or



$$\log \Delta B_c = \log a + b \log \tau_{*ds} + c \log d_* + d \log \left( \frac{k_s}{d_s} \right) \quad (5.33a)$$

the calibration parameters  $a$ ,  $b$ ,  $c$ , and  $d$  are obtained using the EXCEL multiple regression analysis toolbox. The analysis is applied to the CSU database

$$\Delta B_c = 0.884 \tau_{*ds}^{-0.229} d_*^{0.32} \left( \frac{k_s}{d_s} \right)^{0.333} \quad (5.33b)$$

Substituting (5.33b) into (5.30), and solving for  $V_p$ , one obtains

$$V_p = \left\{ 6.47 \tan^{-1} \left( \frac{Re_*}{25.88} \right) + \frac{1}{2\kappa} \ln \left[ 1 + \left( \frac{Re_*}{25.88} \right)^2 \right] - 0.884 \tau_{*ds}^{-0.229} d_*^{0.32} \left( \frac{k_s}{d_s} \right)^{0.333} \right\} \times u_* \quad (5.34)$$

The agreement between  $\Delta B$  and  $\Delta B_c$  is shown in Fig. 5.9. There is a reasonable good fit ( $R^2 = 0.9$ ) between calculated and observed  $\Delta B$ .

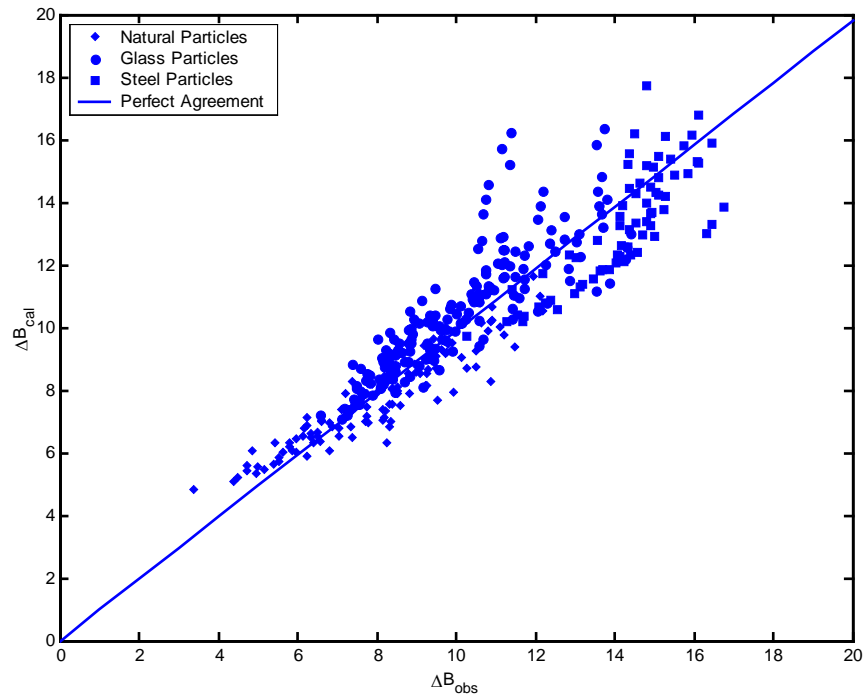


**Figure 5.9:  $\Delta B_{cal}$  vs  $\Delta B_{obs}$  using Eq. (5.33b) for CSU data**

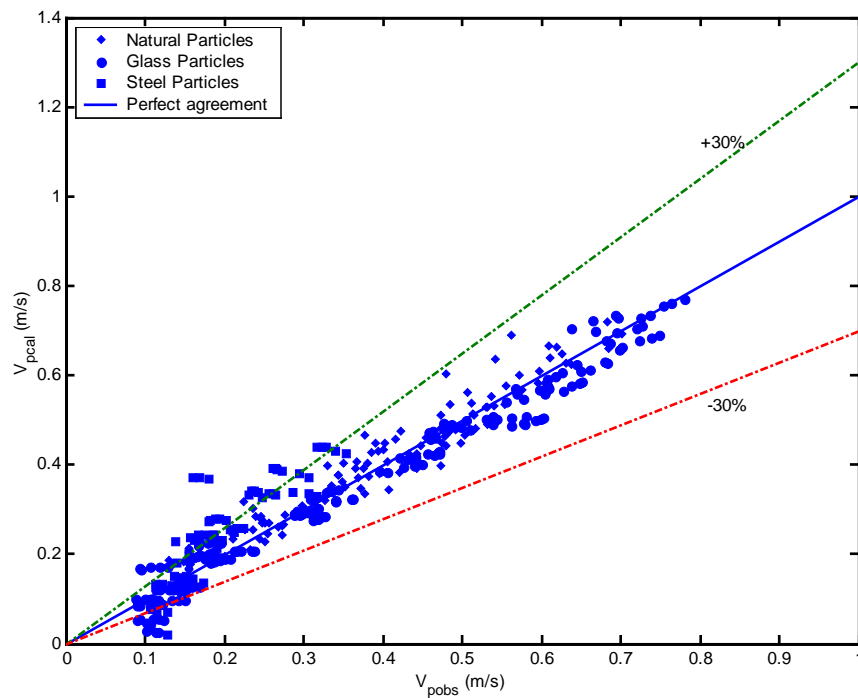


**Figure 5.10: Comparison between Calculated and Observed  $V_p$  using Eq. (5.34)**

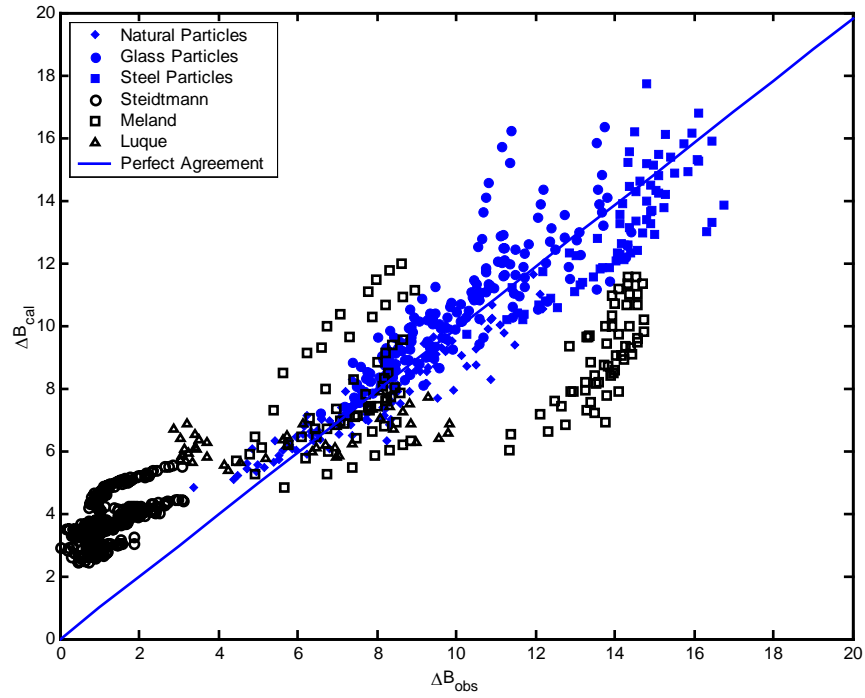


Figure 5.11:  $\Delta B_{cal}$  vs  $\Delta B_{obs}$  using Eq. (5.33b) for total data

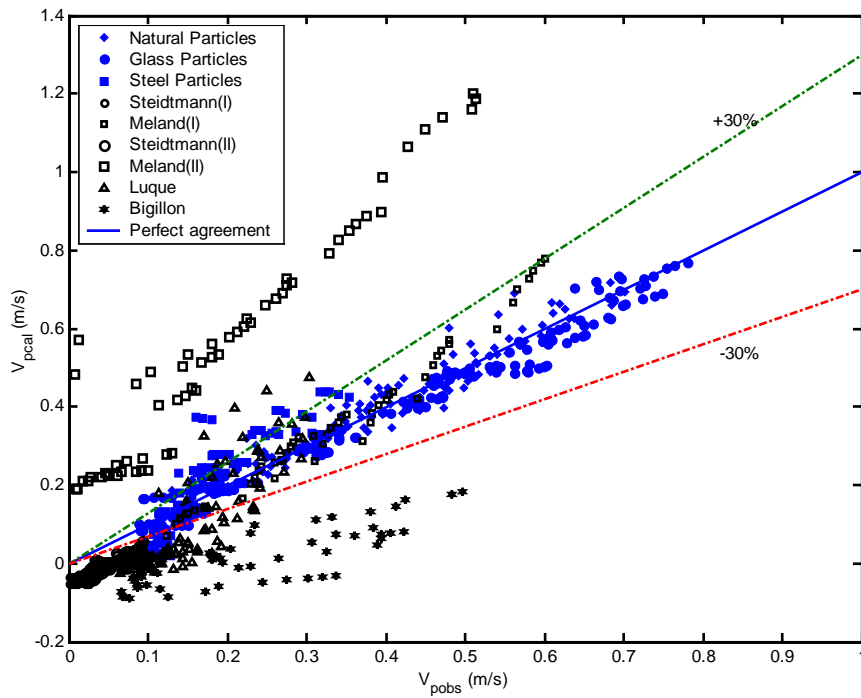
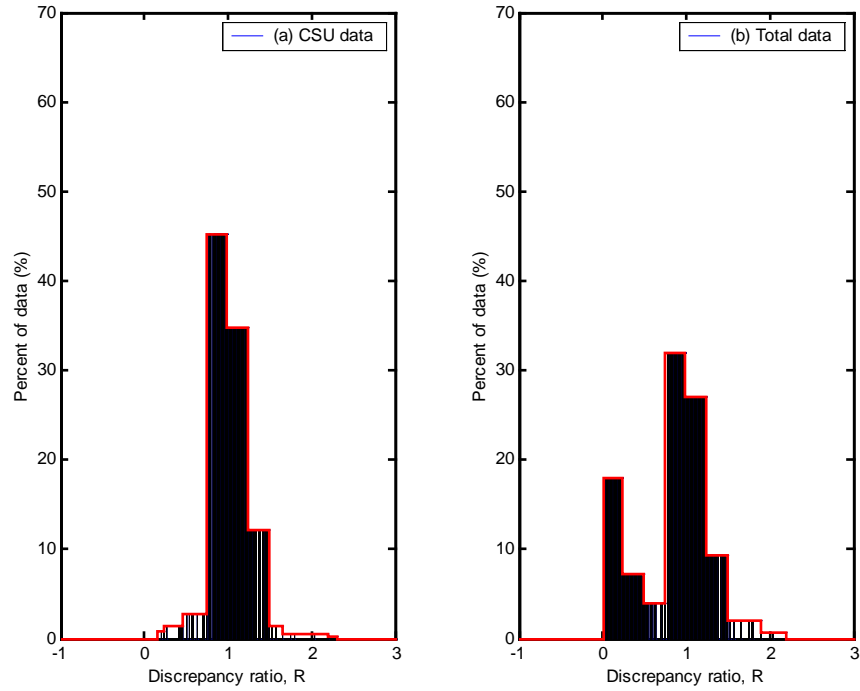


Figure 5.12: Comparison between Calculated and Observed  $V_p$  using Eq. (5.34)



**Figure 5.13: Discrepancy Ratio Distribution of  $V_p$  using Eq. (5.34)**

The analysis is applied to the Total database

$$\Delta B_c = 0.096 \tau_{*ds}^{-0.048} d_*^{0.93} \left( \frac{k_s}{d_s} \right)^{0.61} \quad (5.33c)$$

Substituting (5.33c) into (5.30), and solving for  $V_p$ , one obtains

$$V_p = \left\{ 6.47 \tan^{-1} \left( \frac{Re_*}{25.88} \right) + \frac{1}{2\kappa} \ln \left[ 1 + \left( \frac{Re_*}{25.88} \right)^2 \right] - 0.096 \tau_{*ds}^{-0.048} d_*^{0.93} \left( \frac{k_s}{d_s} \right)^{0.61} \right\} \times u_* \quad (5.35)$$

where:  $Re_* = u_* d_s / \nu$ , shear velocity  $u_* = [g R_n S]^{1/2}$  (m/s),  $d_s$  = particle size (mm),  $k_s$  = bed roughness (mm),  $\nu$  = fluid kinematic viscosity ( $m^2/s$ ),  $G$  = particle specific gravity,  $g$  = gravitational acceleration ( $m/s^2$ ), and Shields parameter  $\tau_{*ds} = u_*^2 / (G-1)gd_s$ , and  $\kappa$  = von Karman constant (0.4);

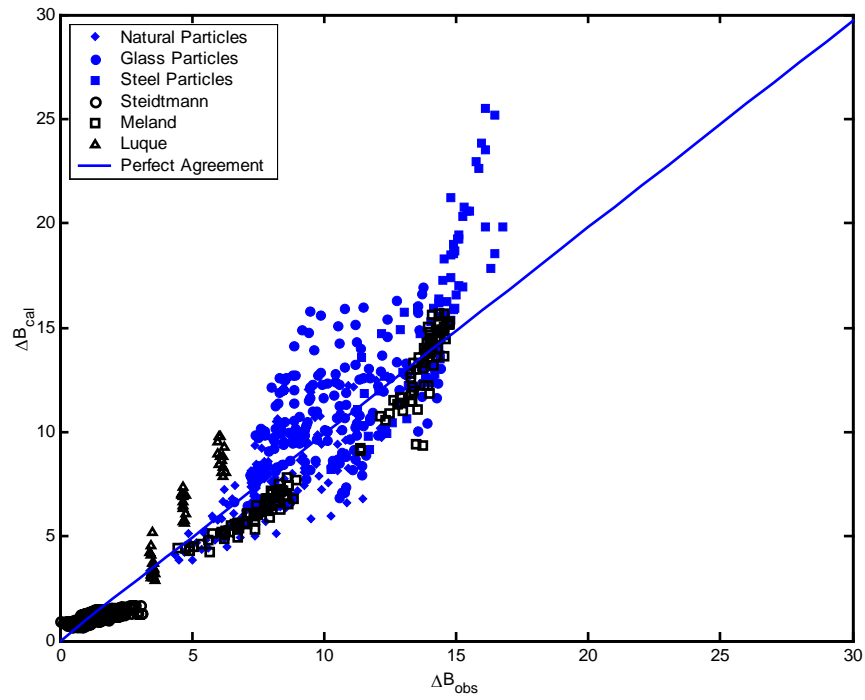


Figure 5.14:  $\Delta B_{cal}$  vs  $\Delta B_{obs}$  using (5.33c) for total data

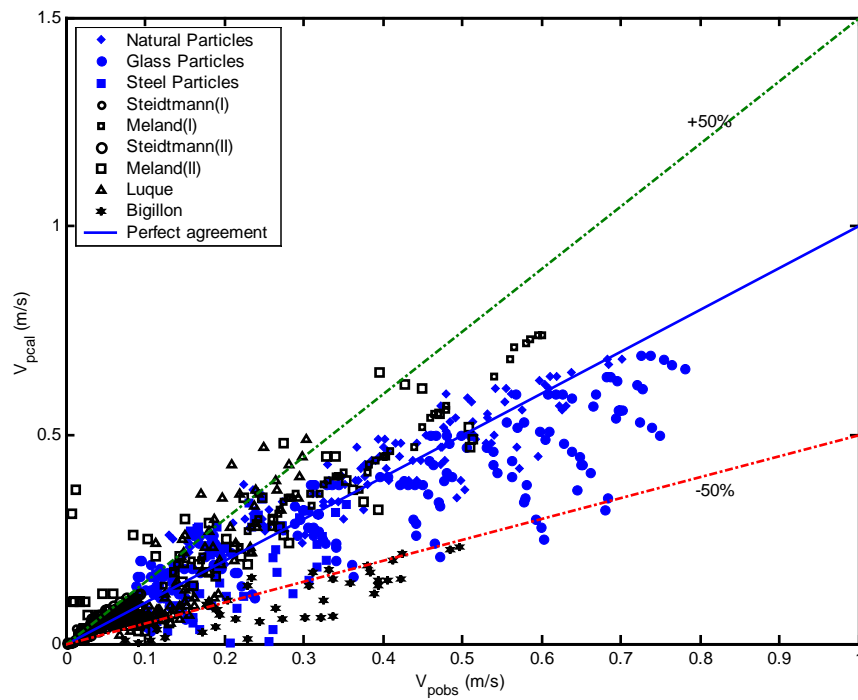
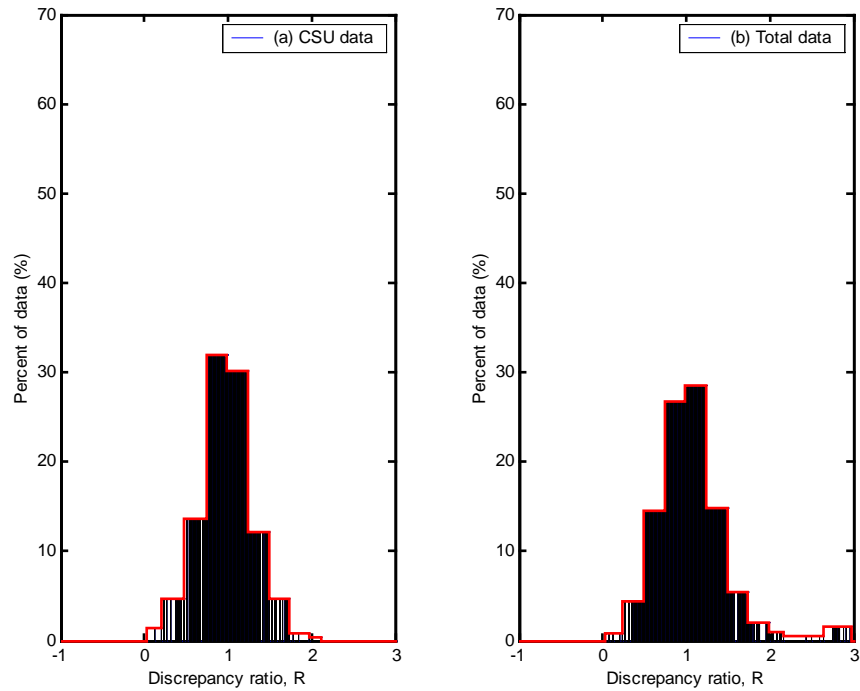


Figure 5.15: Comparison between Calculated and Observed  $V_p$  using Eq. (5.35)



**Figure 5.16: Discrepancy Ratio Distribution of  $V_p$  using Eq. (5.35)**

The bedload particle velocity can be calculated by Eq. (5.34), Fig. 5.12, shows the comparison between calculated and observed rolling bedload particle velocity  $V_p$  using Eq. (5.34); and Fig. 5.13, shows the discrepancy ratio distribution for  $V_p$  using Eq. (5.34). The comparison between calculated and observed particle velocity using the proposed formula is summarized in Table 5.1. A discrepancy ratio method is used to indicate the goodness of fit between calculated and observed values. It can be seen that the percentages of data falling within the range of discrepancy ratios between 0.75 to 1.25 were at least 60% using the total database.

Table 5.1: Summary of Comparison between Calculated and Observed  $V_p$

Equation	Data Sources	Data in Range of Discrepancy Ratio, $R_i$ (%)				No. of Data Points	$R^2$
		0.75-1.25	0.5-1.5	0.25-1.75	0-2.0		
(1)	(2)	(3)	(4)	(5)	(6)	(7)	(8)
Eq. (5.34)	CSU	80	95	100	100	356	0.93
	Total <sup>(1)</sup>	60	75	82	100	1018	0.83
Eq. (5.35)	CSU	59.5	84	93.5	100	356	0.68
	Total	54	83	92.5	100	1018	0.82

(1) = Meland (1966) + Luque (1976) + Steidtmann (1982) + Bridge (1984) + CSU (1995) + Bigillon (2001)

## 5.4. ANALYSIS OF THE THRESHOLD CONDITION

The goal of this section is to find the threshold condition in term of bed roughness size required the particle to stop rolling. The first approach is with reference to the CSU data, Fig. 5.17 shows  $\tau_{*ds}/0.047$  against relative roughness  $d_s/k_s$  for different values of  $V_p/u_*$ .

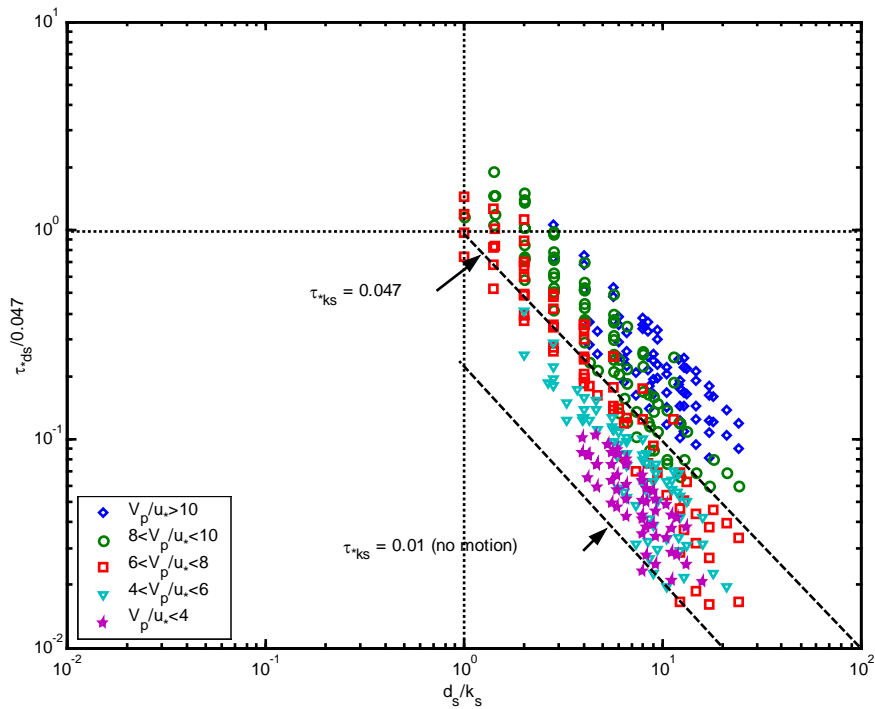


**Figure 5.17:  $\tau_{*ds}/0.047$  vs  $d_s/k_s$ , for different values of  $V_p/u_*$**

Very few particles are shown to move at values of shear stress below

$$\frac{\tau_{*ds}}{0.047} = 0.213 \frac{k_s}{d_s} \quad (5.36)$$

this defines beginning of motion as



$$(\tau_{*k_s})_c = \frac{u_*^2}{(G-1)gd_s} \left( \frac{d_s}{k_s} \right) = \left[ \frac{u_*^2}{(G-1)gk_s} \right]_c = 0.213 \times 0.047 = 0.01 \quad (5.37)$$

The result describes above  $(\tau_{*k_s})_c \approx 0.01$ . Fig. 5.17 shows there are a few data points have the values of  $\tau_{*k_s} < 0.01$ .

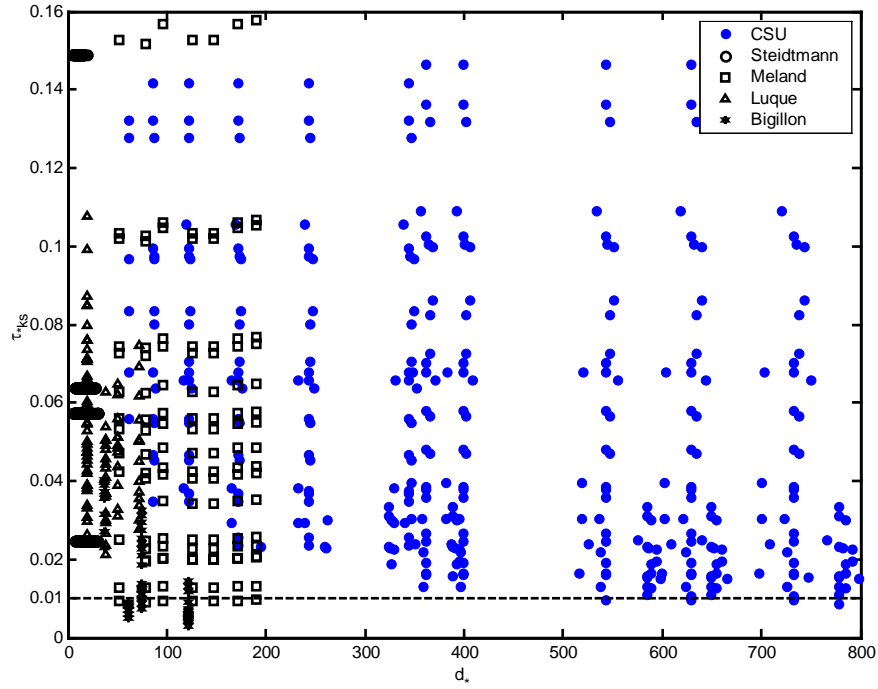


**Figure 5.18:  $\tau_{*k_s}$  vs  $d_*$  for different databases**

The second approach is to find the bed roughness size  $k_s$  that correspond to  $V_p = 0$  in (5.31). Accordingly, threshold condition occurs from Eq. (5.34) when

$$k_{sc} = d_s \left\{ \frac{\left[ 6.47 \tan^{-1} \left( \frac{Re_*}{25.88} \right) + \frac{1}{2\kappa} \ln \left[ 1 + \left( \frac{Re_*}{25.88} \right)^2 \right] \right]^{0.333}}{0.884 \tau_*^{-0.229} d_*^{0.32}} \right\} \quad (5.38)$$

Threshold condition, or  $V_p = 0$  (no motion), is obtained when  $k_s = k_{sc}$ . Particles move when  $k_s < k_{sc}$ , and stop when  $k_s \geq k_{sc}$ .

## 5.5. SUMMARY

Two functions of the transport velocity of a single particle on a smooth bed Eq. (5.28) and on a rough bed Eq. (5.34) are defined through theoretical and empirical analysis. The results show that the bedload particle velocity on smooth beds is approximately equal to the flow at the center of the particles. The roughness function  $\Delta B$  describes the effect of bed roughness on reducing transport velocity of rolling bedload particles. This function  $\Delta B$  varies with bed slope  $S$ , flow depth  $y$  (mm), viscosity of the fluid  $\nu$  ( $m^2/s$ ), particle size  $d_s$  (mm), bed roughness  $k_s$  (mm), specific gravity of the particles  $G$ , and gravitational acceleration  $g$  ( $m/s^2$ ). The proposed bedload particle velocity formula, Eq. (5.34) reduces to Eq. (5.28) when  $k_s \rightarrow 0$ . When  $k_s = d_s$ ,  $V_p \sim (5 - 11)u_*$ , and  $\tau_{*d_s}$  decreases when  $V_p \rightarrow 0$ . Particles reach incipient motion when  $\tau_{*k_s} \approx 0.01$ , or when  $k_s = k_{sc}$  defined in Eq. (5.38).

# CHAPTER 6

## LABORATORY AND FIELD APPLICATIONS

In this chapter, a general procedure for the calculation of bedload particle velocity is presented. This procedure is illustrated through a detailed example problem, followed with field applications.

### 6.1. PROPOSED METHOD

#### 1. Input data

- Particle diameter  $d_s$  (mm)
- Flow depth  $y$  (mm)
- Bed slope  $S_f$

- Bed roughness  $k_s$  (mm)
- Flow viscosity  $\nu$  ( $m^2/s$ )
- Particle specific gravity  $G$

2. Calculation of the basic parameters

- Shear velocity  $u_* = [gR_h S_f]^{1/2}$  (m/s)
- Shields particle parameter  $\tau_{*d_s} = u_*^2 / (G-1)gd_s$
- Shields roughness parameter  $\tau_{*k_s} = u_*^2 / (G-1)gk_s$
- Boundary relative roughness  $d_s/k_s$ , and  $k_s/d_s$
- Particle shear Reynolds number  $Re_* = u_* d_s / \nu$
- Dimensionless particle diameter  $d_* = d_s [(G-1)g/\nu^2]^{1/3}$

3. Calculation of bed roughness critical  $k_{sc}$  from Eqs. (5.37) and (5.38) to determine the motion of the particle.

4. Calculation of  $V_{p\text{smooth}}$  use Eq. (5.28);  $V_p$  use Eqs. (5.34), (5.35), and may also use Eq. (4.20).

## 6.2. TESTING EXISTING FORMULAS WITH ENTIRE DATABASE

Figs. 6.1, 6.3 and 6.5 illustrate the comparison between calculated and observed bedload particle velocity  $V_p$ , by applying the Meland and Norrman (1966), Fernandez Luque and van Beek (1976), and Bridge and Dominic (1984) equations to all assembled data. Figs. 6.2, 6.4 and 6.6 show a discrepancy ratio distribution for Meland and

Norrman, Fernandez Luque and van Beek, and Bridge and Dominic equations respectively. Results show that Fernandez Luque and van Beek, and Bridge and Dominic predict their own data very well, but none of Meland and Norrman, Fernandez Luque and van Beek, and Bridge and Dominic equations compare well with the entire database.

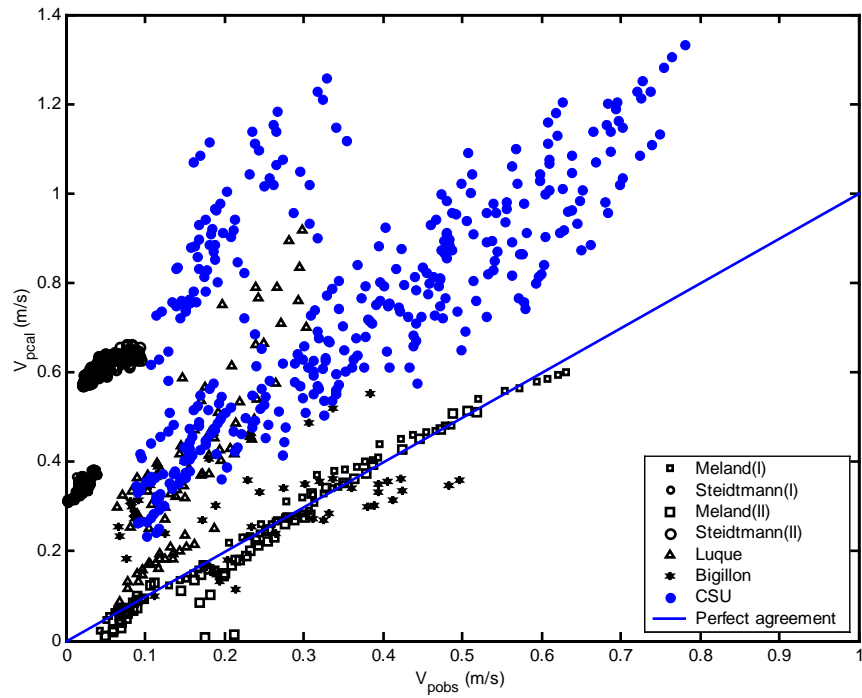


Figure 6.1: Comparison between Calculated and Observed  $V_p$  using Eq. (2.9)

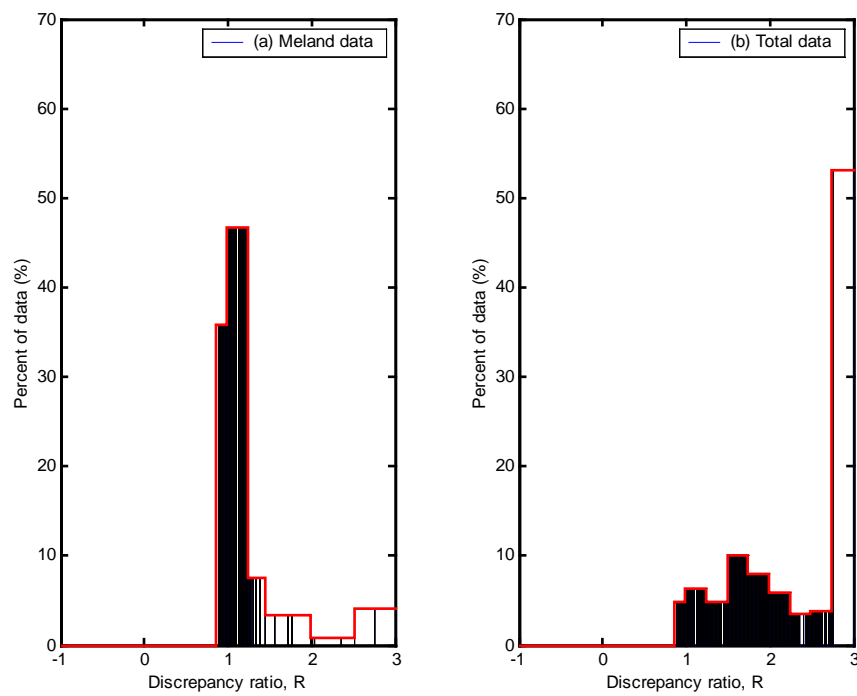


Figure 6.2: Discrepancy Ratio Distribution of  $V_p$  using Eq. (2.9)

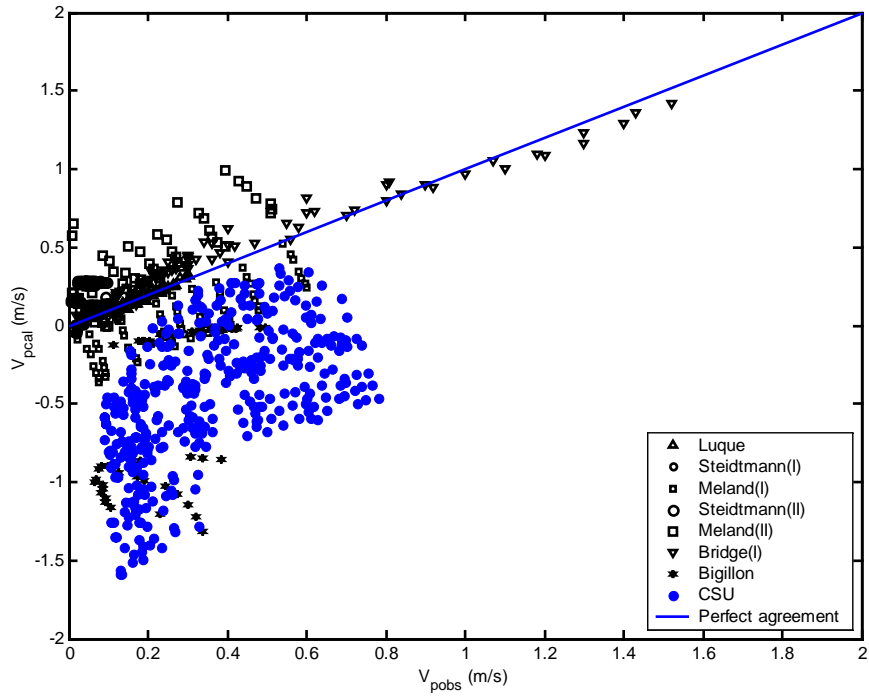


Figure 6.3: Comparison between Calculated and Observed  $V_p$  using Eq. (2.15)

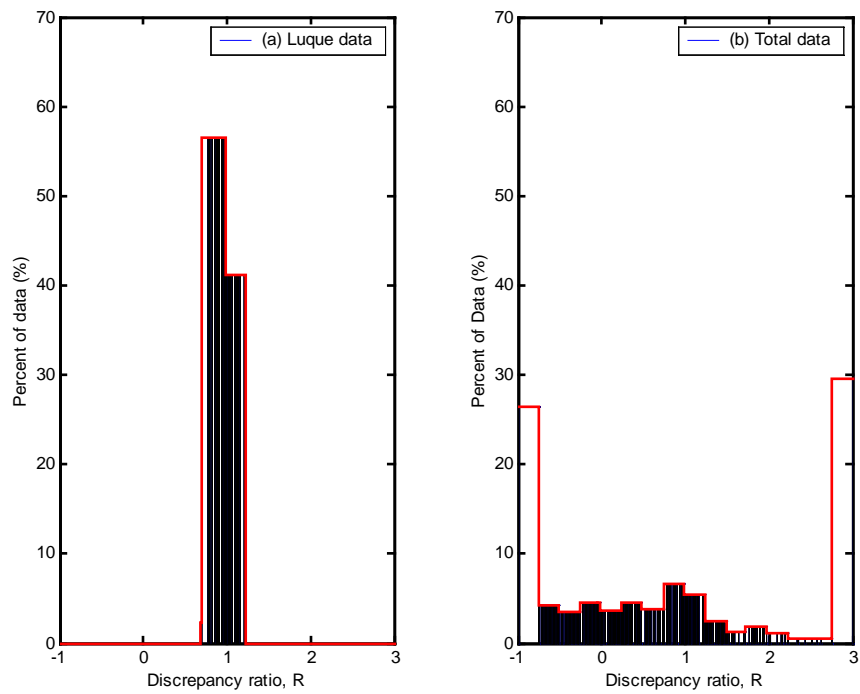


Figure 6.4: Discrepancy Ratio Distribution of  $V_p$  using Eq. (2.15)

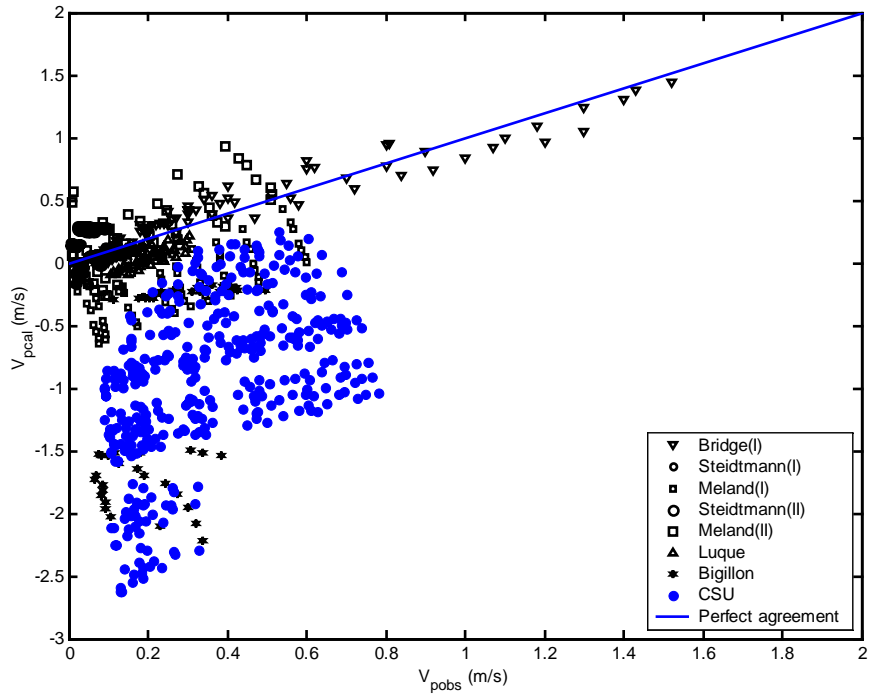


Figure 6.5: Comparison between Calculated and Observed  $V_p$  using Eq. (2.22)

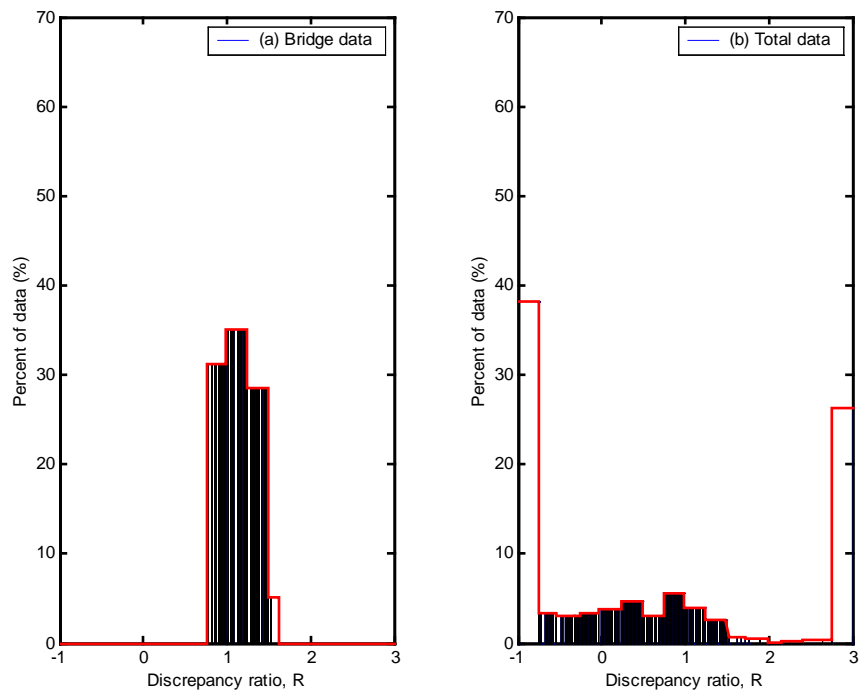


Figure 6.6: Discrepancy Ratio Distribution of  $V_p$  using Eq. (2.22)



In Table 6.1, the discrepancy ratio method indicates the goodness of fit between calculated and observed results. The percentages of data falling within the range of discrepancy ratios between 0.75 to 1.25 is 83% using Meland and Norrman's database and reduces to 12% when using the total database. Similarly, for Fernandez Luque and van Beek (1976), the percentages of data falling within the range of discrepancy ratios between 0.75 to 1.25 is 98% using Fernandez Luque and van Beek's database and reduces to 12% when using the total database. For Bridge and Dominic (1984), the percentages of data falling within the range of discrepancy ratios between 0.75 to 1.25 is 68% using Bridge and Dominic's database and reduces to 8.5% when using the total database. There is clear indication that equations of Meland and Norrman, Fernandez Luque and van Beek, and Bridge and Dominic fail to predict bedload particle velocity when applied the database from other sources.

Table 6.1: Summary of Comparison between Calculated and Observed  $V_p$

Equations  (1)	Data Sources  (2)	Data in Range of Discrepancy Ratio, $R_i$ (%)				No. of Data Points  (7)	$R^2$  (8)
		0.75-1.25	0.5-1.5	0.25-1.75	0-2.0		
		(3)	(4)	(5)	(6)		
Meland and Norrman (1966)	Meland	83	95	100	100	120	0.95
	Total <sup>(1)</sup>	12	17	28	100	1018	-0.4
Fernandez Luque and van Beek (1976)	Luque	98	100	100	100	85	0.93
	Total <sup>(1)</sup>	12	20	28	100	1018	-0.096
Bridge and Dominic (1984)	Bridge	68	96.5	100	100	77	0.93
	Total <sup>(1)</sup>	8.5	16	22.5	100	1018	-0.27

Where: (1) = Meland (1966) + Luque (1976) + Steidtmann (1982) + Bridge (1984) + CSU (1995) + Bigillon (2001)

### 6.3. HALFMOON CREEK, COLORADO

Dixon and Ryan (2000) conducted the data collection on 6/9/2000 at the Halfmoon Creek near Leadville, Colorado to observe the bed-load with the underwater video camera. The original movie was obtained from Dr. Bunte at the Engineering Research Center, Colorado State University. At Halfmoon Creek, they observed slurries of sand and pea gravel moving along the bed of the stream. Saltating particles in the coarse sand to fine gravel size class were typically moving too quickly to distinguish them when observing the video frame by frame. These smaller particles, however, were easily seen

while the video was moving at a normal or slow motion speed. Larger particles in the medium to coarse gravel size class were moving slower and were easily view frame by frame. Occasionally sweeps were observed that would briefly entrain small to medium sized gravel.

In some other cases a larger particle would turn over and come to rest. For example, at Halfmoon Creek they observed a relatively large particle (b-axis = 46 mm) move into the frame and come to rest behind a similar sized stationary particle (Fig. 6.7). This particle adjusted its orientation slightly during the next 17 seconds. The particle then rolled over and came to rest downstream against a partially buried large cobble (Fig. 6.8). The particle adjusted its position slightly during next 7 minutes and 19 seconds as smaller particles filled in and subsequently scoured away both on top and beneath. Just before the particle moved out of the view frame, there was a sweep of sediment followed by the particle being struck by another particle (b-axis = 26 mm) that initiated its movement out of the view frame (Fig. 6.9).



**Figure 6.7: Track of a single particle at Halfmoon Creek (Dixon and Ryan, 2000); a) the particle move into view and comes to rest.**

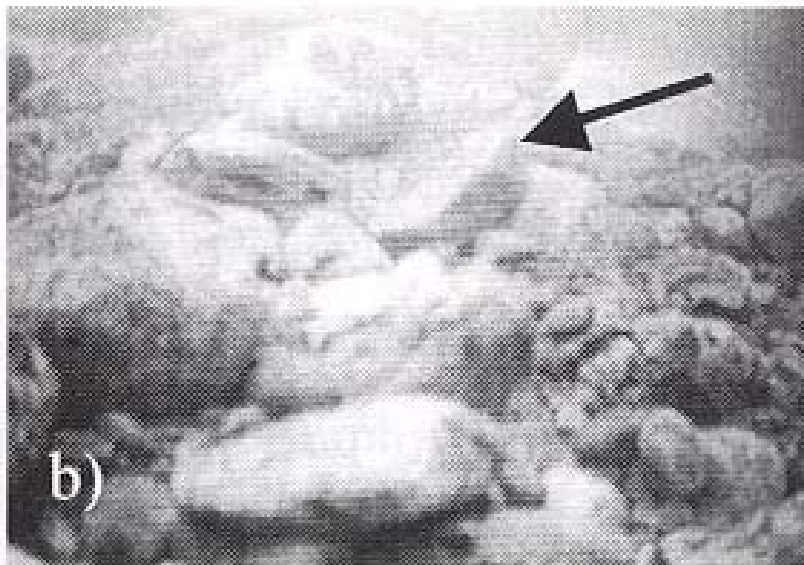


**Figure 6.8: Track of a single particle at Halfmoon Creek (Dixon and Ryan, 2000); b) after 17 seconds the particle moves 23 mm and comes to rest again.**

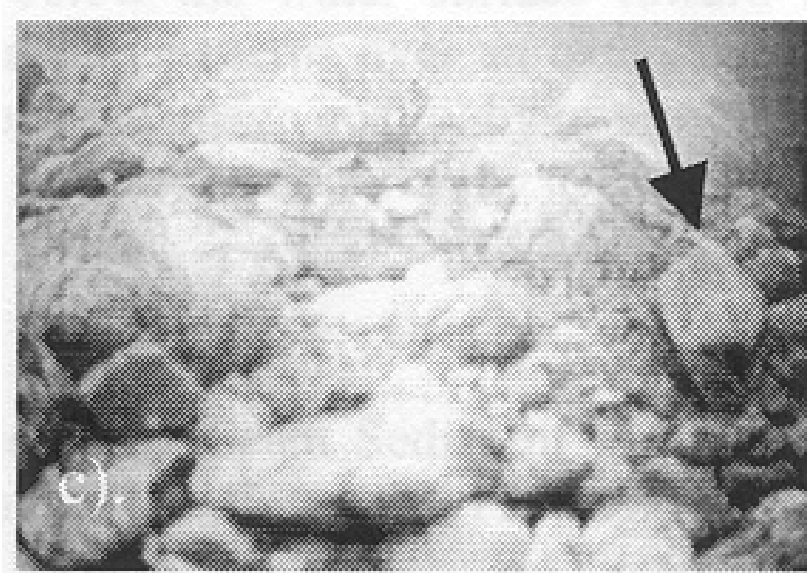


**Figure 6.9: Track of a single particle at Halfmoon Creek (Dixon and Ryan, 2000); c) after being stationary for over 7 minutes, the particle moves out of the view.**

Due to the lack of measured data, assumptions have been made to estimate bedload particle velocity conducted by Dixon and Ryan (2000). The estimated flow and sediment properties include:

1. Input data: Particle size  $d_s = 40$  mm, bed slope  $S_f = 0.005$ , flow rate  $Q = 5.2$  m<sup>3</sup>/s, mean flow velocity  $u_f = 1.27$  m/s, bed roughness  $k_s = 50$  mm, mean flow depth  $y = 480$  mm;
2. Calculation of basic parameters
  - Shear velocity  $u_* = [gR_h S_f]^{1/2} = [9.81 \times 0.48 \times 0.005]^{1/2} = 0.153$  m/s
  - Shields particle parameter  $\tau_{*ds} = u_*^2 / (G-1)gd_s = (0.153)^2 / (2.65-1) \times 9.81 \times 0.04 = 0.036$
  - Shields roughness parameter  $\tau_{*ks} = u_*^2 / (G-1)gk_s = (0.153)^2 / (2.65-1) \times 9.81 \times 0.05 = 0.029$

- Boundary relative roughness  $d_s/k_s = 40/50 = 0.8$ , and  $k_s/d_s = 1.25$
  - Particle shear Reynolds number  $Re_* = u_* d_s / \nu = 0.153 \times 0.04 / 1.004 \times 10^{-6} = 6096$
  - Dimensionless particle diameter  $d_* = d_s [(G-1)g/v^2]^{1/3} = 1009$
3. Calculation of bed roughness critical  $k_{sc}$  from Eqs. (5.37) and (5.38) to determine the motion of the particle; From Eq. (5.37), one obtains  $k_{sc1} = (0.153)^2 / (2.65-1) \times 9.81 \times 0.01 = 140$  mm which is comparable to  $k_{sc2} = 110$  mm, obtained from Eq. (5.38).
4. Calculation of  $V_{psmooth} = 3.64$  m/s by using Eq. (5.28);  $V_p = 1.4$  m/s, and 0.79 m/s by using Eqs. (4.20), and (5.34) respectively. Similarly, applied the above procedures for different  $d_s$ ,  $k_s$ , and the results is shown in Fig. 6.10.

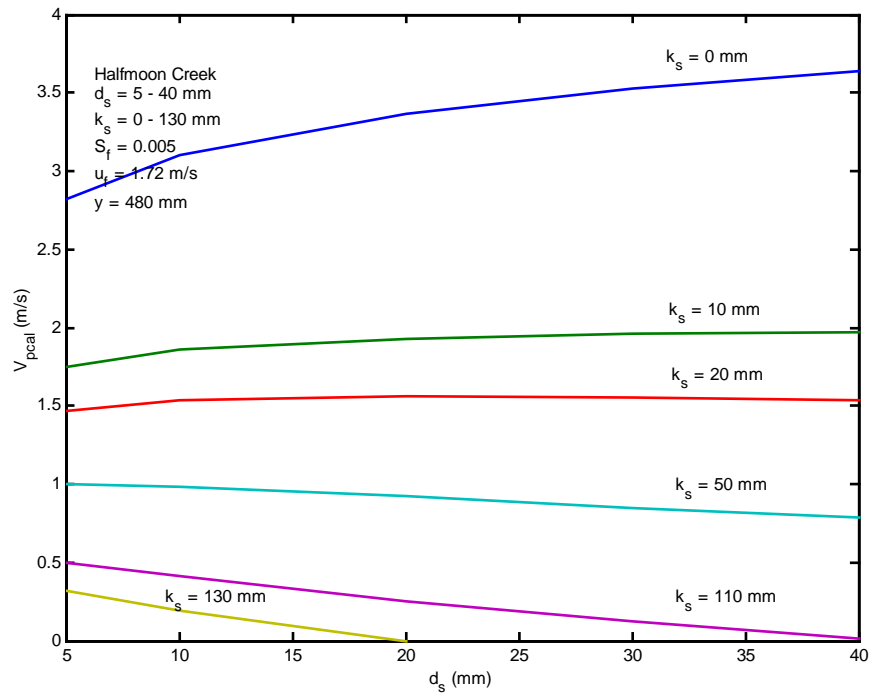


**Figure 6.10: Predicted  $V_p$  using Eq. (5.34) for different values of  $d_s$  and  $k_s$**

#### 6.4. AVILA MOUNTAIN, VENEZUELA

Mountain Avila, located on the north of Venezuela, witnessed on December 16<sup>th</sup>, 1999, a severe debris flows occurring over an area of about 500 km<sup>2</sup>. As a faulted-block mountain, the Avila region has abundant neotectonic uplift. Altitude steeply ascends from sea level to 2000 m within only 6-9 km from the ridge to the beach. Average sediment deposition in the river canyon was about 2-3 m and essentially buried most of the standing houses to the rafters. Water level marks as high as 7 m were observed in some of the buildings. The debris surges destroyed approximately 60% of the structures in the town of Tanaguarena and resulted in approximately 100 casualties. The mining operation (Cantera Cerro Grande) reports damages in excess of 3 million dollars in lost structures

and equipment. Structures in the canyon sustained impact damage from debris and boulders in surges. Some structures were completely destroyed by impact, scour and exposure to high velocity flows. Foundations were undermined by scour and collapsed. High velocity surges with boulders and debris were experienced across the entire canyon bottom as the channel conveyance velocity was lost. The structures that remain standing were buried in a coarse-grained mixture of boulders, cobbles, sand and debris (Bello et al., 2000). Fig. 6.11 shows an aerial view of Caraballeda looking Southwest with newly opened channels in the foreground and center right of photograph; Figs. 6.12, and 6.14 shows road damaged in Los Corales; Fig. 6.13 shows an aerial view of Caraballeda looking North with a massive deposition of coarse sediment delivered by debris flows and flash floods in Los Corales section; Fig. 6.15 shows a view of Los Corales with deposited boulder on the road; Fig. 6.16 shows Big boulders transported by debris flow on a fairly smooth bed; Fig. 6.17 Big boulder transported by debris flow in December 1999 in Caraballeda; Fig. 6.18 shows an aerial view of Los Corales sector of Caraballeda with damage to apartment building; Fig. 6.19 shows a view of Los Corales with damage to an apartment building; Fig. 6.20 shows a control canal for debris and mudflow at the Saint Julian Ravine.



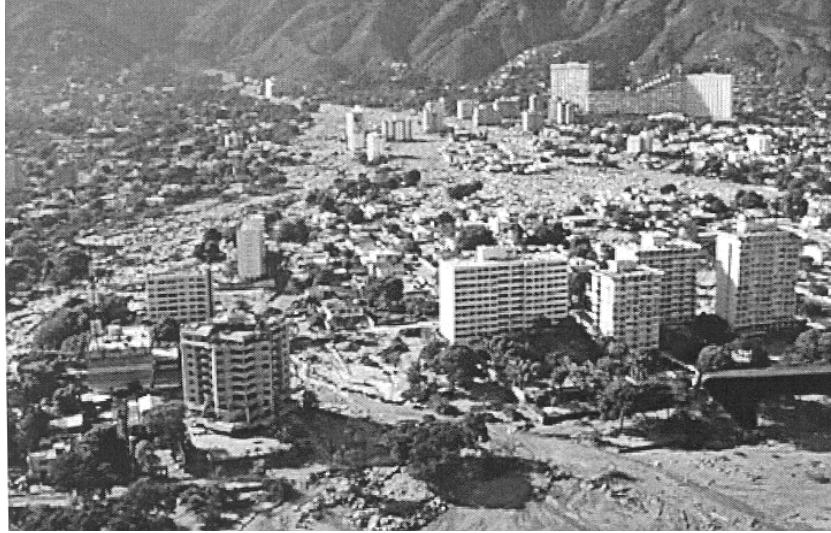


**Figure 6.11: Aerial view of Caraballeda looking Southwest (Larsen et al., 2000)**



**Figure 6.12: View of road damaged in Los Corales, Leon and Rojas, 2000 (personal communication)**



**Figure 6.13: Aerial view of Caraballeda looking North (Larsen et al., 2000)**



**Figure 6.14: View of road damaged in Los Corales, Leon and Rojas, 2000 (personal communication)**





**Figure 6.15: View of deposited boulders on the road in Los Corales, Leon and Rojas, 2000 (personal communication)**



**Figure 6.16: Big boulder transported by debris flow, Leon and Rojas, 2000 (personal communication)**

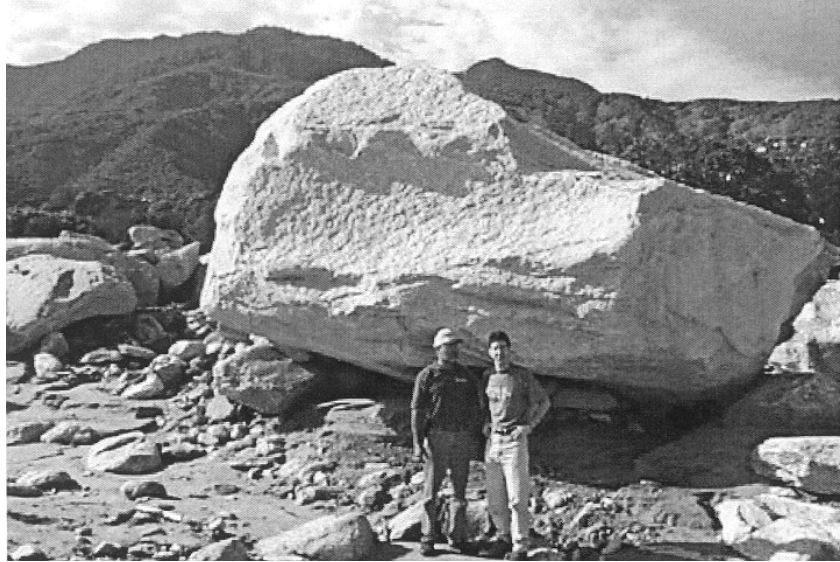


**Figure 6.17: Boulder transported by debris flow in December 1999 (Larsen et al., 2000)**



**Figure 6.18: Aerial view of Los Corales sector of Caraballeda (Larsen et al., 2000)**



**Figure 6.19: View of damaged to apartment building in Los Corales, Leon and Rojas, 2000 (personal communication)**



**Figure 6.20: Control canal for debris flow at the Saint Julian Ravine, Leon and Rojas, 2000 (personal communication)**

This particular example problem is derived from the measurement of field data, due to the insufficient of the nature of the database, some assumptions have been made. Given a uniform flow with  $T_{\text{water}} = 20^{\circ}\text{C}$ ,  $\nu_{\text{water}} = 1.004 \times 10^{-6} \text{ m}^2/\text{s}$ , particle diameter  $d_s = 0.1\text{-}3 \text{ m}$ ,  $G = 2.65$ ,  $k_s = 0\text{-}250 \text{ mm}$ , bed slope  $S_f = 0.01$  (Leon and Rojas, 2000, personal communication), flow depth  $y = 3 \text{ m}$  (Bello et al., 2000), determine the rolling bedload particle velocity,  $V_{\text{pcal}} = ?$

Solution:

1) Particle size  $d_s = 2 \text{ m}$ , bed slope  $S_f = 0.01$ , bed roughness  $k_s = 150 \text{ mm}$ , mean flow depth  $y = 3 \text{ m}$ ;

2) Calculation of basic parameters

- Shear velocity  $u_* = [gR_h S_f]^{1/2} = [9.81 \times 3 \times 0.01]^{1/2} = 0.54 \text{ m/s}$
- Shields particle parameter  $\tau_{*d_s} = u_*^2 / (G-1)gd_s = (0.54)^2 / (2.65-1) \times 9.81 \times 2 = 0.009$
- Shields roughness parameter  $\tau_{*k_s} = u_*^2 / (G-1)gk_s = (0.54)^2 / (2.65-1) \times 9.81 \times 0.15 = 0.12$
- Boundary relative roughness  $d_s/k_s = 13.33$ , and  $k_s/d_s = 0.075$
- Particle shear Reynolds number  $Re_* = u_* d_s / \nu = 0.54 \times 2 / 1.004 \times 10^{-6} = 1075697$
- Dimensionless particle diameter  $d_* = d_s [(G-1)g/\nu^2]^{1/3} = 50457$

3) Calculation of bed roughness critical  $k_{sc}$  from Eqs. (5.37) and (5.38) to determine the motion of the particle; From Eq. (5.37), one obtains  $k_{sc1} = (0.54)^2 / (2.65 - 1) \times 9.81 \times 0.01 = 1.8$  m which is about ten times  $k_{sc2} = 170$  mm, obtained from Eq. (5.38).

4) Calculation of  $V_{psmooth} = 19.85$  m/s by using Eq. (5.28);  $V_p = 0.9$  m/s by using Eq. (5.34). Similarly, applied the above procedures for different  $d_s$ , and  $k_s$ , and the results is shown in Fig. 6.21, where, proposed formula Eq. (5.34) gives realistic estimates of particle velocity values, and therefore it could help define particle velocities during devastating floods.

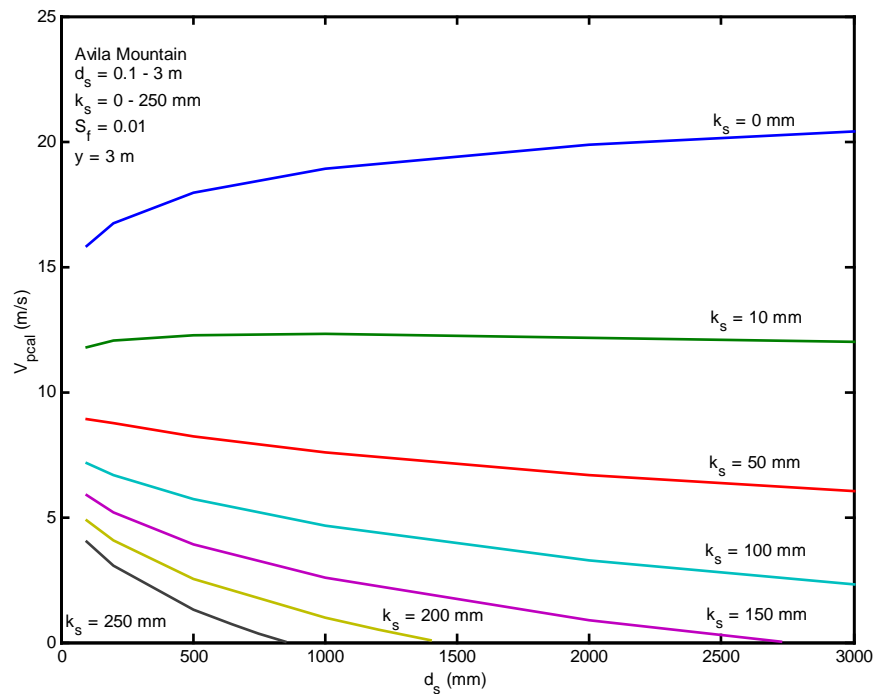


Figure 6.21: Predicted  $V_p$  using Eq. (5.34) for different values of  $d_s$  and  $k_s$

# CHAPTER 7

## SUMMMARY AND CONCLUSIONS

This study aims at defining the bedload particle velocity in smooth and rough open channels as a function of the following variables: bed slope  $S_f$ , flow depth  $y$ , viscosity of the fluid  $\nu$ , particle size  $d_s$ , bed roughness  $k_s$ , particle specific gravity  $G$ , and gravitational acceleration  $g$ .

Sources of data used in this analysis include 6 laboratory data sets for a total of 1018 points collected from different sources. In previous studies documented in the literature, 120 points could be obtained from Meland and Norrman (1966), 85 points from Fernandez Luque and van Beek (1976), 330 points from Steidtmann (1982), and 77 points from Bridge and Dominic (1984). Additionally, 356 points were collected at CSU on plates with bed roughness set at 1.2 mm, 1.7 mm, 2.4 mm, and 3.4mm, and 50 points from Bigillon (2001), with bed roughness set at 1.5 mm and 3 mm. Each set of data contains a complete record for flow and bedload particles information. These data are limited to the particle sizes with median diameters in the range of 0.21 to 29.3 mm, bed



roughness in the range of 0.19 to 7.76 mm, average flow velocity in the range of 0.22 to 1.00 m/s, shear velocity in the range of 0.0097 to 0.1108 m/s, flow depth in the range of 2.13 to 180 mm, and slope in the range of 0.00073 to 0.05.

The existing formulas such as Meland and Norrman (1966), Fernandez Luque and van Beek (1976), and Bridge and Dominic (1984) are verified with the laboratory measurements. Results show that all of the existing formulas fail to predict  $V_p$  when applied to the data sources other than their own database.

The analysis of the data leads to the following conclusions:

- (1) For a smooth bed ( $k_s = 0$ ), the rolling bedload particle velocity  $V_p$  increases with particle sizes  $d_s$ ;
- (2) For a rough bed ( $k_s > 0$ ), particle velocity decreases with particle density  $G$ , thus lighter particles move faster than heavier ones; and on a very rough boundary  $V_p$  decreases with particle sizes;
- (3) Bedload particles move at values of the Shields parameter  $\tau_{*ds}$  below the critical value of  $\tau_{*dsc} = 0.047$ ;
- (4) Very few of the observed particles moved at values of Shields roughness parameter  $\tau_{*ks}$  less than 0.01;
- (5) Particles are observed to move at values of the Shields roughness parameter  $0.01 < \tau_{*ks} < 0.15$ ;
- (6) The ratio of particle velocity  $V_p$  to mean flow velocity  $u_f$  lies in the range of 0.2 to 0.9, while Kalinske (1942) suggested 0.9 to 1.0;

(7) The ratio of particle velocity  $V_p$  to shear velocity  $u_*$  lies in the range of 2.5 to 12.5, compared to the values cited in the literature  $6.0 < V_p/u_* < 14.3$ ;

New methods for predicting transport velocities of bedload particles in rough and smooth open channels are examined. Two approaches for transport velocities of bedload particles were considered. The first approach combines dimensional analysis and regression analysis to define bedload particle velocity as a power function of the Shields parameter  $\tau_*$ , boundary relative roughness  $k_s/d_s$ , dimensionless particle diameter  $d_*$ , and excess specific gravity  $(G-1)$ . The second approach considers the transport velocity of a single particle on a smooth bed. The reduction in particle velocity due to bed roughness is then examined through a theoretical and empirical analysis. Results show that the bedload particle velocity on smooth beds is approximately equal to the flow velocity at the center of the particle. Bed roughness decreases the transport velocity of rolling bedload particles.

Comparatively, The first approach gives satisfactory results, except when  $k_s$  equals 0, then  $V_p$  goes to  $\infty$ , and when  $k_s$  is large,  $V_p$  does not stop (unbounded); for the second approach  $V_{pmax}$  when  $k_s$  equals 0, and when  $V_p$  equals 0, then values of  $k_s$  follow the criteria a and b described in Chapter 5 (section 5.4) and there is an insufficient evidence to suggest that one criteria is better than other.

The analysis shows that the proposed formula, Eq. (5.34) provides much better predictions than the existing formulas. Plots showing the comparison between calculated and observed bedload particle velocity and the discrepancy ratio distribution are shown in Figs. 5.12, and 5.13 respectively; the discrepancy ratio for the predictions of bedload particle velocity using the newly proposed formula, Eq. (5.34) are normally distributed

and have higher density (close to perfect agreement) than all other formulas. Predictions with extreme discrepancy ratios ( $R_i < -1.0$  and  $R_i > 3.0$ ) are very limited in utility; and less than 2.5 % of data with discrepancy ratio  $R_i < 0.75$  and  $R_i > 1.25$ . The statistical results of calculated  $V_p$  are shown in Table 5.1, which indicate that the newly proposed formula Eq. (5.34) gives the best prediction amongst all formulas. In addition, the proposed formula, Eq. (5.34) is also verified with the most current laboratory data from Bigillon (2001). Field application to Halfmoon Creek (Dixon and Ryan, 2000), and the devastating flood of the Avila Mountain in Venezuela in December 1999 (Leon and Rojas, 2000, personal communication), the results give realistic estimates of particle velocities.

# REFERENCES

- Abbott, J. E. and Francis, J. R. D. 1977. "Saltation and suspension trajectories of solid grains in a water stream." *Philos. Trans. Roy. Soc. London*, 284 (1321): 225-254p.
- Aguirre, M. A., Calvo, A., Henrique, C., Ippolito, I., and Bideau, D. 1997. "Stopping distance: A way to understand energy dissipation in a granular flow experimentally modeled." *Powders and Grains 97*, Behringer & Jenkins (eds), ISBN 90 5410 884 3, 471-473p.
- Aksoy, S. 1973. "Fluid forces acting on a sphere near a boundary." *Proc. 15<sup>th</sup> Congress, IAHR*, 121-224p.
- Alonso, C. V. 1980. "Selecting a formula to Estimate Sediment Transport in Non-Vegetated Channels." *CREAMS: A Field Scale Model for Chemicals, Runoff, Erosion from Agricultural Management Systems*, Conservation Research Report No. 26, United States Department of Agriculture, 1980
- Alonso, C. V. and C. Mendoza, 1992. "Near-Bed Sediment Concentration in Gravel Bedded Streams." *Water Resources Research WRERAQ*; Vol. 28, No. 9, (September 1992): 2459-2468.
- Ancey, C., Evesque, P. and Coussot, P. 1996. "Motion of a single bead on a bead row theoretical investigations." *J. Phys. I, France*, 6:725-751p.
- Ancey, C., Evesque, P. and Coussot, P. 1997. "Analogy between granular flows down an inclined channel and the motion of a bead down a bumpy line." *Powders and Grains 97*, Proceedings of the 3<sup>rd</sup> Int'l. Conf. On Powders and Grains, 475-478p.

- Andrews, E. D. 1984. "Bed-Material Entrainment and Hydraulic Geometry of Gravel-Bed Rivers in Colorado." Geological Society of America Bulletin; V. 95, No. 3, (March 1984): 371-378.
- Andrews, E. D. 1983. "Entrainment of Gravel from Naturally Sorted Riverbed Material." U.S. Geological Survey, Geological Society of America Bulletin. V. 94 (October 1983): 1225-1231.
- Andrews, E. D. and G. Parker, 1987. "Formation of a Coarse Surface Layer as the Response to Gravel Mobility." Sediment Transfer in Gravel-Bed Rivers. John Wiley & Sons; New York., p 269-300.
- Andrews, E. D. and J. D. Smith, 1992. "A Theoretical Model for Calculating Marginal Bedload Transport Rates of Gravel. In Dynamics of Gravel-Bed Rivers." ed., by P. Billi, R. D. Hey, C. R. Thorne & P. Tacconi, John Wiley & Sons Ltd.
- Ashworth, P. J. and R. I. Ferguson, 1989. "Size-Selective Entrainment of Bed Load in Gravel Bed Streams. Water Resources Research WRERA0; Vol. 25, No.4, (April 1989): 627-634.
- Ashworth, P. J. and R. I. Ferguson, 1989. "Size-Selective Entrainment of Bed Load in Gravel Bed Streams. Water Resources Research WRERA0; Vol. 25, No.4, (April 1989): 627-634.
- Bagnold, R. A. 1956. "The flow of cohesionless grains in fluids." Philos. Trans. R. Soc. London Ser. A, 249, 235-297.
- Bagnold, R. A. 1973. "The nature of saltation and of bed-load transport in water." Proc. R. Soc. London Ser. A, 332, 473-504.

- Bagnold, R. A., 1977. "Bed Load Transport by Natural Rivers." *Water Resources Research*, Vol. 13, No. 2 (April 1977).
- Bello, M. E., O'Brien, J. S., Lopez, J. L., and Garcia-Martinez, R., 2000. "Simulation of flooding and debris flows in the Cerro Grande River." *Hydrologic and Geomorphologic Evaluation of the debris flows*.
- Best, J., Bennet, S., Bridge, J. and Leeder, M. 1997. "Turbulence modulation and particle velocities over flat sand beds at low transport rates." *J. Hydraulic Engineering*, Vol. 123, No. 12, 1118-1129p.
- Bigillon, F. 2001. "Etude du mouvement bidimensionnel d'une particule dans un courant d'eau sur forte pente." Ph.D.'s dissertation, Universite Grenoble 1- Joseph Fourier, U.F.R de Mechanique.
- Bouvard, M. and Petkovic, S. 1985. "Vertical dispersion of spherical, heavy particles in turbulent open channel flow." *J. Hydraulic Research*, Vol. 23, No. 1, 5-19p.
- Bray, D. I. 1972. "Generalized Regime-Type Analysis of Alberta Rivers." Thesis presented to the University of Alberta, at Edmonton, Alberta, Canada, in 1972, in partial fulfillment of the requirements for the degree of Doctor of Philosophy.
- Brayshaw, A. C. 1985. "Bed Microtopography and Entrainment Thresholds in Gravel-Bed Rivers." *Geological Society of America Bulletin*; Vol. 96, No. 2, (February 1985): 218-223.
- Brayshaw, A. C., Lynne E. Frostick, and Ian Reid, 1983. "The Hydrodynamics of Particle Clusters and Sediment Entrainment in Coarse Alluvial Channels." *Sedimentology*, Editors: M. E. Tucker, Durham, P. H. Bridges, Derby and J. S. Bridge, Binghamton. Volume 30, No. 1.

- Bridge, J. S. 1981a. "A discussion of Bagnold's (1956) bedload transport theory in relation to recent developments in bedload modeling." *Earth Surf. Proc.*, 6, 187-190.
- Bridge, J. S. 1981b. "Bed shear stress over sub aqueous dunes, and the transition to upper-stage plane beds." *Sedimentology*, 28, 33-36.
- Bridge, J. S. 1982a. "Bed shear stress over sub aqueous dunes, and the transition to upper-stage plane beds: Reply." *Sedimentology*, 29, 744-747.
- Bridge, J. S. 1982b. "Hydraulic interpretation of grain-size distributions using a physical model for bedload transport: Reply." *J. Sediment. Petrol.*, 52 1336-1338.
- Bridge, J. S., and Javis, J. 1982. The dynamics of river bend: A study in flow and sedimentary processes, *sedimentology*, 29, 499-541, 1982.
- Bridge, J. S. and Dominic, D. F. 1984. "Bed load grain velocities and sediment transport rates." *J. Water Resources Research*, 20(4): 476-490p.
- Bridge, J. S. and Bennett, S. J. 1992. "A model for the entrainment and transport of sediment grains of mixed sizes, shapes and densities." *J. Water Resources Research*, Vol. 28, No. 2, 337-363p.
- Brownlie, W. R. 1981. "Prediction of flow depth and sediment discharge in open channels." California Institute of Technology, W. M. Keck Laboratory of Hydraulics and Water Resources, Report No. KH-R-43A.
- Burkham, D. E. and Dawdy D. R. 1976. "Resistance Equation for Alluvial Channel Flow." *Journal of the Hydraulics Division, Proceedings ASCE*, Vol. 102, No. HY10.

- Burrows, R. L. and Harrold, P. E. 1983. "Sediment Transport in the Tanana River near Fairbanks, Alaska, 1980-81." United States Geological Survey. Water Resources Investigation Report 83-4064.
- Burrows, R. L. and Emmett, W. W. and Parks, B. 1981. "Sediment Transport in the Tanana River near Fairbanks, Alaska, 1977-1979." United States Geological Survey. Water Resources Investigation Report 81-20.
- Carling, P. A. 1983. "Threshold of Coarse Sediment Transport in Broad and Narrow Natural Streams." *Earth Surface Processes and Landforms* Vol. 8: 1-18.
- Carson, M. A. and G. A. Griffiths, 1985. "Tractive Stress and the Onset of Bed Particle Movement in Gravel Stream Channels: Different Equations for Different Purposes." *J. Hydrology JHYDA7*; Vol. 79, No. 3/4.
- Carty, J. 1957. "Resistance coefficients for sphere on plane boundary." B. S. Thesis, MIT.
- Chang, Howard H. 1988. "Fluvial Processes in River Engineering." New York: John Wiley & Sons.
- Cheng, D. H. and Clyde, C. G. 1972. "Instantaneous hydrodynamic lift and drag forces on large roughness elements in turbulent open channel flow." *Int'l Sedimentation, Symp. to Honor H. A. Einstein*, pp3-1:20.
- Cheng, N-S. 1997. "Simplified settling velocity formula for sediment particle." *J. Hydraulic Engineering*, Vol. 123, No. 2, 149-152p.
- Cheng, N-S. 1997. "Effect of concentration on settling velocity of sediment particles." *J. Hydraulic Engineering*, Vol. 123, No. 8, 728-731p.



- Chien, N. and Wan, Z. H. 1983. "Sediment transport mechanics." Science Press, Beijing, China (in Chinese).
- Chiew, Y-M. and Parker, G. 1994. "Incipient sediment motion on non-horizontal slopes." J. Hydraulic Engineering, Vol. 32, No. 5, 649-660p.
- Childers, Dallas, Stephen E. Hammond, and William P. Johnson, 1988. "Hydrologic Data for Computation of Sediment Discharge, Toutle and North Fork Toutle Rivers near Mount St. Helens, Washington, Water Years 1980-84." U.S. Geological Survey Open-File Report 87-548. Vancouver, Washington.
- Church, M., J. F. Wolcott, and W. K. Fletcher, 1991. "Test of Equal Mobility in Fluvial Sediment Transport: Behavior of the sand Fraction." Water Resources Research WRERAQ; Vol. 27, No. 11, (November 1991): 2941-2951.
- Clauser, F. H. 1954. "Turbulent boundary layers in adverse pressure gradients." J. Aeronautical Science, Vol. 21, pp. 91-108p.
- Colby, B. R. 1964. "Discharge of sands and mean velocity relationship in sand bed streams." Sediment Transport in Alluvial Channels, Geological Survey Professional Paper 462-A.
- Coleman, N. L. 1967. "A theoretical and experimental study of drag and lift forces acting on a sphere resting on hypothetical stream bed." Proc. 12<sup>th</sup> Cong. Intern. Assoc. Hydr. Res., 3.
- Coleman, N. L. 1981. "Velocity profiles with suspended sediment." J. Hydraulic Research, Vol. 19, No. 3, 211-229p.

- Copeland, R. R., and Thomas, W. A. 1989. "Corte Madera Creek Sedimentation Study." Technical Report HL-89-6, Final Report, Waterways Experiment Station, Corps of Engineers, Vicksburg, MS 39181, p46 +appendix. April 1989.
- Davis, A. C., Ellett, B. G. S. and Jacob, R. P. 1998. "Flow measurement in sloping channels with rectangular free overfall." *J. Hydraulic Engineering*, Vol. 124, No. 7, 760-763p.
- Dixon, M. and Ryan S. 2000 "Using an underwater video camera for observing bedload transport in mountain stream." Proc. of the 7<sup>th</sup> Interagency Sedimentation Conference, March 25 to 29, 2000, Reno, Nevada.
- Dominic, D. F. 1983. "Evaluation of bedload sediment transport models." Master's thesis, State Univ. of N. Y. at Binghamton.
- Einstein, H. A. 1950. "The bed load function for sediment transport in open channel flows." Technical Report No. 1026, USDA Soil Conservation Service, Washington D.C.
- Einstein, H. A. and El-Sami, E. A. 1949. "Hydrodynamic forces on a rough wall." *Rev. Modern Physics*, 21(3), 520-524p.
- Einstein, H. A. 1942. "Formulas for the Transport of Bed-Load." *Transactions of the American Society Civil Engineers*, Vol. 107.
- Emmett, W. W. and Seitz. 1974. "Suspended and Bed load sediment transport in the Snake and Clearwater Rivers in the vicinity of Lewiston, Idaho." U.S. Geological Survey Basic-Data Report.
- Engelund, F. and J. Fredsoe, 1976. "A sediment transport model for straight alluvial channels." *Nordic Hydrol.*, 7, 293-306.

- Engelund, F., and J. Fredsoe, 1982a. "Sediment ripples and dunes." *Ann. Rev. Fluid Mech.*, 14, 13-37.
- Fenton and Abbot, 1977. "Initial Movement of Grain on a StreamBed: The effects of Relative Intrusion." *Proceedings of the Royal Society of London, A*, Vol. 352.
- Fernandez Luque, R. and van Beek, R. 1976. "Erosion and transport of bed load sediment." *J. Hydraulic Research*, 14(2): 127-144p.
- Fleming, C. A., and J. N. Hunt, 1976. "A mathematical sediment transport model for unidirectional flows." *Proc. Inst. Civ. Eng.*, 61, 297-310.
- Francis, J. R. D. 1973. "Experiments on the motion of solitary grains along the bed of a water stream." *Proc. Roy. Soc. London A* 332:443-471p.
- Garde, R. and Sethuraman, S. 1969. "Variation of drag coefficient of a sphere rolling along a boundary." *La Houille Blanche*, No 7. (or this paper can also be found in *Selected Works of R. J. Garde*, Hydraulic Engineering Section, Civil Engineering Department, University of Roorkee, India, 76-81p.
- Gessler, J. 1976. "Stochastic Aspects of Incipient Grain Motion on Riverbeds." *Stochastic Approaches to Water Resources*, Volume II; Chapter 25, Colorado State University, Fort Collins, (1976): 25-1 – 25-6.
- Gessler, J. 1971. "Beginning and ceasing of sediment motion." *River Mechanics*, Fort Collins, Colorado, H. W. Shen, ed., 1, 7-1 – 7-22.
- Gilbert, G. B. 1914. "Transport of Debris by Running Water." *U.S. Geological Survey Professional Paper.*, 86, 1914.
- Gilbert, G. K. 1914. "The transportation of debris by running water." *USGS Prof. Paper* No. 86, 259.

- Gomez, B. and M. Church, 1989. "Assessment of Bed Load Sediment Transport Formulae for Gravel Bed Rivers." Water Resources Research WRERAO; Vol. 25, No. 6, (June 1989): 1161-1186.
- Graf, W. H. 1984. "Hydraulics of sediment transport." Water Resources Publications, LLC.
- Guy, H. P. and Norman, V. W. 1970. "Field methods for measurement of Fluvial Sediment." U.S. Geological Survey Techniques of Water Resources Investigations, Book 3. U.S. Government Printing Office, Washington.
- Helley, E. J., and Smith Einchell, 1971. "Development and calibration of a pressure difference bed load sampler." U.S. Geological Survey Open-File Report.
- Hubbell, D. W., H. H. Stevens, Jr., J. V. Skinner, and J. P. Beverage, 1987. "Laboratory Data on Coarse-Sediment Transport for Bedload Sampler Calibrations. U.S. Geological Survey Water-Supply Paper 2299, Denver, Colorado.
- Ikeda, S. 1971. "Some studies on the mechanics of bed load transport." Proc. Jpn. Soc. Civ. Eng. 185:61-69.
- Ikeda, H. and Iseya, F. 1988. "Experimental study of heterogeneous sediment transport." Environmental Research Center, University of Tsukuba, ISSN 0286-5408.
- Ippen, A. T. and Verma, R. P. 1955. "Motion of particles on bed of a turbulent stream." Trans. Am. Soc. Civ. Eng. 921-938p.
- Jan, C. D. 1992. "Movement of a sphere moving over smooth and rough inclines." Ph. D. dissertation., University of California at Berkeley, California.
- Jan, C. D. and Chen, J. C. 1998. "Movements of a sphere rolling down an inclined plane." Journal of Hydraulics Research., ASCE. Vol. 35, No. 5.

- Jones, M. L., and Seitz, H. R., 1980. "Sediment transport in the Snake and Clearwater Rivers in the vicinity of Lewiston, Idaho." United States Geological Survey Open-File Report 80-690.
- Julien, P. Y., Chen, Y. C. 1989. "Experimental study of horizontal lamination in a recirculating flume." Report CER88-89-PYJ-YC14, CSU, May 1989,63p.
- Julien, P. Y. and Lan, Y. Q. 1989. "Experimental formation of alluvial deposits in a wide rectangular flume." Report CER89-90PYJ-YQL2, CSU, July 1989, 29p.
- Julien, P. Y. and Lan, Y. Q. 1990. "Laboratory experiments on sedimentation, lamination and descicattion of sediment mixtures." Report CER89-90PYJ-15, CSU, May 1990, 165p.
- Julien, P. Y. 1995. "Erosion and Sedimentation" Cambridge University Press.
- Julien, P. Y., Meier, C. I. and Blackard, B. 1995. "Laboratory measurements of bed load particle velocities." Report CER95-96PYJ-MCI-BB., Department of Civil Engineering, Colorado State University, Fort Collins, Colorado.
- Julien, P. Y., Lan Y. Q, and Raslan, Y. 1997. "Experimental mechanics of sand stratification." Powders and Grains 97, Proceedings of the 3<sup>rd</sup> Int'l. Conf. On Powders and Grains, 487-490p.
- Julien, P. Y. and Guo, J. 1997. "Transport velocities of individual particles over smooth open channel bed." Report CER97-98PYJ-GJ1., Department of Civil Engineering, Colorado State University, Fort Collins, Colorado.
- Julien, P. Y. and Leon, C. 2000. "Mud floods, mudflows and debris flows classification, rheology and structural design."
- Julien, P. Y. 2002. "River Mechanics." Cambridge University Press.

- Kalinske, A. A. 1942. "Discussion of " Settling velocity and flume behavior of non-spherical particles" by Krumbein, W. C., EOS Trans. AGU 23:632-633p.
- Kalinske, A. A. 1947. "Movement of sediment as bedload in rivers." Eos. Trans. AGU, 28, 615-620.
- Karim, M. F. and Kennedy, J. F. 1984. "A short list of sediment transport equations." Iowa Institute of Hydraulic Research, The University of Iowa, Iowa City, Iowa 52242, July 1984, p33.
- Klimek, K. E. 1997. "Spherical particle velocities on rough dry surfaces." M.S. Thesis, Department of Civil Engineering, Colorado State University, Fort Collins, Colorado.
- Kirkgoz, M. S. 1989. "Turbulent velocity profiles for smooth and rough open channel flow." J. Hydraulic Engineering, ASCE, 115(11), 1543-1561p.
- Kirkgoz, M. S. and Ardiclioglu, M. 1997. "Velocity profile of developing and developed open channel flow." J. Hydraulic Engineering, ASCE. Vol. 123, No. 12, 1099-1105p.
- Knott, James M., and Stephen W. Lipscomb, 1983. "Sediment Discharge Data for Selected Sites in the Susitna River Basin Alaska, 1981-82." U.S. Geological Survey Open-File Report 83-870, Prepared in cooperation with the Alaska Power Authority. U.S. Department of the Interior Geological Survey. Anchorage, Alaska.
- Knott, James M., and Stephen W. Lipscomb, 1985. "Sediment Discharge Data for Selected Sites in the Susitna River Basin Alaska, October 1982 to February

- 1984.” U.S. Geological Survey Open-File Report 85-157, prepared in cooperation with the Alaska Power Authority. United States Department of the Interior.
- Knott, James M., Stephen W. Lipscomb, and Terry W. Lewis, 1986. “Sediment Transport Characteristics of Selected Streams in the Susitna River Basin, Alaska, October 1983 to September 1984.” U.S. Geological Survey Open-File Report 86-424W, Prepared in cooperation with the Alaska Power Authority. U.S. Department of the Interior Geological Survey.
- Knott, James M., Stephen W. Lipscomb, and Terry W. Lewis, 1987. “Sediment Transport Characteristics of Selected Streams in the Susitna River Basin, Alaska: Data for Water Year 1985 and Trends in Bedload Discharge, 1981-85.” U.S. Geological Survey Open-File Report 87-229. Prepared in cooperation with the Alaska Power Authority. U.S. Department of the Interior Geological Survey.
- Komar, P. D. 1987. “Selective Grain Entrainment by a Current from a Bed of Mixed Sizes: A Reanalysis.” *J. Sedimentary Petrology*, Vol. 57, No. 2, (March 1987):203-211.
- Krumbein, W. C. 1942. “Settling velocities and flume behavior of non-spherical particles.” *EOS Trans. AGU* 23:621-632p.
- Kuhnle, R. A. 1993. “Incipient motion of sand gravel sediment mixtures.” *J. Hydraulic Engineering*, Vol. 119, No. 12, 1400-1415p.
- Kundu, P. K. 1990. “Fluid Mechanics.” Academic Press, Inc.
- Lamberti A. and Paris E. 1992. “Analysis of armouring processes through laboratory experiment.” *Dynamics of Gravel-Bed Rivers*. Edited by Billi, P., Hey R. D., Trome C. R., Tacconil P., John Wiley & Sons LTD, West Sussex, England.

- Larsen, M. C. and Sierra, H. T. 2000. "Preliminary observations: flash-flood and landslide disaster of December, 1999, north coast of Venezuela."
- Laursen, E. M. 1958. "The Total Load of Streams." J. Hydraulics Division, Proceedings ASCE, Vol. 84, No. HY1, February 1958. P 1530-1 –1530-36.
- Lee, H-Y. and Hsu, I-S. 1996. "Particle spinning motion during saltating process." J. Hydraulic Engineering, Vol. 122, No. 10, 587-590p.
- Limerinos, J. T. 1970. "Determination of the Manning Coefficient from Measured Bed Roughness in Natural Channels." Water Supply Paper 1898b, U.S. Geological Survey.
- Ling, C-H. 1995. "Criteria for incipient motion of spherical sediment particles." J. Hydraulic Engineering, Vol. 121, No. 6, 472-478p.
- Low, H. S. 1989. "Effect of sediment density on bedload transport." J. of Hydraulic Engineering, Vol. 115, No. 1, 124-138p.
- Mantz, P. A. 1977. "Incipient transport of fine grains and flakes by fluids: Extended Shields diagram." J. Hydraul. Div. Am. Soc. Civ. Eng., 103, 601-614.
- Mantz, P. A. 1980. "Low sediment transport rates over flat bed." J. Hydraul. Div. Am. Soc. Civ. Eng., 106, 1173-1189.
- Meland, N. and Norrman, J. O. 1966. "Transport velocities of single particles in bed load motion." Geografiska Annaler 48 A (4):165-182p.
- Meier, C. I. 1995. "Transport velocities of single bed load grains in hydraulically smooth open channel flow." Master's thesis, Department of Civil Engineering, Colorado State University, Fort Collins, Colorado.



- Meyer-Peter, E. and Muller, R. 1948. "Formulas for bed load transport." Stockholm, Sweden, International Association for Hydraulic Structures Research, 2<sup>nd</sup> meeting., p. 39-64.
- Milhous, R. T., J. B. Bradley, and C. L. Loeffler, 1986. "Sediment Transport Simulation an Armoured Stream." Proceedings of the 4<sup>th</sup> Federal Interagency Sedimentation Conference; March 24-27, 1986, Las Vegas, Nevada. Volume II, p 270-280.
- Milhous, R. T. 1973. "Sediment Transport in Gravel-Bottomed Stream." Thesis, Oregon State University.
- Miller, R. L., and R. J. Byrne, 1966. "The angle of repose for a single grain on a fixed rough bed, *Sedimentology*, 6, 303-314.
- Miller, M. C., McCave, I. N. and Komar, P. D. 1977. "Threshold of sediment motion under unidirectional currents." *J. Sedimentology*, 24, 507-527p.
- Muste, M. and Patel, V. C. 1997. "Velocity profiles for particles and liquid in open channel flow with suspended sediment." *J. Hydraulic Engineering*, Vol. 123, No. 9, 742-751p.
- Naden, P. S. 1981. "Gravel in motion." working Pap. 321, School of Geogr., Univ of Leeds, Leeds, U.K.
- Nezu, I. and Rodi, W. 1986. "Open channel flow measurements with a lazer doppler anemometer." *J. Hydr. Engrg., ASCE*, 112(5), 335-355p.
- Nino, Y., Garcia, M. and Ayala, L. 1994. "Gravel saltation, 1. Experiments." *J. of Water Resources Research*, Vol. 30, No. 6, 1907-1914p.
- Parsons, D. A. 1972. "The speed of sand grains in laminar flow over a smooth bed." In: Shen, H. W. (Ed). *Sedimentation Symposium to honor Einstein*, H. A.

- Paintal, A. S., 1971. "Concept of critical Shear Stress in Loose Boundary Open Channels." J. Hydraulic Research No. 1 pp 90-113.
- Parker, G. 1990. "Surface-Based Bedload Transport Relation for Gravel Rivers." J. Hydraulic Research JHYRAF; Vol. 28, No. 4, (1990):427-437.
- Parker, G., S. Dhamotharan, and H. Stefan, 1982. "Model Experiments on Mobile, Paved Gravel Bed Streams." Water Resources Research; Vol. 18, No.5, (October 1982):1395-1408.
- Parker, G., and P. C. Klingeman, 1982. "On Why Gravel Bed Streams are Paved." Water Resources Research; Vol. 18, No. 5, (October 1982):1409-1423.
- Parker, G., P. C. Klingeman, and D. G. McLean, 1982b. "Bedload and Size Distribution in Paved Gravel-Bed Streams." J. Hydraulic Division, Proceedings of the ASCE; Vol. 108, No. HY4, (April 1982):544-571.
- Rakoczi, L. 1991. "Field tracer investigations of grain sorting in gravel bed river." Proc. of International Grain Sorting Seminar, October 21-26, 1991, Ascona, Switzerland., 77-92.
- Riguidel F-X., Jullien, R., Ristow, G. H., Hansen, A. and Bideau, D. 1994. "Behaviour of a sphere on a rough inclined plane." J. Physics I, France, 4 (1994), 261-272p.
- Ristow, G. H. Riguidel, F-X. and Bideau, D. 1994. "Different characteristics of the motion of a single particle on a bumpy inclined line." J. Phys. I, France, 4 (1994), 1161-1172p.
- Romanovskiy, V. V. 1977. "Investigation of the speed of bed load movement." Soviet Hydrol. 16(2):108-112.

- Shen, H. W., and Lu, J. Y. 1983. "Development and Prediction of Bed Armouring." *J. Hydraulic Engineering*, Vol. 109, No. 4.
- Shields, A. 1936. "Application of Similarity Principles and Turbulence Research to Bed-Load." English translation by W. P. Ott and J. C. van Uchelon, California Institute of Technology.
- Shulits, S. 1935. "The Schoklitsch Bed Load Formula." *Engineering*, London, England, June 21, 1935, pp 644-646 and June 28, 1935, p687.
- Simons, D. B. and Senturk, F. 1992. "Sediment Transport Technology." Water Resources Publication, Fort Collins, Colorado.
- Song, T., Chiew, Y-M. and Chin, C. O. 1998. "Effect of bed load movement on flow friction factor." *J. Hydraulic Engineering*, ASCE. Vol. 124, No. 2, 165-175p.
- Song, T. and Chiew, Y-M. 1997. "Settling characteristics of sediments in moving Bingham fluid." *J. Hydraulic Engineering*, Vol. 123, No. 9, 812-815p.
- Steidtmann J. R. 1982. "Size-density sorting of sand-size spheres during deposition from bedload transport and implications concerning hydraulic equivalence." *J. Sedimentology*. 29, 877-883p.
- Sumer, B. M., and B. Oguz, 1978. "Particle motions near the bottom in turbulent flow in an open channel." *J. Fluid Mech.*, 86, 109-127.
- Sumer, B. M., and R. Diegaard, 1981. "Particle motions near the bottom in turbulent flow in an open channel, 2." *J. Fluid Mech.*, 109, 311-337.
- Sumer, B. M., Kozakiewicz, A., Fredsoe, J. and Deigaard, R. 1996. "Velocity and concentration profiles in sheet flow layer of movable bed." *J. Hydraulic Engineering*, Vol. 122, No. 10, 549-558p.

- Tait, S. J., Willets, B. B. and Maizels, J. K. 1992. "Laboratory observations of bed armouring and changes in bedload composition." Dynamics of Gravel-Bed Rivers, edited by Billi, P., Hey, R. D., Trorne, C. R., Tacconil, P., John Wiley & Sons LTD, West Sussex, England.
- Tominaga, A. and Nezu, I. 1992. "Velocity profiles in steep open channel flows." J. Hydraulic Engineering, Vol. 118, No. 1, 73-90p.
- Van Rijn, L. C. 1984. "Sediment transport, Part I: Bedload transport." J. Hydraulic Engineering, Vol. 110, No. 10, 1431-1456p.
- Van Rijn, L. C. 1984. "Sediment transport, Part II: Suspended load transport." J. of Hydraulic Engineering, Vol. 111, No. 11, 1613-1641p.
- Vanoni, V. A. 1975. "Sedimentation Engineering." Edited by Vito A. Vanoni, 1975. ASCE, Manuals and Reports on Engineering Practice No. 54.
- Von Karman, T. 1930. "Mechanische Ahnlichkeit und turbulenz." Gottinger Nachrichten Math. Phys. Klasse, 58-60 (in German).
- White, F. M. 1991. Viscous Flows. 2<sup>nd</sup> Ed., McGraw-Hill, Inc.
- Wiberg, P. L. 1987. "Mechanics of bed load sediment transport." Ph.D. dissertation, University of Washington, Seattle, Washington.
- Wiberg, P. L. and Smith, J. D. 1989. "Model for calculating bedload transport of sediment." J. Hydraulic Engineering, Vol. 115, No. 1, 101-123p.
- Wilcock, P. R. 1988. "Methods for Estimating the Critical Shear Stress of Individual Fractions in Mixed-Size Sediment." Water Resources Research WRERA0; Vol. 24, No. 7, (July 1988):1127-1135.

- Wilcock, P. R. and J. B. Southard, 1988. "Experimental Study of Incipient Motion in Mixed-Sized Sediment." *Water Resources Research* WRERA0; Vol. 24, No. 7, (July 1988):1137-1151.
- Williams, G. P. and D. L. Rosgen, 1989. "Measured Total Sediment Loads (Suspended and Bedloads) for 93 United States Streams." U.S. Geological Survey, Open-File Report 89-67, U.S. Department of Interior Geological Survey, Denver, Colorado.
- Wilson, K. C. 1966. "Bedload transport at high shear stress." *J. Hydraul. Div. Am. Soc. Civ. Eng.*, 92, 49-59.
- Wolman, M. G. 1954. "A Method of Sampling Coarse River bed Material." *Trans. American Geophy. Union*, 35(6).
- Xie, H., Wei, F., and Cui P. 2000. "Causes and characteristics of the Avila debris flows in Venezuela."
- Yalin, M. S. 1977. "Mechanics of sediment transport." 2<sup>nd</sup> ed., Pergamon, New York, Oxford.
- Yalin, M. S., and E. Karahan, 1979. "Inception of sediment transport, *J. Hydraul. Div. Am. Soc. Civ. Eng.*, 105, 1433-1443.
- Yang, C. T., 1973. "Incipient motion and sediment transport." *J. Hydraulics Division, ASCE*, Vol. 99, No. HY10, October 1973.
- Yang, C. T. 1984. "Unit Stream Power Equation for Gravel." *J. Hydraulic Division, ASCE*, Vol. 110, No. HY12, 1984.
- Yarin, L. P. and Hetsroni, G. 1994. "Turbulence intensity in dilute two phase flows-1: Effect of particle-size distribution on the turbulence of the carrier fluid." *Int. J. Multiphase Flow*, Vol. 20, No. 1, pp. 1-15.